3-D Surface-Wave Estimation and Separation Using an Iterative Closed-Loop Approach*

Tomohide Ishiyama[1] and Gerrit Blacquiere[2]

Search and Discovery Article #41898 (2016)**
Posted September 26, 2016

*Adapted from oral presentation given at AAPG GEO-2016, 12th Middle East Geosciences Conference & Exhibition, Manama, Bahrain, March 7-10, 2016

[1]Inpex, Tokyo, Japan (tomohide.ishiyama@inpex.co.jp)
[2]Delft University of Technology, Delft, Netherlands

Abstract

Surface waves in seismic data are often dominant and mask primaries in land or shallow-water environments. Separating them from the primaries is of great importance either for removing them as noise for reservoir imaging and characterization, or for considering them as signal for near-surface characterization. However, their complex properties, such as dispersion, multi-modality and spatial variability, make the surface-wave separation significantly challenging in processing. To address the challenges, we introduced a method of 3-D surface-wave estimation and separation using an iterative closed-loop approach.

The closed loop contains a relatively simple forward model of surface waves and adaptive subtraction of the forward-modelled surface waves from the observed surface waves, making it possible to evaluate the residual between them. In this approach, the surface-wave model is parameterized by the frequency-dependent slowness and source properties for each surface-wave mode. The optimal model parameters are estimated in an iterative way such that the residual is minimized and, consequently, the approach solves the inverse problem.

We applied this method to several data sets to demonstrate its virtues, such as real 3D geophone/hydrophone seismic data onshore/offshore Abu Dhabi where ground-roll/mud-roll is significantly dominant in land/shallow-water environments. Through the examples, we observed that the method successfully estimates and separates out the surface waves from the seismic data to consequently obtain the subsurface signals. The method provides a better result than a conventional slowness/velocity-based filtering method which cannot handle both surface waves and subsurface signals overlapping each other. We also observed its wide range of applicability to under-sampled, asymmetrically sampled, irregularly sampled and blended seismic data. This suggests the possibility of relaxing requirements for seismic survey parameters in terms of surface-wave separation and, therefore, offers flexibility as well as potential effort reduction with respect to seismic surveys. It should be noted that recent advances in acquisition, such as point receivers and a large amount of stations, make the method more effective because of the improved spatial sampling of surface waves without negative array effects.

References Cited

Ernst, F., 2013. Modal Elastic Inversion: 75th EAGE Conference & Exhibition, Extended Abstracts.

Ishiyama, T., 2015, Surface-Wave Separation and its Impact on Seismic Survey Design: PhD Thesis, Delft University of Technology, Delft, Netherlands, p. 170.

Ishiyama, T., G. Blacquiere, E. Verschuur, and W.A. Mulder, 2015, 3-D Surface-Wave Estimation and Separation Using a Closed-Loop Approach: Geophysical Prospecting. doi:10.1111/1365-2478.12370

Ishiyama, T., G. Blacquiere, and W.A. Mulder, 2015, The Impact of Surface-Wave Separation on Seismic Survey Design: 77th EAGE Conference and Exhibition, IFEMA, Madrid, Spain, 1-4 June 2015, 5 p.

Ishiyama, T., G. Blacquiere, and D.J. Verschuur, 2014, 3D Surface-Wave Estimation and Separation: A Closed-Loop Approach: 84th SEG Annual Meeting Technical Program Expanded Abstracts, v. 33, p. 4263-4267.

Ishiyama, T., G. Blacquiere, and D.J. Verschuur, 2014, 3D Surface-Wave Estimation and Separation Using a Closed-Loop Approach: 76th EAGE Conference & Exhibition Extended Abstracts.

Le Meur, D., N. Benjamin, L. Twigger, K. Garceran, L. Delmas, and G. Poulain, 2010, Adaptive Attenuation of Surface-Wave Noise: First Break, v. 28/9, p. 83-88.

Le Meur, D., N. Benjamin, R. Cole, and M. Al Harthy, 2008, Adaptive Groundroll Filtering: 70th EAGE Conference & Exhibition Extended Abstracts.

Strobbia, C., A. Zarkhidze, R. May, J. Quigley, P. Bilsby, 2011, Attenuation of Aliased Coherent Noise: Model-Based Attenuation for Complex Dispersive Waves: First Break, v. 29/8, 93-100.

Strobbia, C., P. Vermeer, A. Laake, A. Glushchenko, S. Re, 2010, Surface Waves: Processing, Inversion and Removal: First Break, v. 28/8, p. 85-91.

Yilmaz, O., 2001, Seismic Data Analysis: Society of Exploration Geophysics, Tulsa, OK, 2017 p.

GEO 2016

12th Middle East Geosciences Conference and Exhibition

Conference: 7 – 10 March 2016

Exhibition: 8 – 10 March 2016

BAHRAIN INTERNATIONAL EXHIBITION AND CONVENTION CENTRE

3-D Surface-wave estimation and separation using an iterative closed-loop approach

Tomohide Ishiyama, Inpex Corporation and
Gerrit Blacquiere, Delft University of Technology

AAPG

EAGE
EUROPEAN ASSOCIATION OF GEOSCIENTISTS & ENGINEERS

SEG
Society of Exploration Geophysicists
The international society of applied geophysics

ادارة المعارض العربية
Arabian Exhibition Management

INPEX Group

JODCO

TU Delft
Delft University of Technology

Outline

- Introduction
- Theory and method
- Real data examples
- Conclusions and remarks

Outline

- Introduction
- Theory and method
- Real data examples
- Conclusions and remarks

Surface-wave characteristics

- Surface-wave characteristics in seismic data
  - Higher amplitude
  - Lower frequency
  - Lower velocity

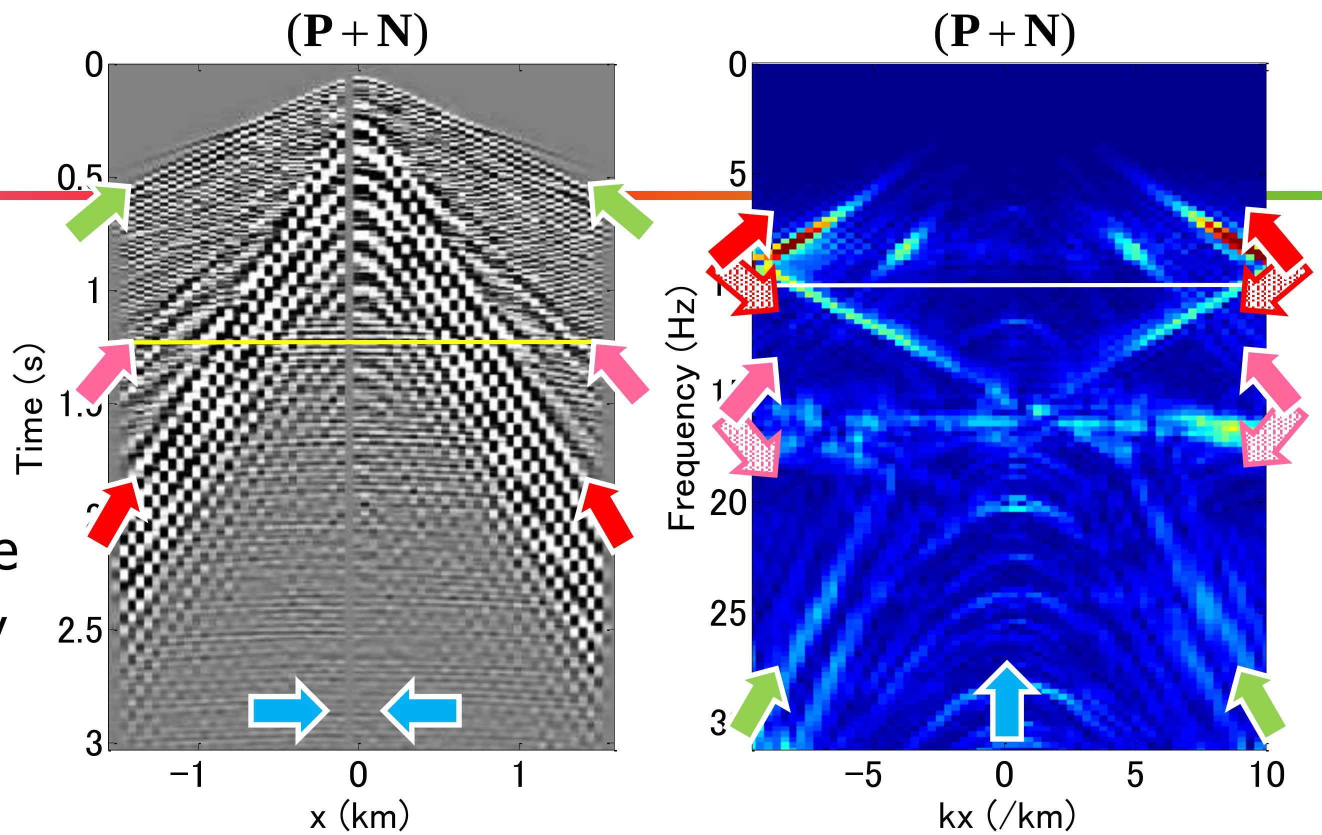

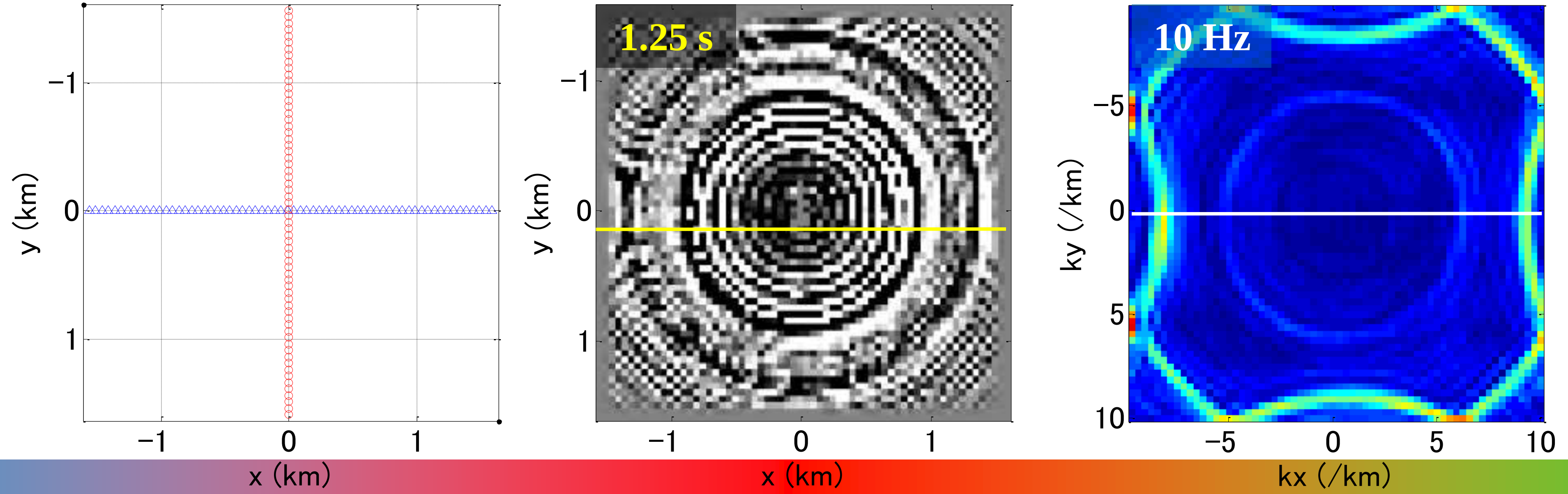

Surface-wave properties

- Dispersive
  - Different frequencies propagate with different velocities.

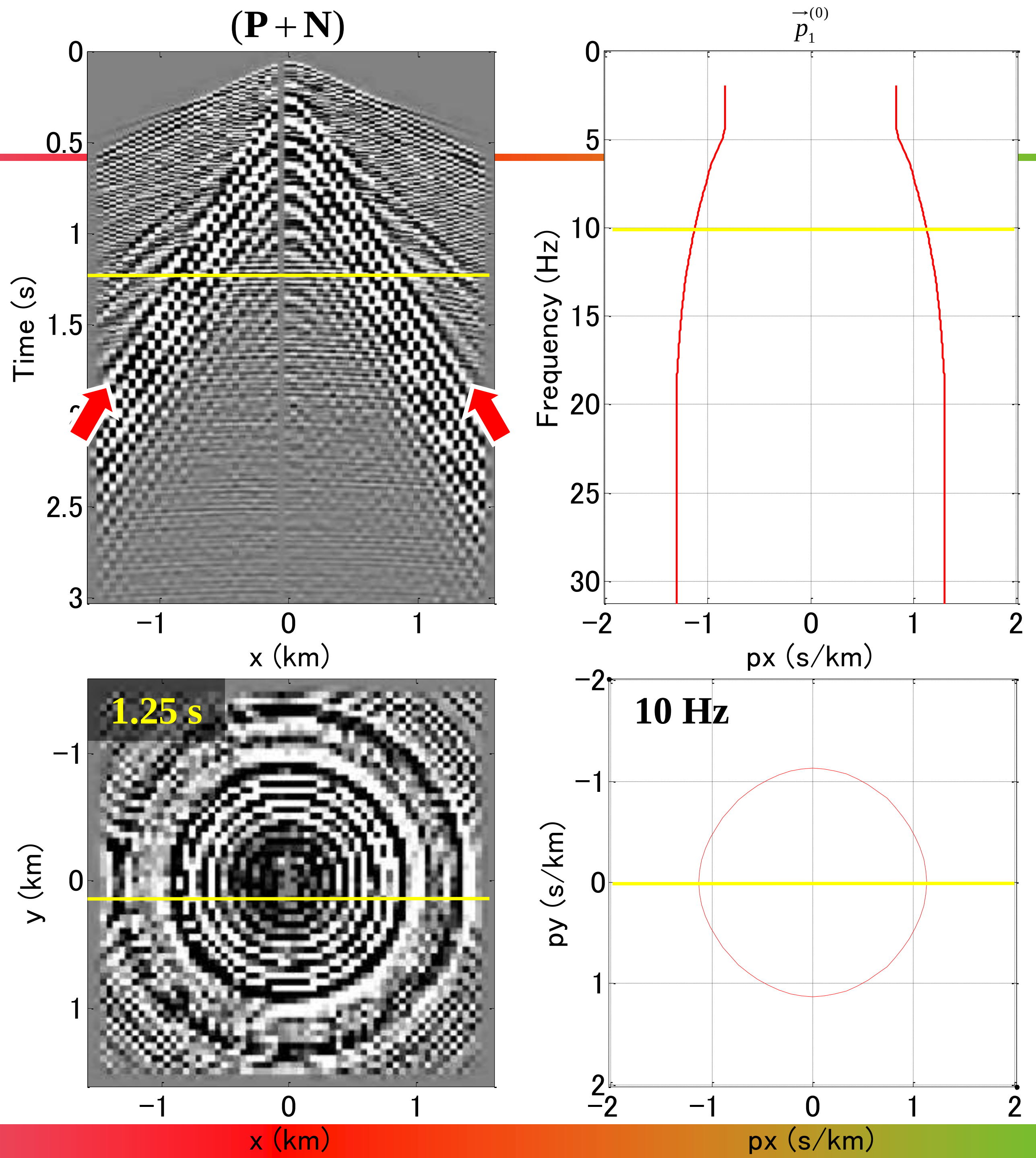

Surface-wave properties

- Dispersive
  - Different frequencies propagate with different velocities.

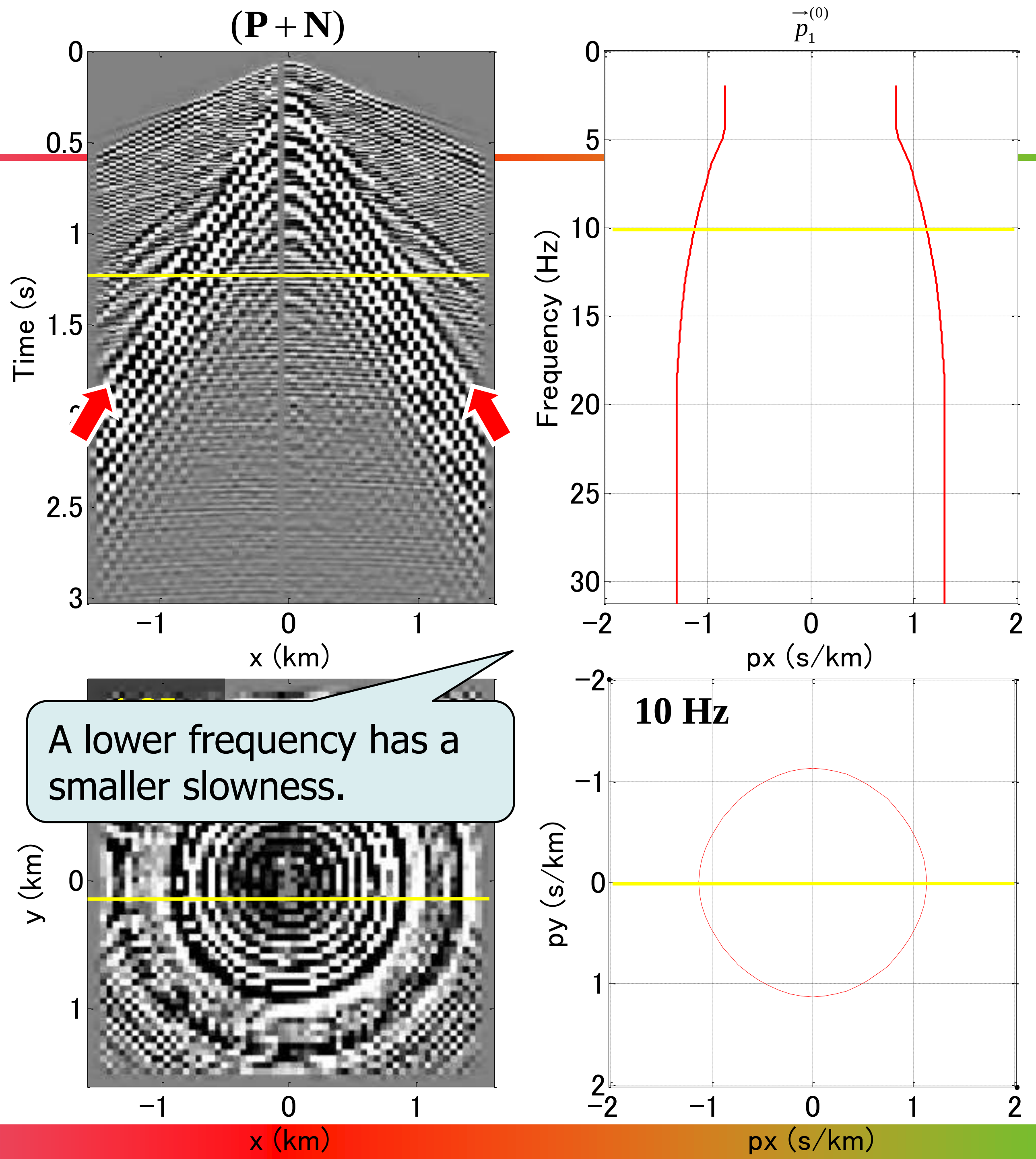

A lower frequency has a smaller slowness.

Surface-wave properties

- Dispersive
- Multi-modal
  - Each frequency propagates with several velocities simultaneously.

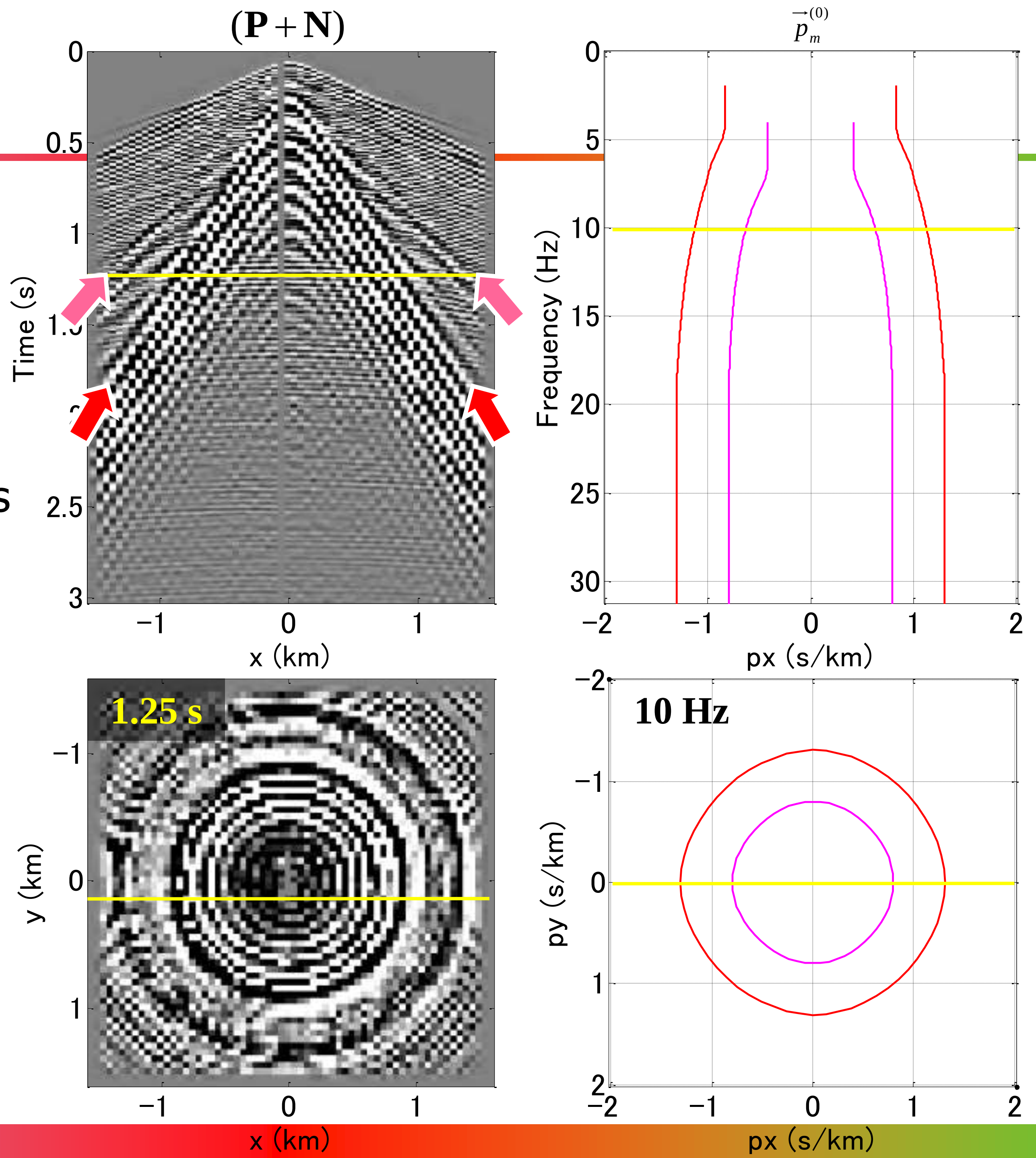

Surface-wave properties

- Dispersive
- Multi-modal
  - Each frequency propagates with several velocities simultaneously.

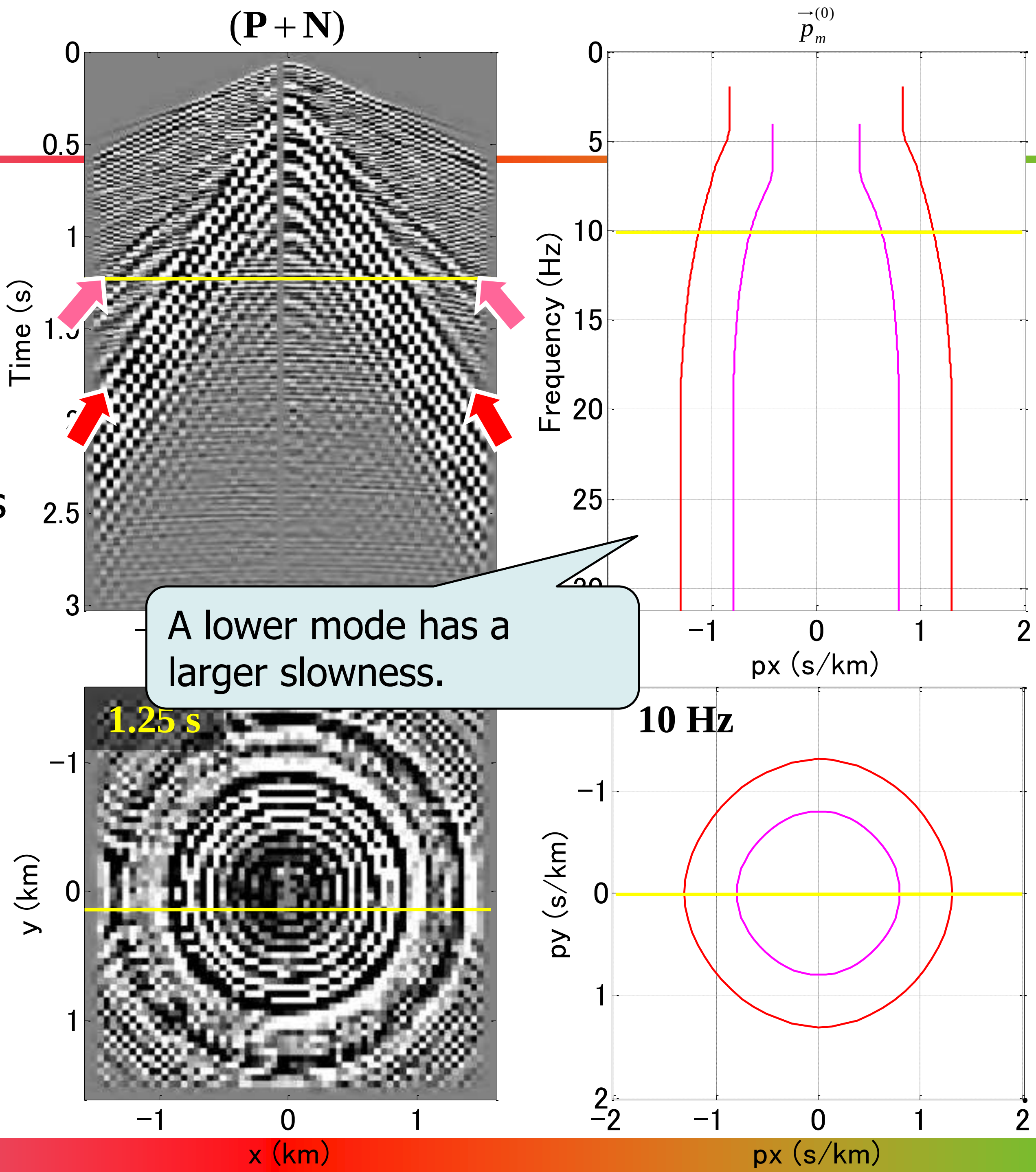

Surface-wave properties

- Dispersive
- Multi-modal
- Spatially variable
  - These properties change spatially in a shot record, and one shot to another.

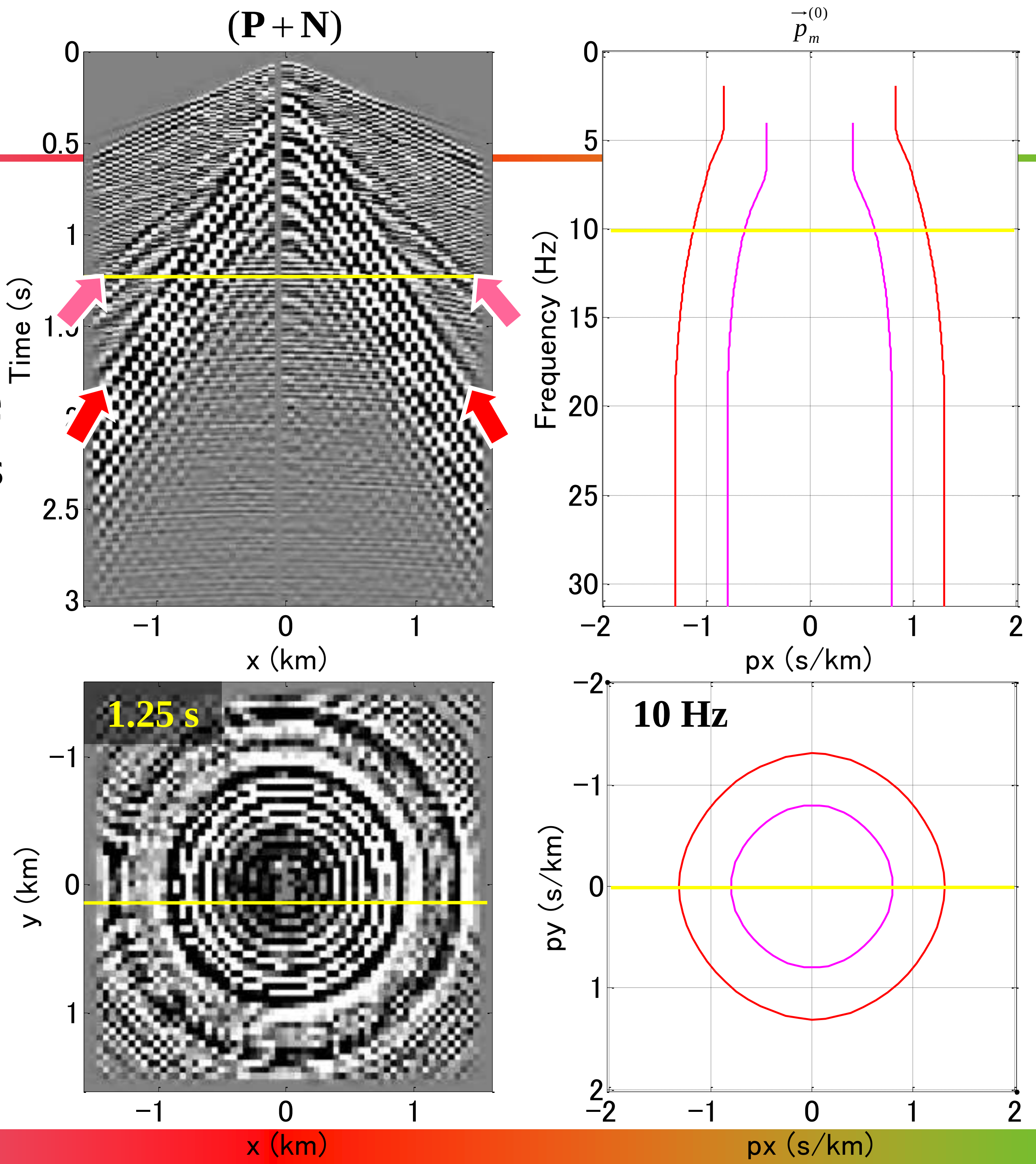

Surface-wave properties

Delphi

- Dispersive
- Multi-modal
- Spatially variable
- Under sampled

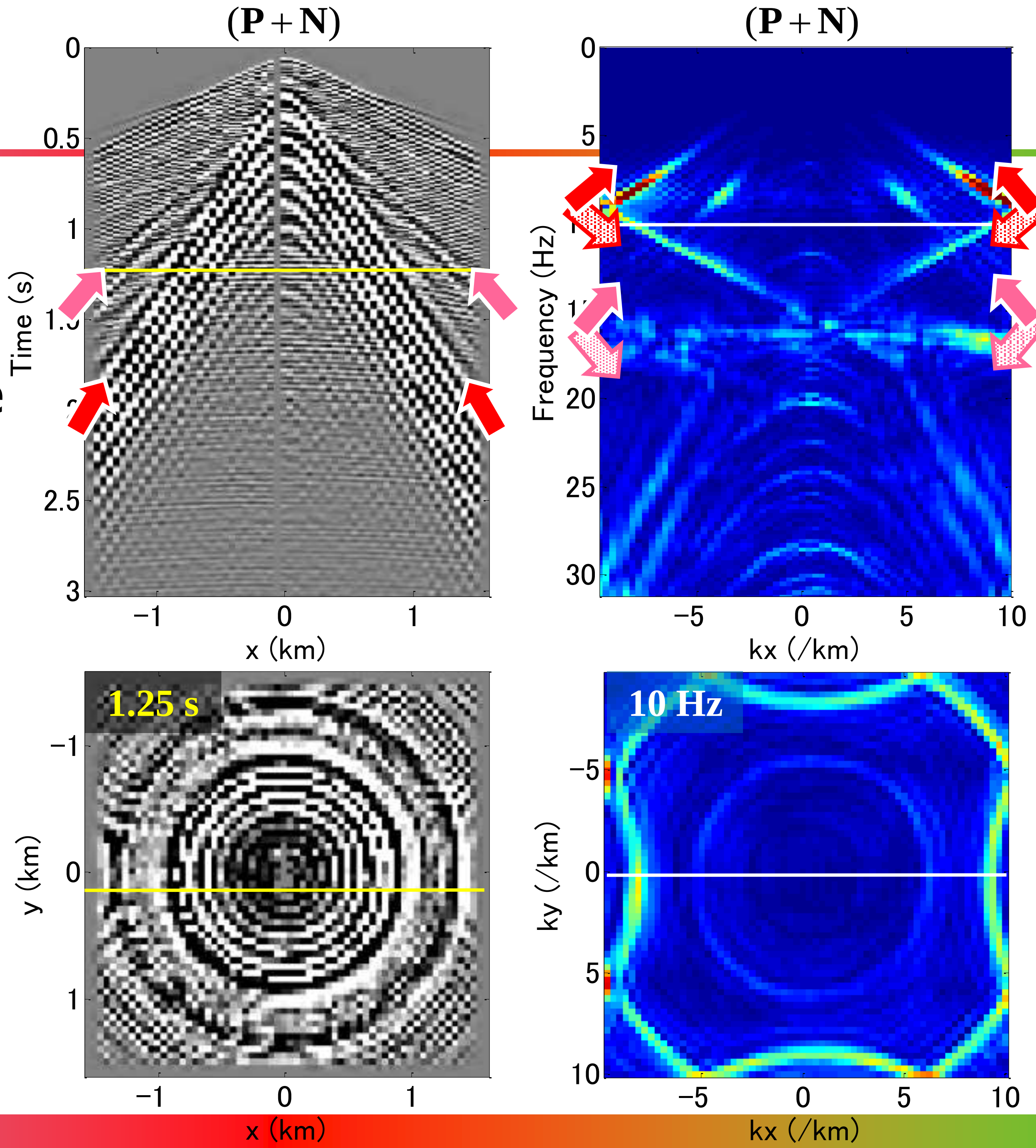

Surface-wave properties

- Dispersive
- Multi-modal
- Spatially variable
- Under sampled

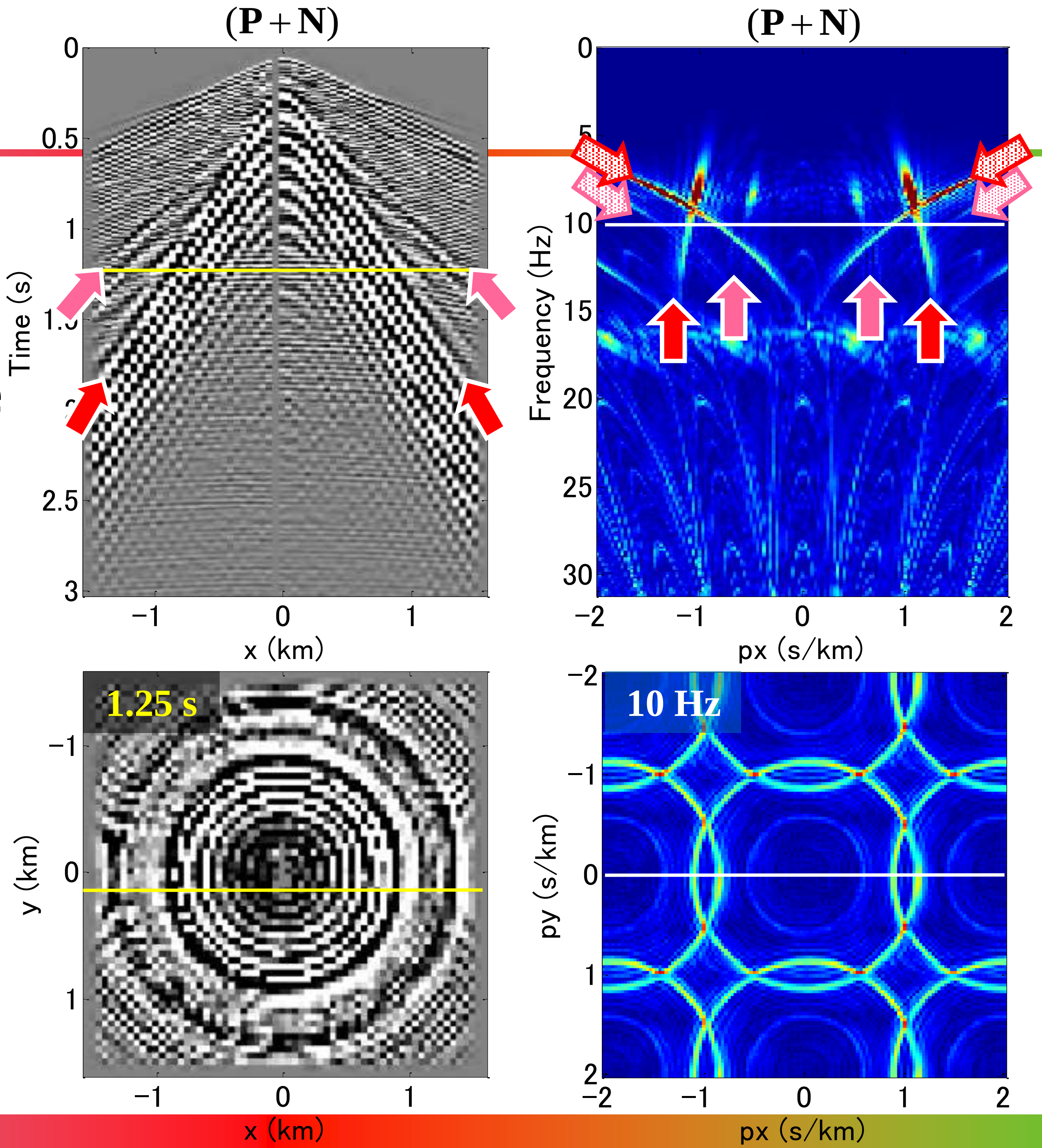

Delphi

Surface-wave properties

- Dispersive
- Multi-modal
- Spatially variable
- Under sampled

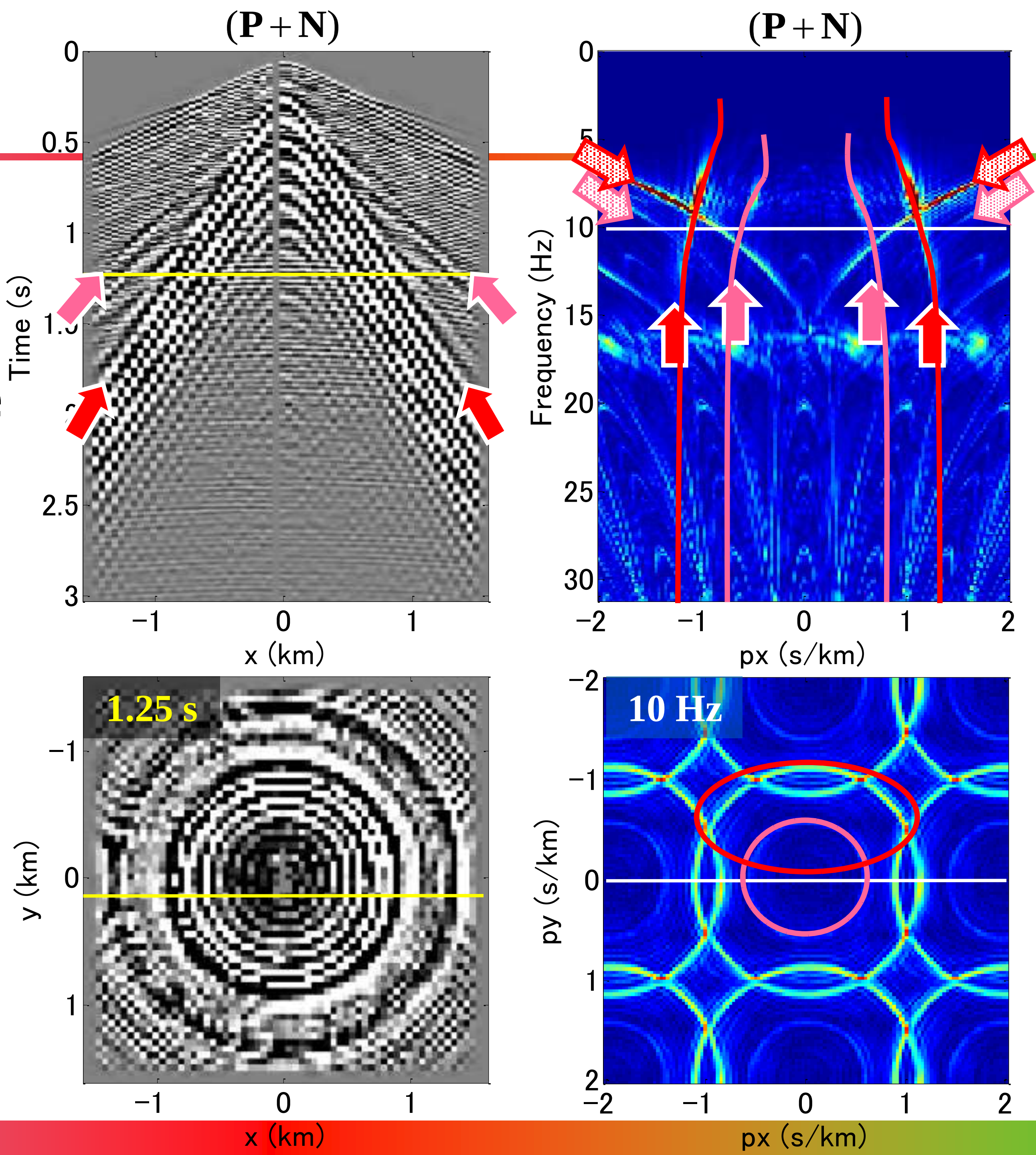

Surface-wave properties

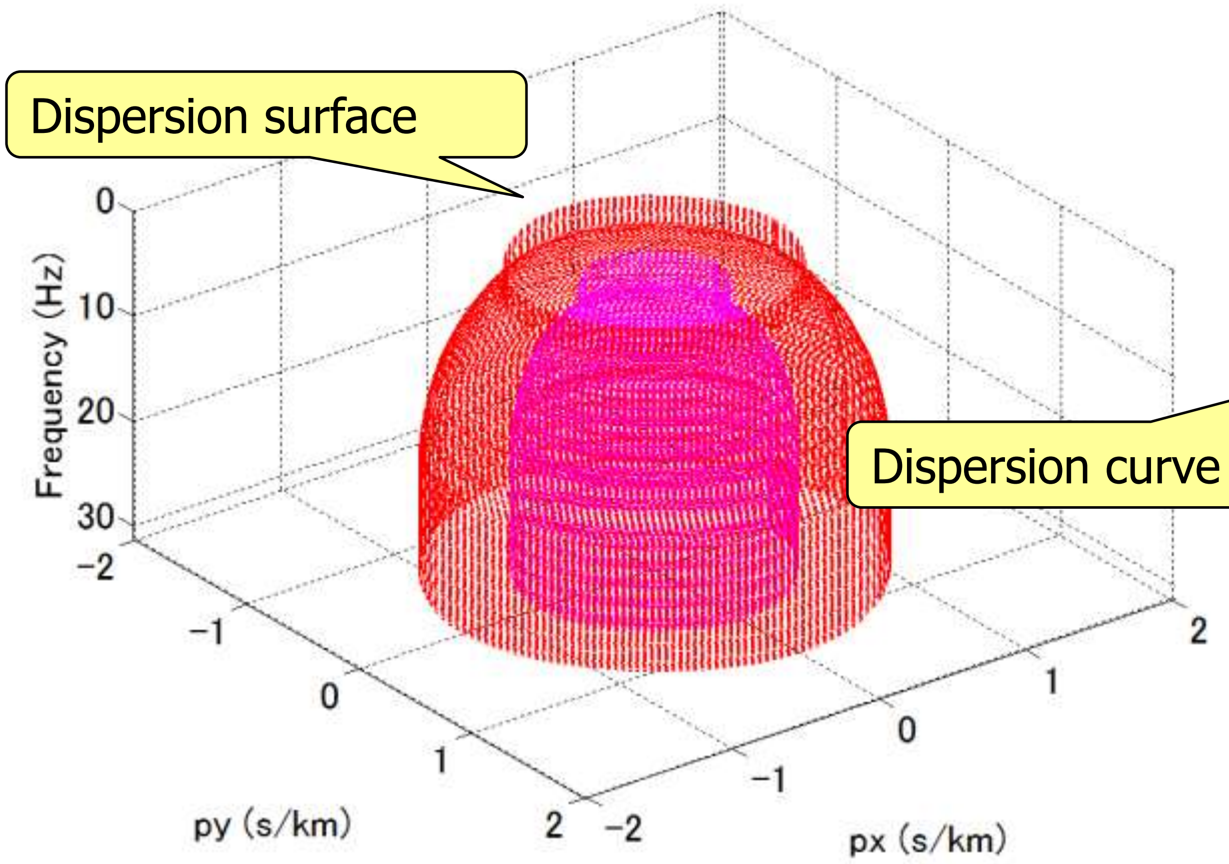

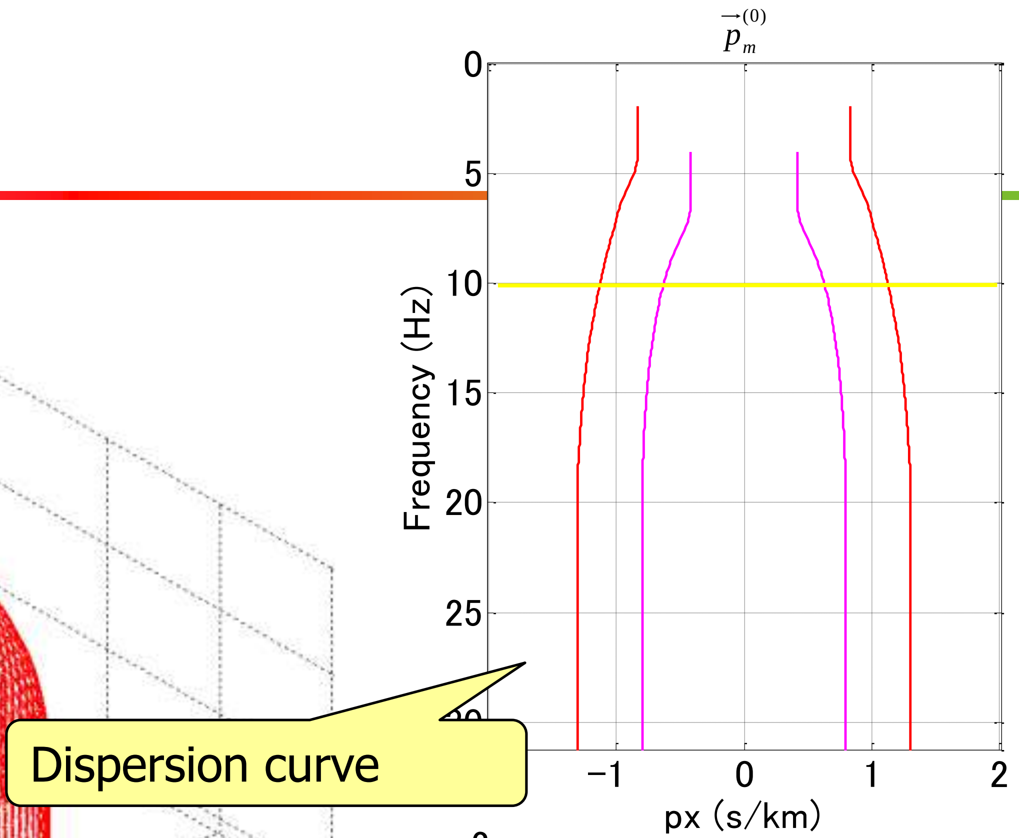

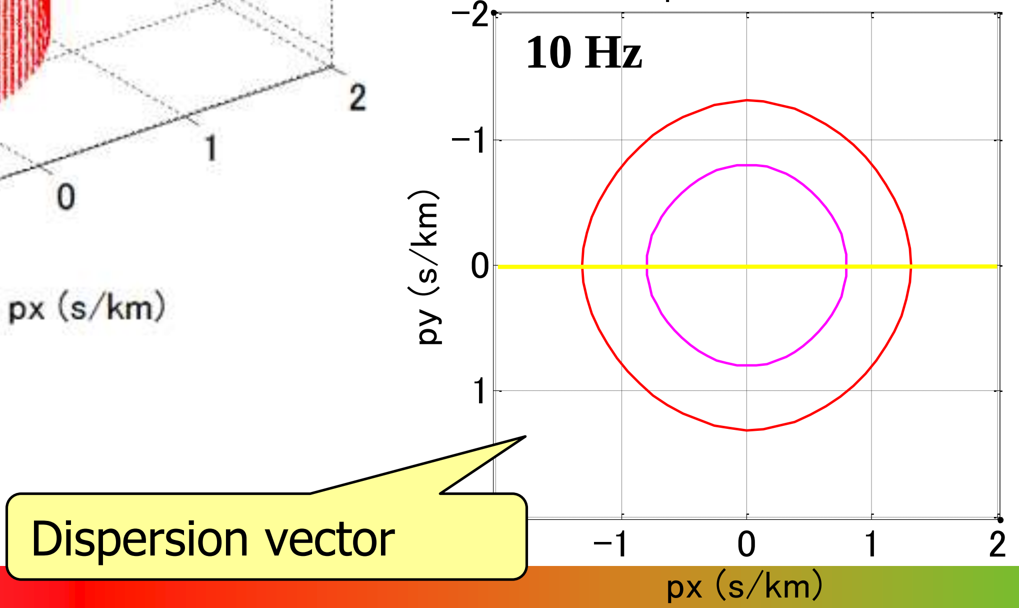

Surface-wave properties

- Dispersive
- Multi-modal
- Spatially variable
- Under sampled
- Irregularly sampled

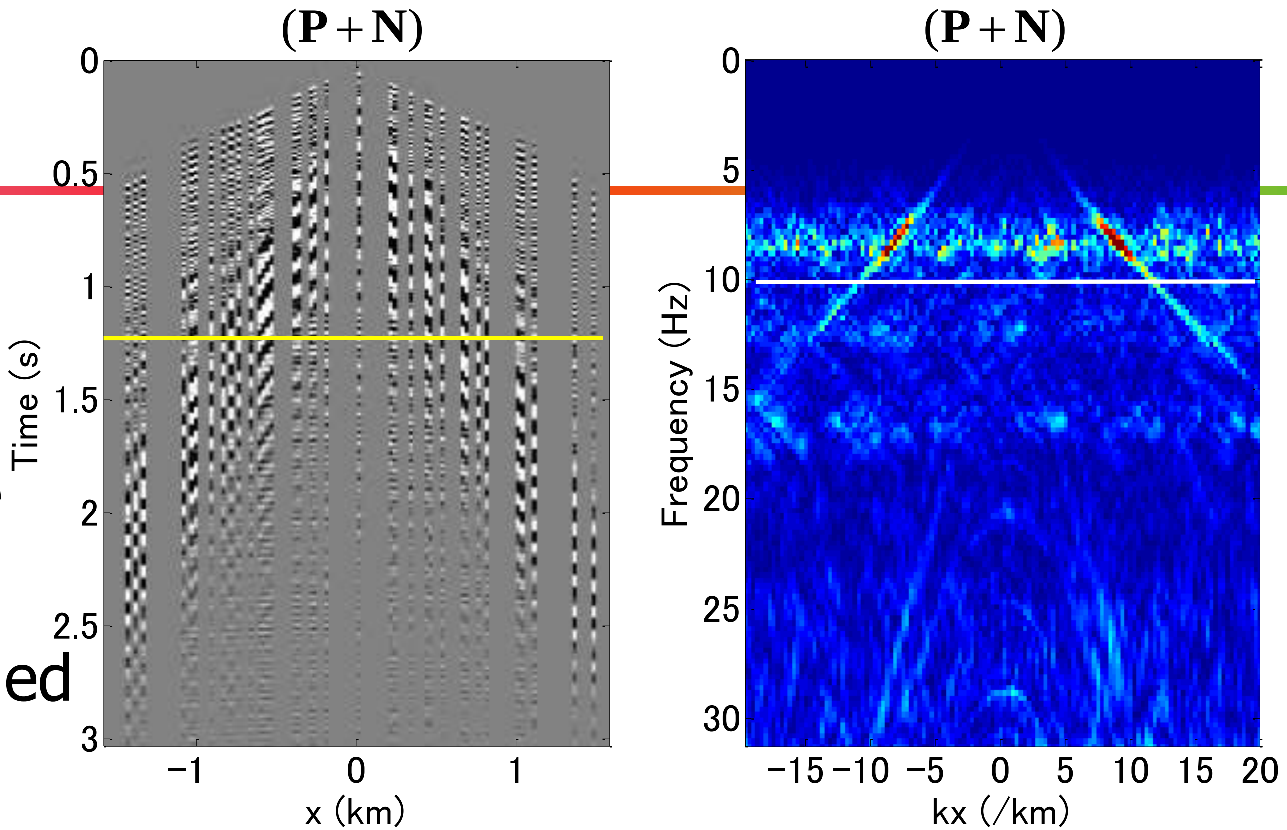

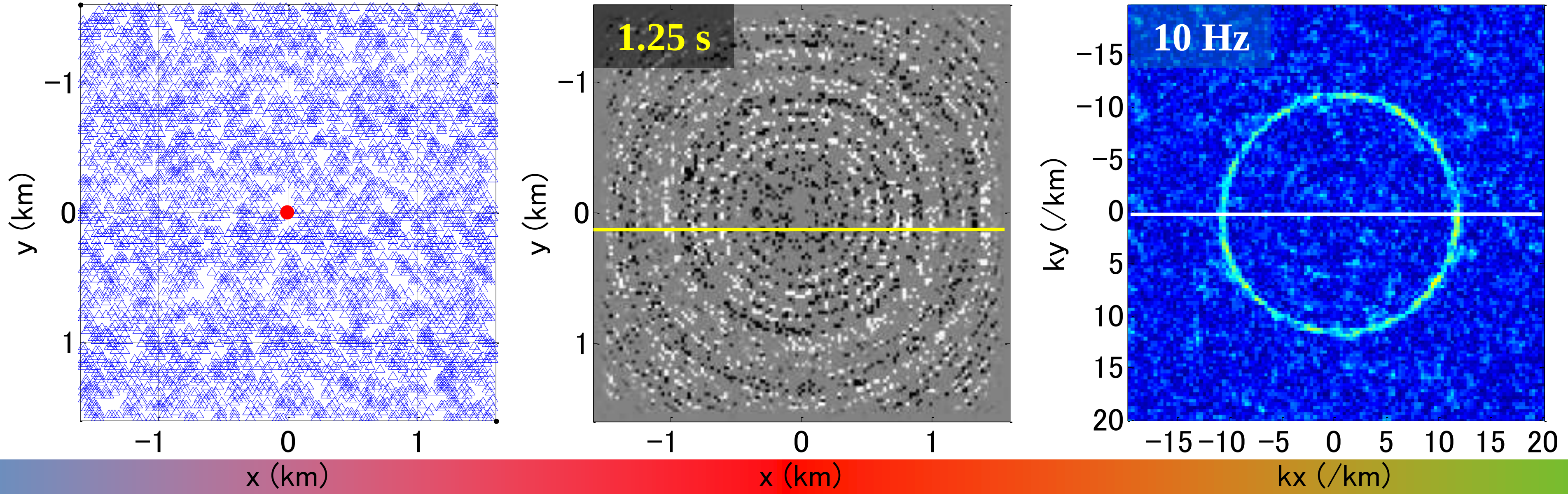

Surface-wave properties

- Dispersive
- Multi-modal
- Spatially variable
- Under sampled
- Irregularly sampled
- Blended

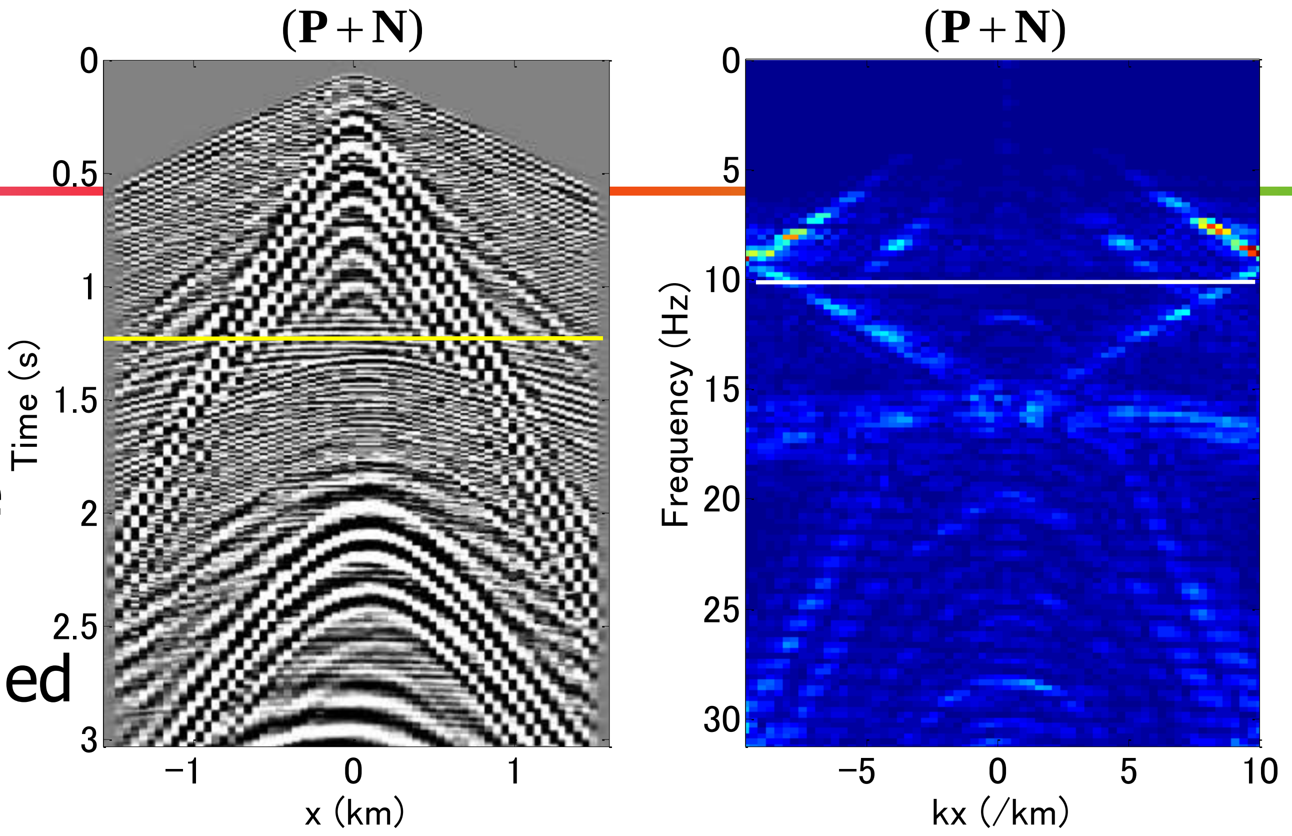

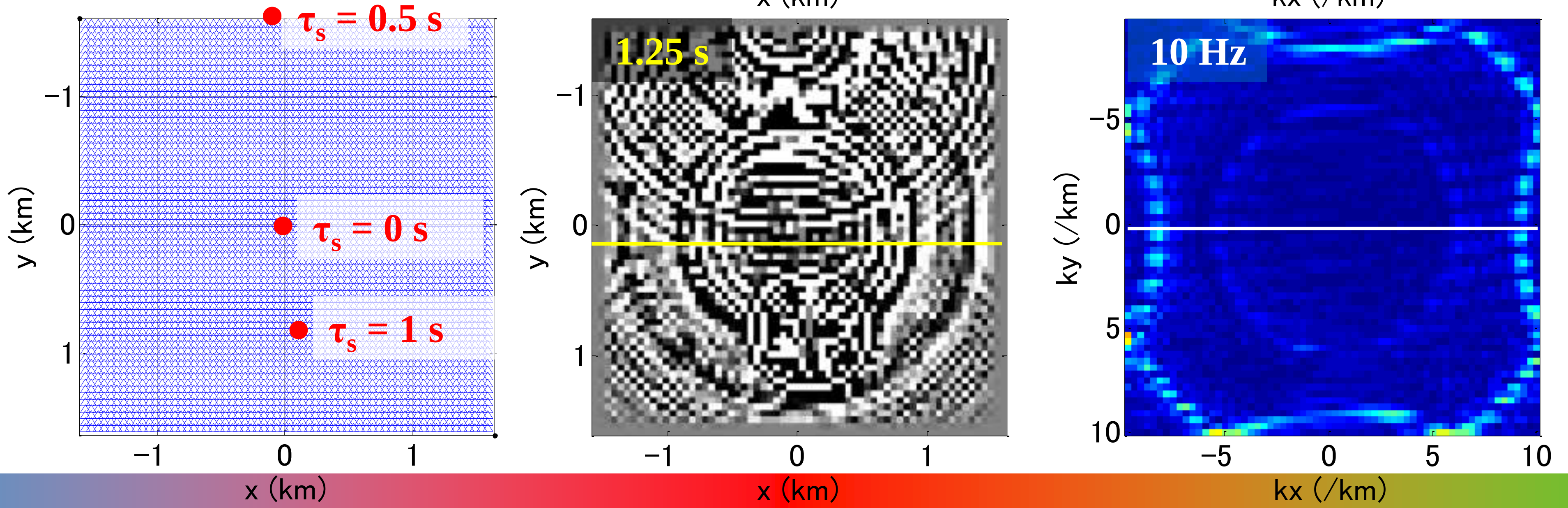

Surface-wave separation

Delphi

Surface waves

– traditionally treated as noise, masking primaries.
– today regarded as signal, for near-surface characterization.

Estimating them and separating them out from seismic data is important for both applications.

$$\mathbf{P}_{tot} = \mathbf{P} + \mathbf{N}$$

N : Surface waves
P : Subsurface signals
(P+N) : Seismic data

Outline

- Introduction
- Theory and method
- Real data examples
- Conclusions and remarks

Forward model

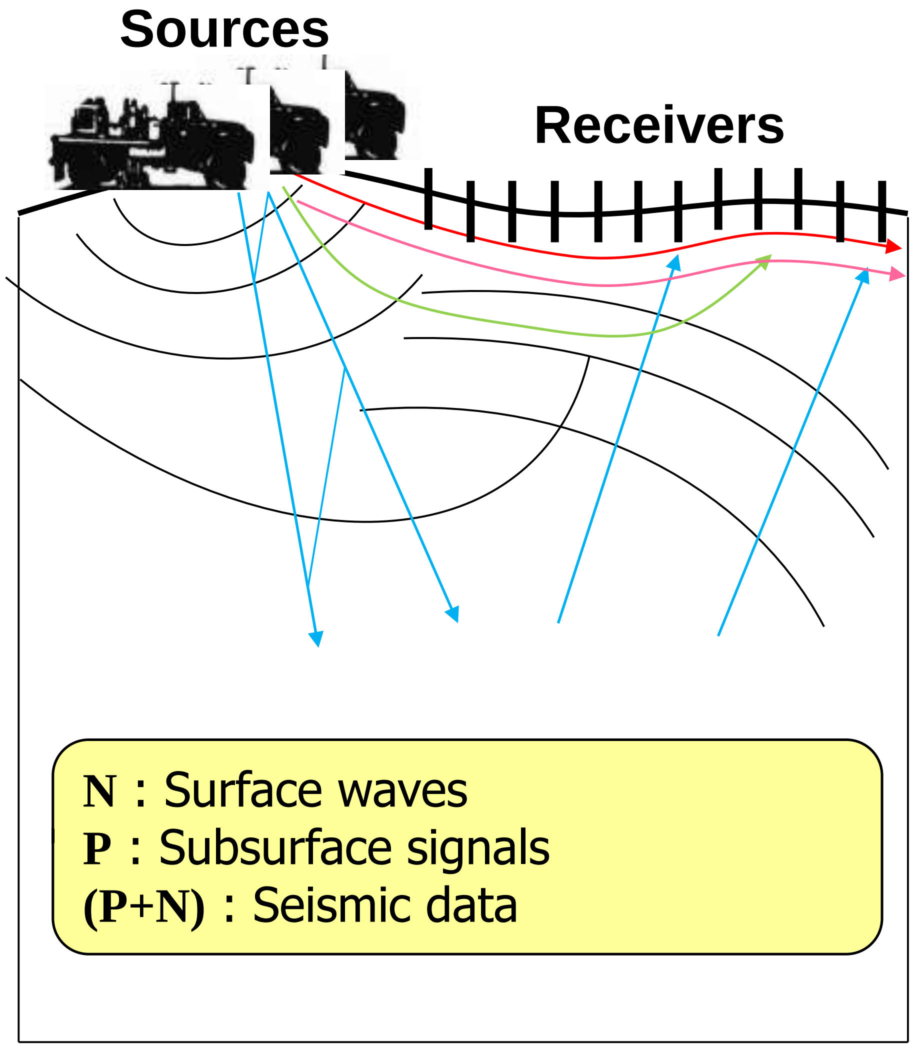

N : Surface waves
P : Subsurface signals
(P+N) : Seismic data

$$\mathbf{P}_{tot} = \mathbf{P} + \mathbf{N}$$

Forward model

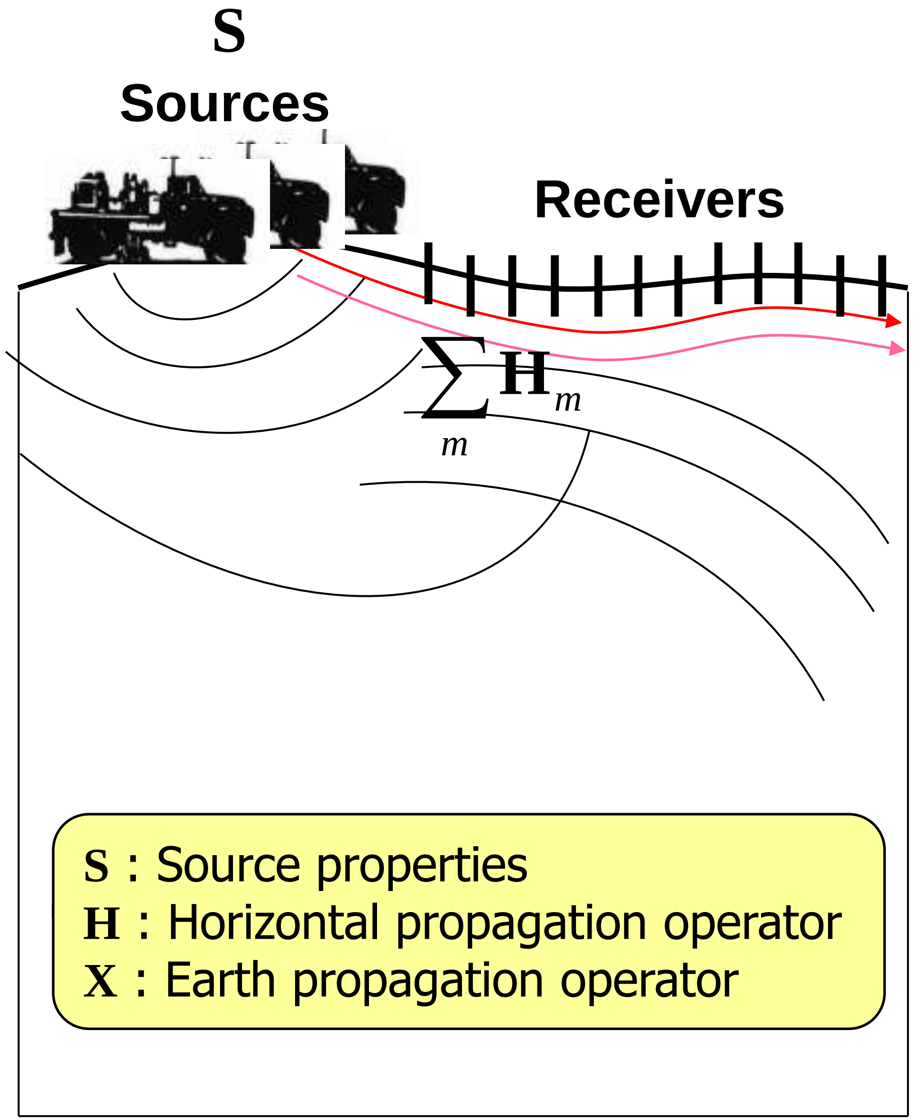

$$\mathbf{N} = \sum_m \mathbf{N}_m$$

$$\mathbf{N}_m = \mathbf{H}_m \mathbf{S}_m$$

$$H_m(\vec{r},\omega) = \left(\frac{e^{-\vec{\lambda}_m(\omega)\cdot\vec{r}}}{\sqrt{|\vec{r}|}}\right) e^{-j\omega\vec{p}_m(\omega)\cdot\vec{r}}$$

Forward m

Multi-modes
m : the number of a surface-wave mode.

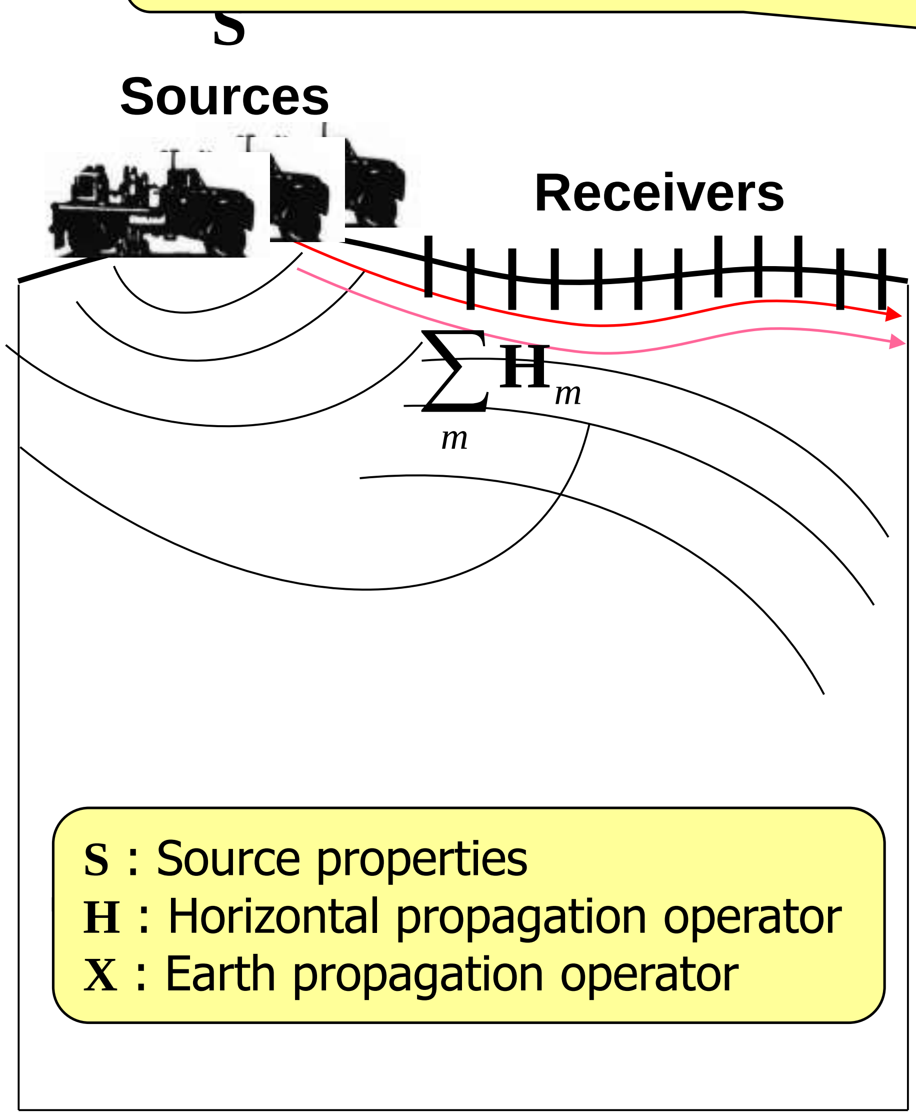

$$\mathbf{N} = \sum_m \mathbf{N}_m$$

$\mathbf{N}_m$ dispersion vector

$$H_m(\vec{r},\omega) = \left(\frac{e^{-\vec{\lambda}_m(\omega)\cdot\vec{r}}}{\sqrt{|\vec{r}|}}\right)e^{-j\omega\vec{p}_m(\omega)\cdot\vec{r}}$$

Travel-time phase shift

Delphi

Forward m

Multi-modes
m : the number of a surface-wave mode.

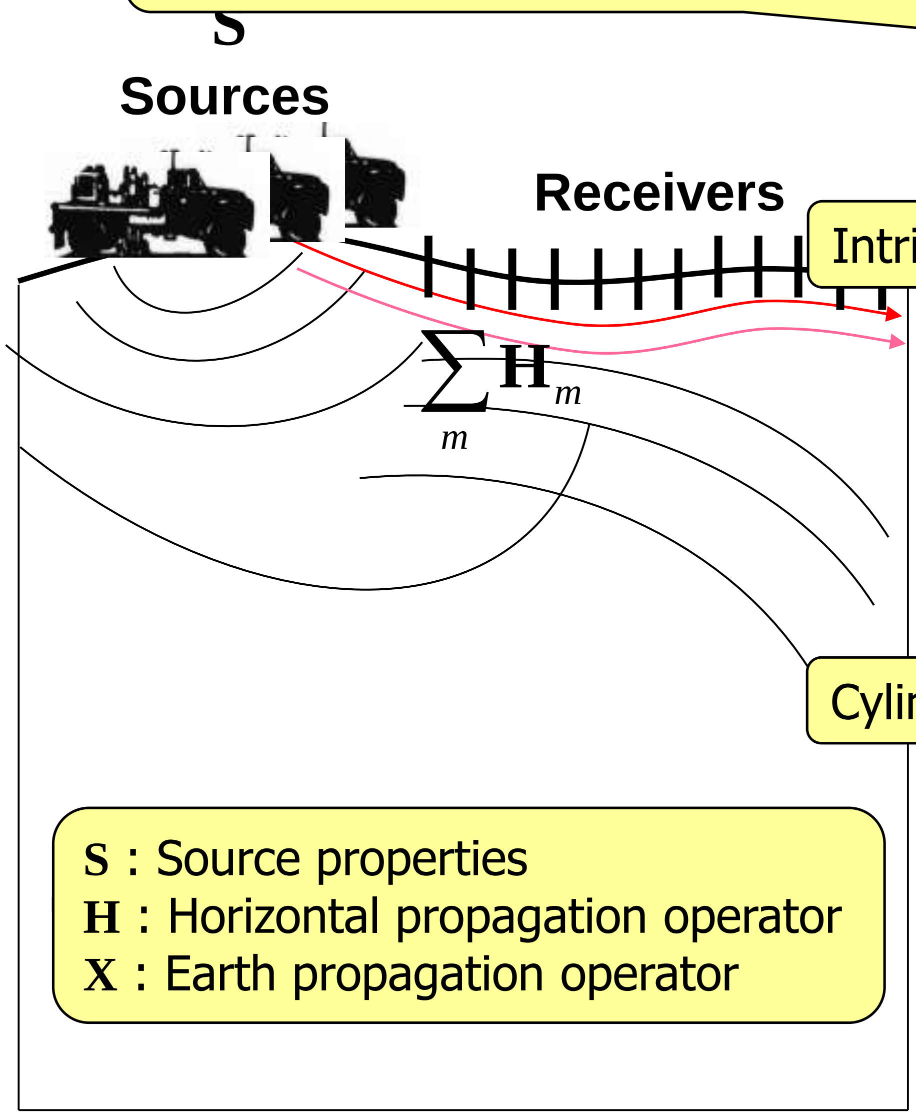

$$\mathbf{N} = \sum_m \mathbf{N}_m$$

Intrinsic attenuation

r

$$H_m(\vec{r},\omega) = \Big(\frac{e^{-\vec{\lambda}_m(\omega)\cdot\vec{r}}}{\sqrt{|\vec{r}|}}\Big)e^{-j\omega\vec{p}_m(\omega)\cdot\vec{r}}$$

Tra me phase shift

Cylindrical spreading

Delphi

Multi-modes

m : the number of a surface-wave mode.

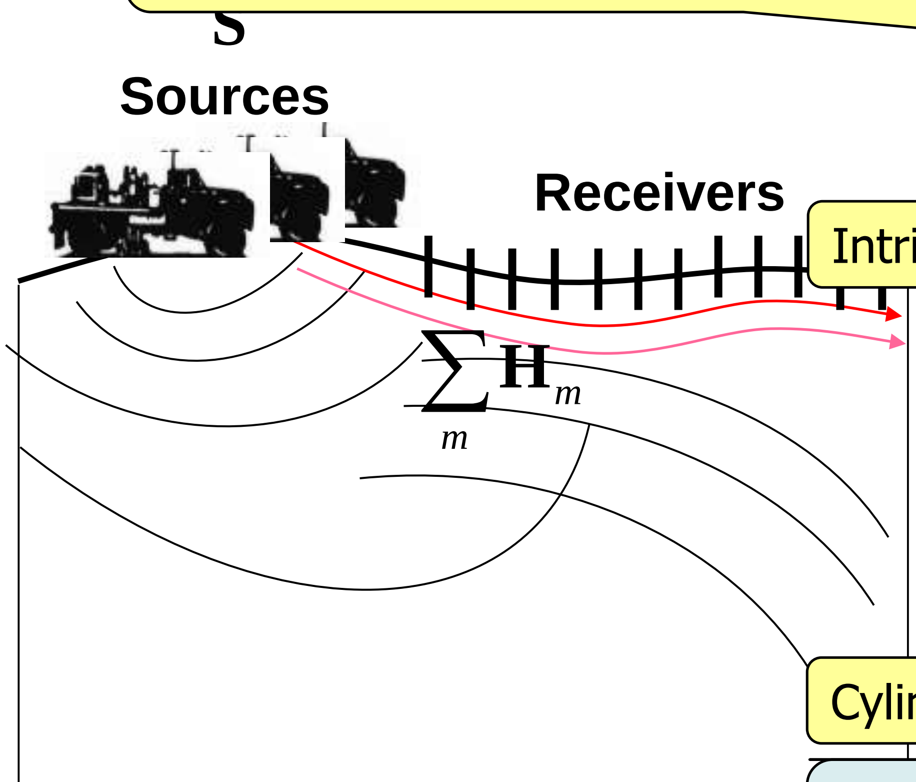

$$\mathbf{N} = \sum_m \mathbf{N}_m$$

Intrinsic attenuation

$$H_m(\vec{r},\omega) = \left(\frac{e^{-\vec{\lambda}_m(\omega)\cdot\vec{r}}}{\sqrt{|\vec{r}|}}\right)e^{-j\omega\vec{p}_m(\omega)\cdot\vec{r}}$$

Cylindrical spreading

The geometrical spreading effect is much larger than the intrinsic attenuation effect.

– $\mathbf{N}$ is parameterized by $\vec{\lambda}_m$, $\vec{p}_m$ and $\mathbf{S}_m$; or $\vec{p}_m$ and $\mathbf{S}_m$ with the assumption that $\vec{\lambda}_m$ is zero.

Inversion

$$\mathbf{J}:\mathbf{A}_m;\mathbf{H}_m,\mathbf{S}_m \xrightarrow[\mathbf{J}=min.]{s.t.} <\mathbf{P}>$$

$$\mathbf{J}=\sum_{\omega}\left\|\mathbf{P}+\Delta\mathbf{N}\right\|^2$$

$$=\sum_{\omega}\left\|(\mathbf{P}+\mathbf{N})-<\mathbf{N}>\right\|^2$$

$$=\sum_{\omega}\left\|(\mathbf{P}+\mathbf{N})-\sum_{m}\mathbf{A}_m\mathbf{H}_m\mathbf{S}_m\right\|^2$$

<N> : Surface-wave estimate
<P> : Subsurface-signal estimate

- The parameters as well as the adaptive filter are solved such that the residual $\mathbf{P}+\Delta\mathbf{N}$ is minimized.
- The minimization scheme works on $<\mathbf{N}>$ only, and $\mathbf{P}$ remains untouched by a signal-protecting scheme.
- In the ideal situation, the resulting residual $\mathbf{P}+\Delta\mathbf{N}$ closely corresponds to $\mathbf{P}$.

Inversion

$$\mathbf{J}:\mathbf{A}_m;\mathbf{H}_m,\mathbf{S}_m \xrightarrow[\mathbf{J}=min.]{s.t.} <\mathbf{P}>$$

$$\mathbf{J}=\sum_{\omega}\left\|\mathbf{P}+\Delta\mathbf{N}\right\|^2$$

$$=\sum_{\omega}\left\|(\mathbf{P}+\mathbf{N})-<\mathbf{N}>\right\|^2$$

$$=\sum_{\omega}\left\|(\mathbf{P}+\mathbf{N})-\sum_{m}\mathbf{A}_m\mathbf{H}_m\mathbf{S}_m\right\|^2$$

A_m : Adaptive filter

Parameters

- The parameters as well as the adaptive filter are solved such that the residual $\mathbf{P}+\Delta\mathbf{N}$ is minimized.
- The minimization scheme works on $<\mathbf{N}>$ only, and $\mathbf{P}$ remains untouched by a rotecting scheme.
- In the ideal situation, the resulting residual $\mathbf{P}+\Delta\mathbf{N}$ closely corresponds to $\mathbf{P}$.

Closed loop

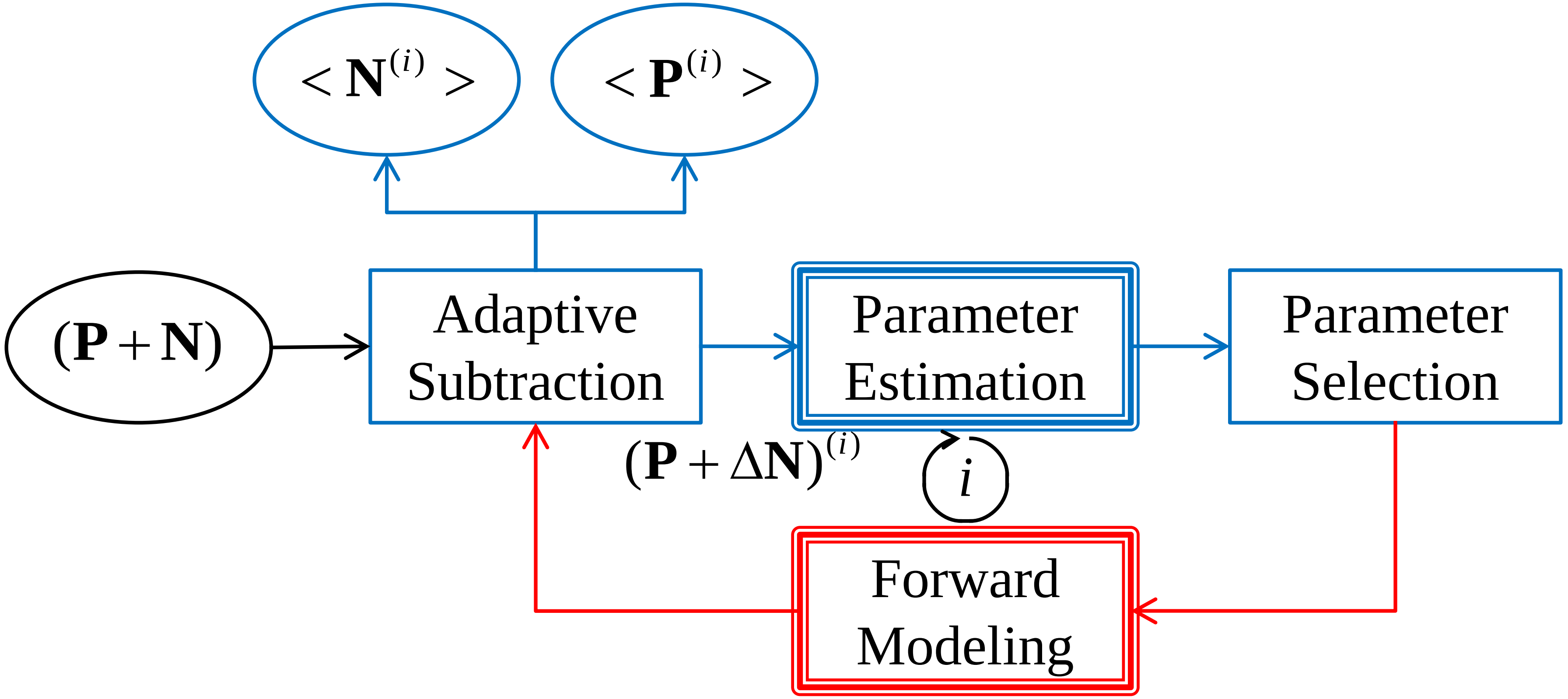

– For each loop, the modal parameters $\vec{p}_m^{(i)}$, $\Delta\mathbf{S}_m^{(i)}$ as well as the modal adaptive filter $\mathbf{A}_m^{(i)}$ (m = 1, 2, …) are estimated.

Closed loop

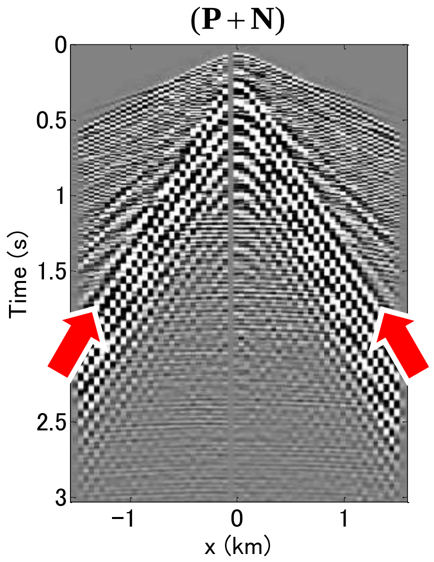
(P + N)
0
0.5
1
1.5
2.5
3
Time (s)
−1
0
1
x (km)

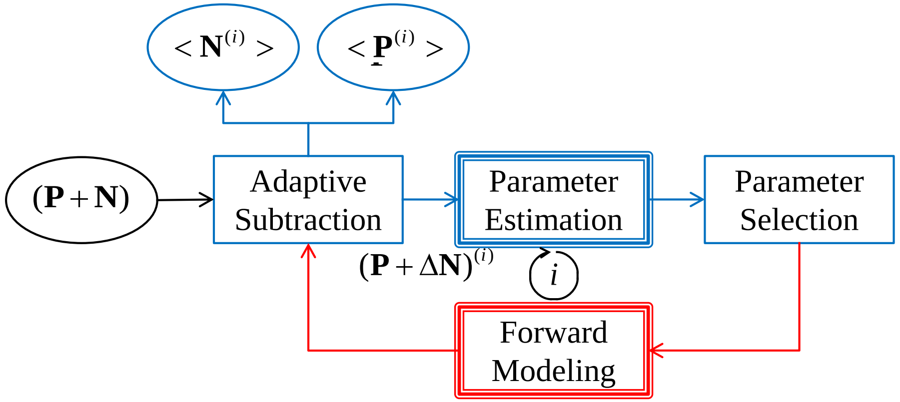
< N(i) >
< P(i) >
(P + N)
Adaptive Subtraction
Parameter Estimation
Parameter Selection
(P + ΔN)(i)
i
Forward Modeling

Closed loop

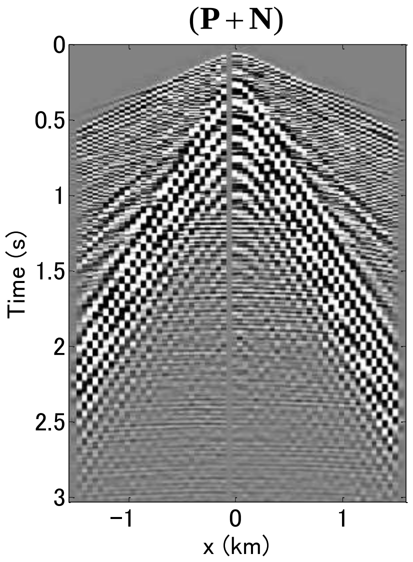
(P + N)
0
0.5
1
1.5
2
2.5
3
Time (s)
−1
0
1
x (km)

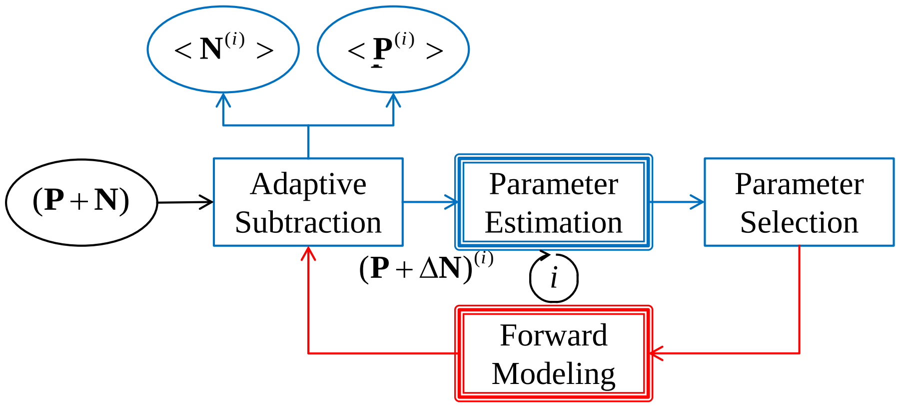
< N^(i) >
< P^(i) >
(P + N)
Adaptive Subtraction
Parameter Estimation
Parameter Selection
(P + ΔN)^(i)
i
Forward Modeling

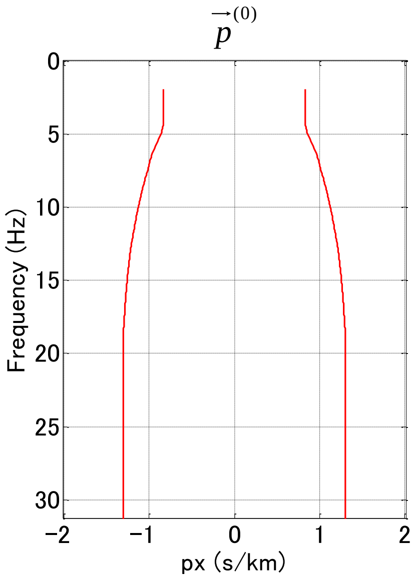
p^(0)
0
5
10
15
20
25
30
Frequency (Hz)
−2
−1
0
1
2
px (s/km)

Closed loop

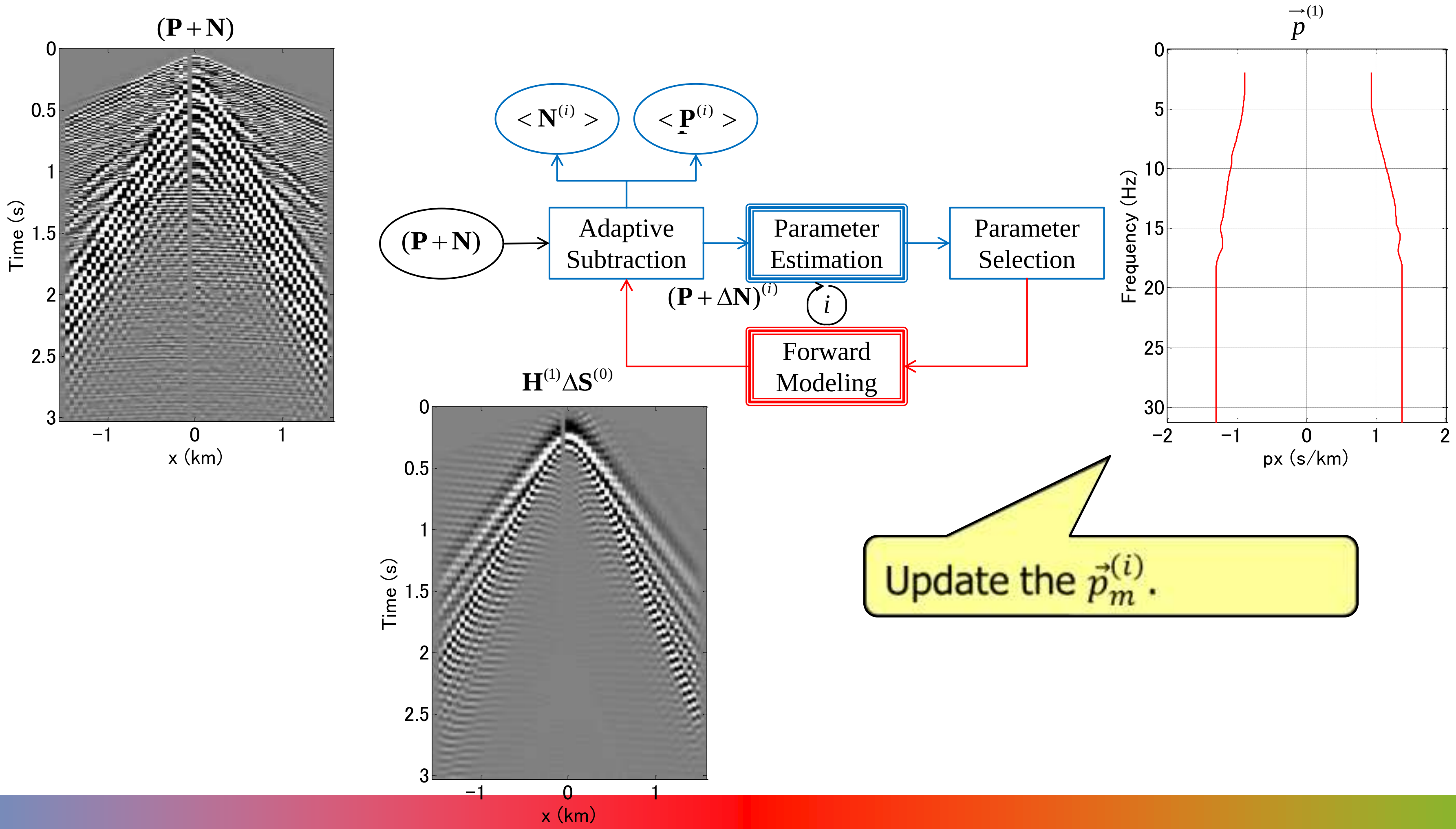

Update the $\vec{p}_m^{(i)}$.

Closed loop

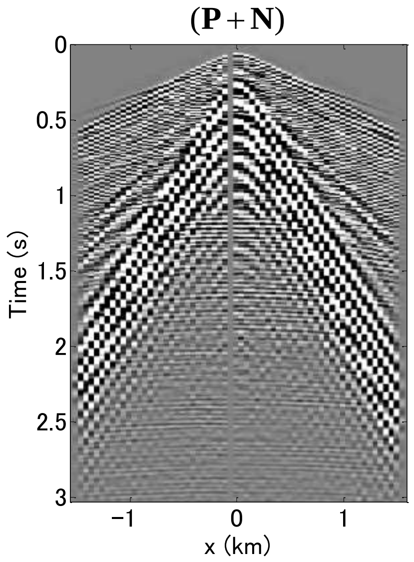

(P + N)
Time (s)
x (km)

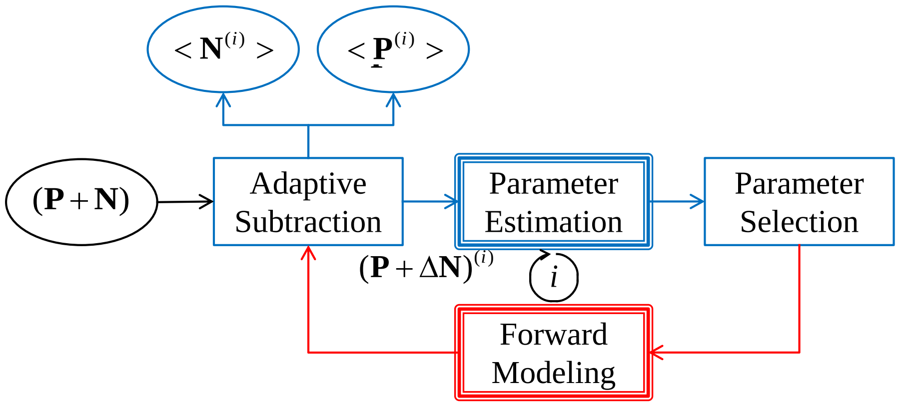

< N^(i) >
< P^(i) >
(P + N)
Adaptive Subtraction
Parameter Estimation
Parameter Selection
(P + ΔN)^(i)
i
Forward Modeling

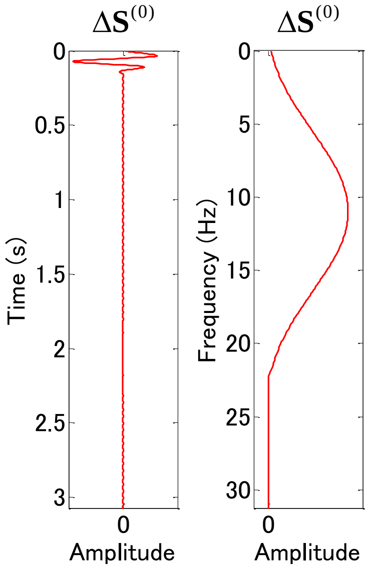

ΔS^(0)
Time (s)
Amplitude
ΔS^(0)
Frequency (Hz)
Amplitude

Closed loop

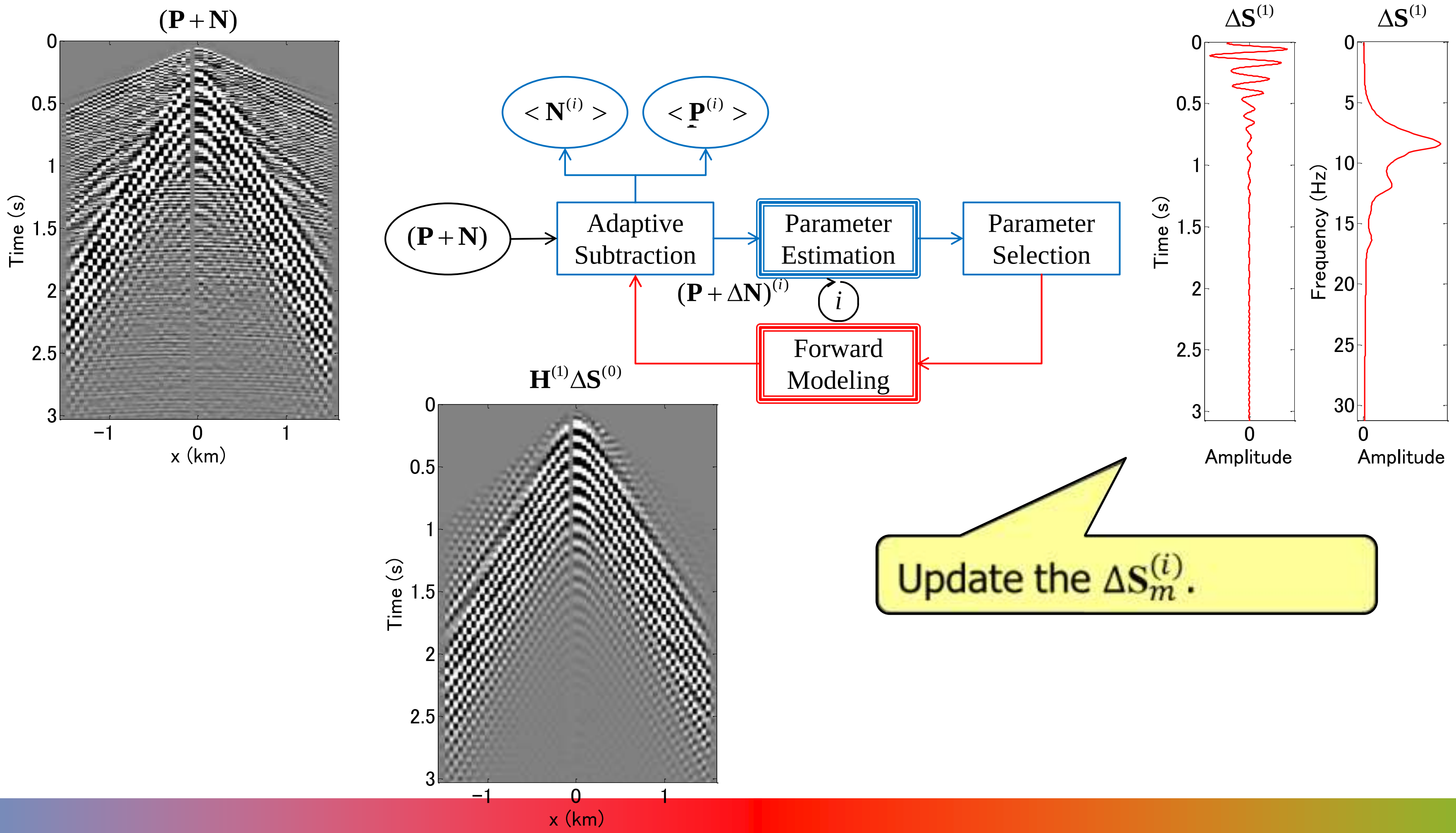

(P + N)
Time (s)
x (km)
< N^(i) >
< P^(i) >
(P + N)
Adaptive Subtraction
Parameter Estimation
Parameter Selection
(P + ΔN)^(i)
i
Forward Modeling
H^(1) ΔS^(0)
Time (s)
x (km)
ΔS^(1)
Time (s)
Amplitude
ΔS^(1)
Frequency (Hz)
Amplitude
Update the $\Delta\mathbf{S}_m^{(i)}$.

Closed loop

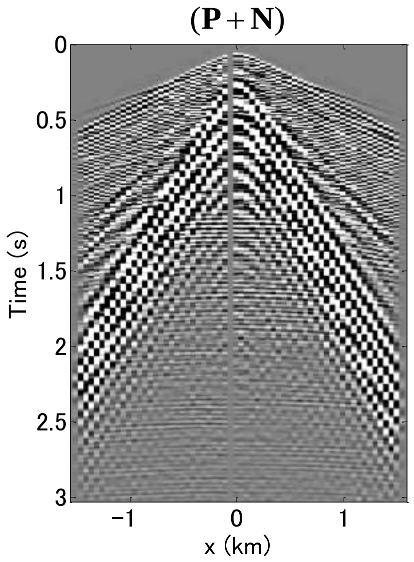

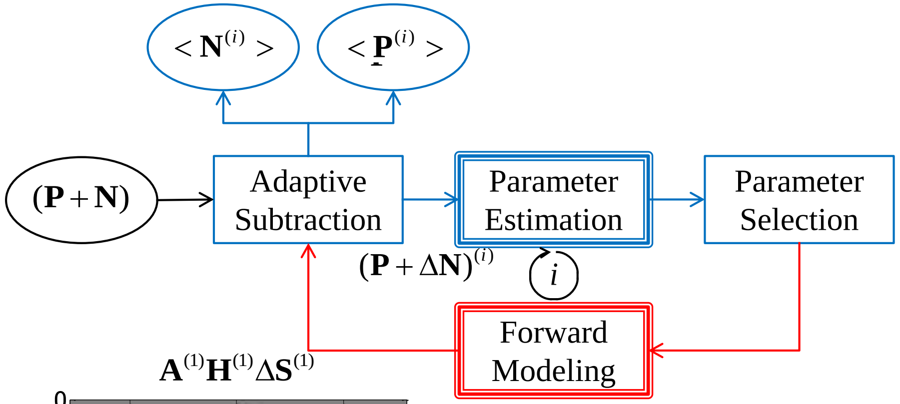

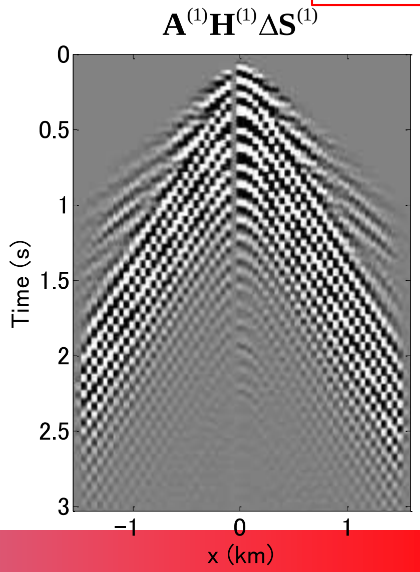

Update the $\mathbf{A}_m^{(i)}$.

Closed loop

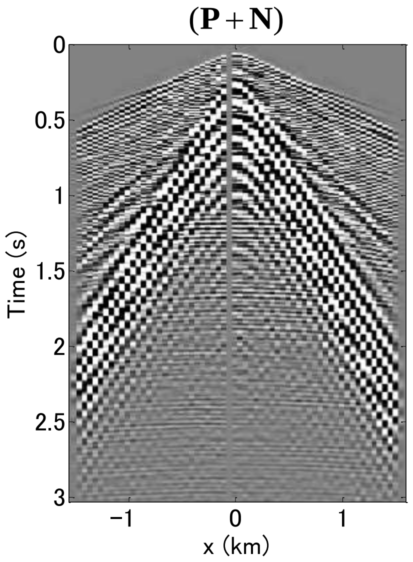

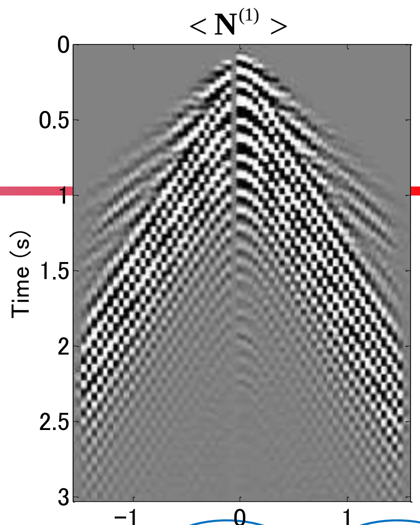

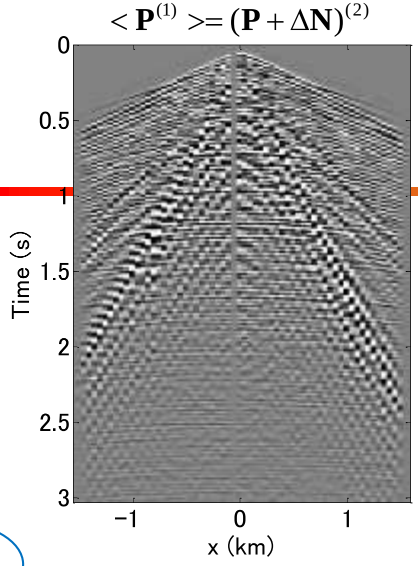

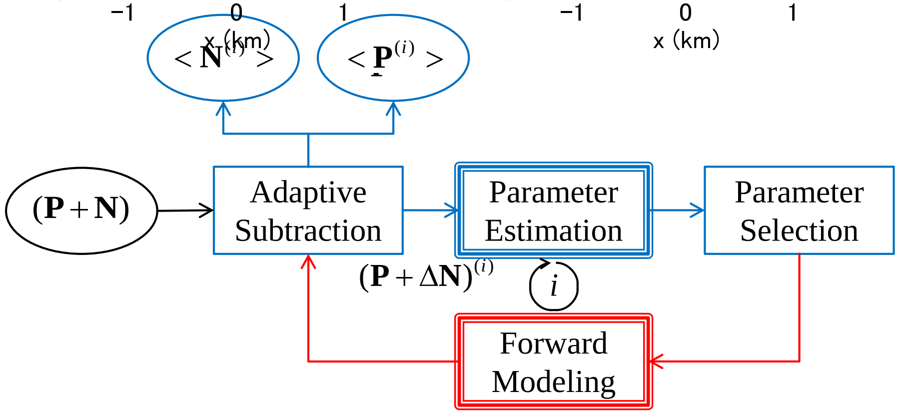

Go to the next loop, etc., etc…

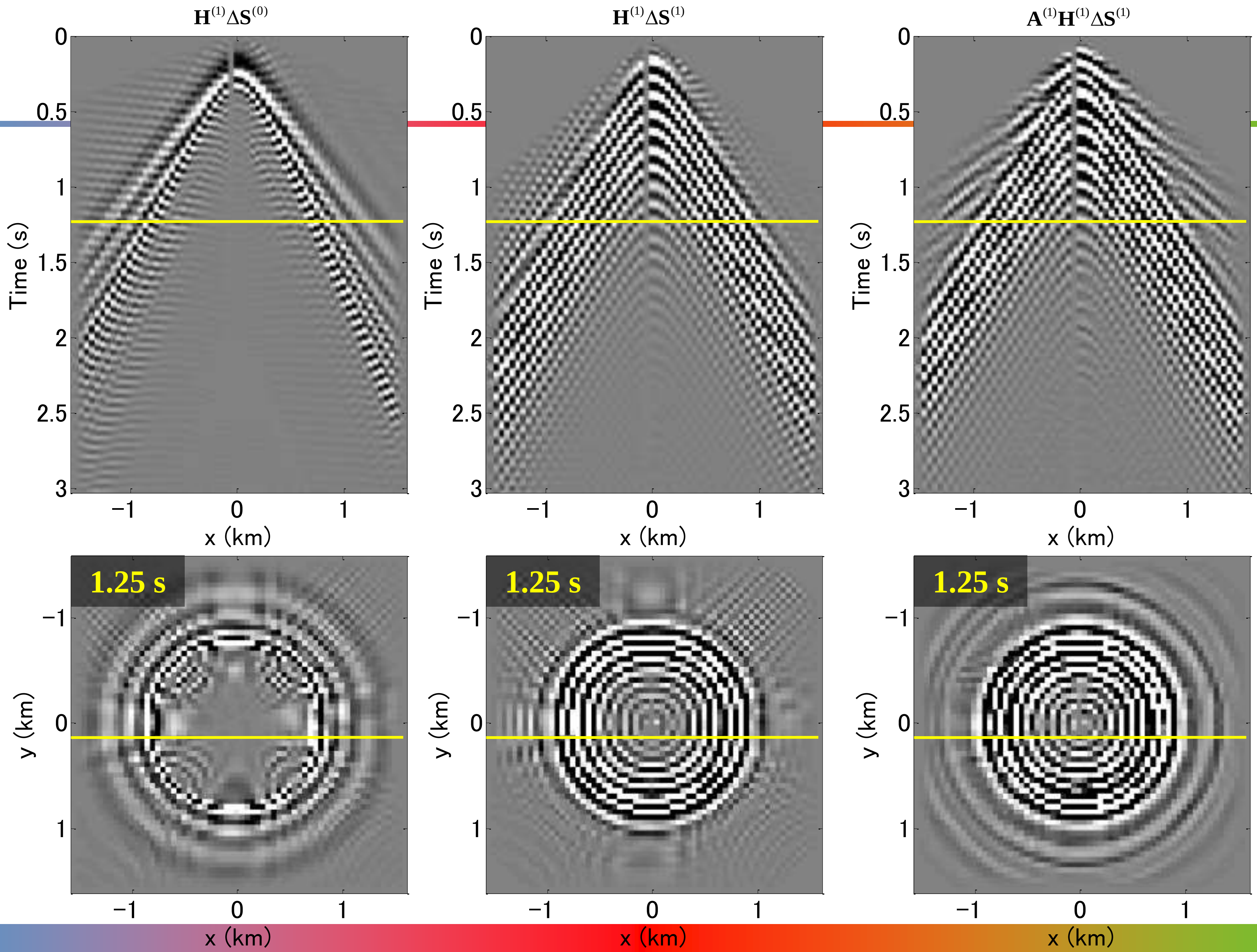

Delphi

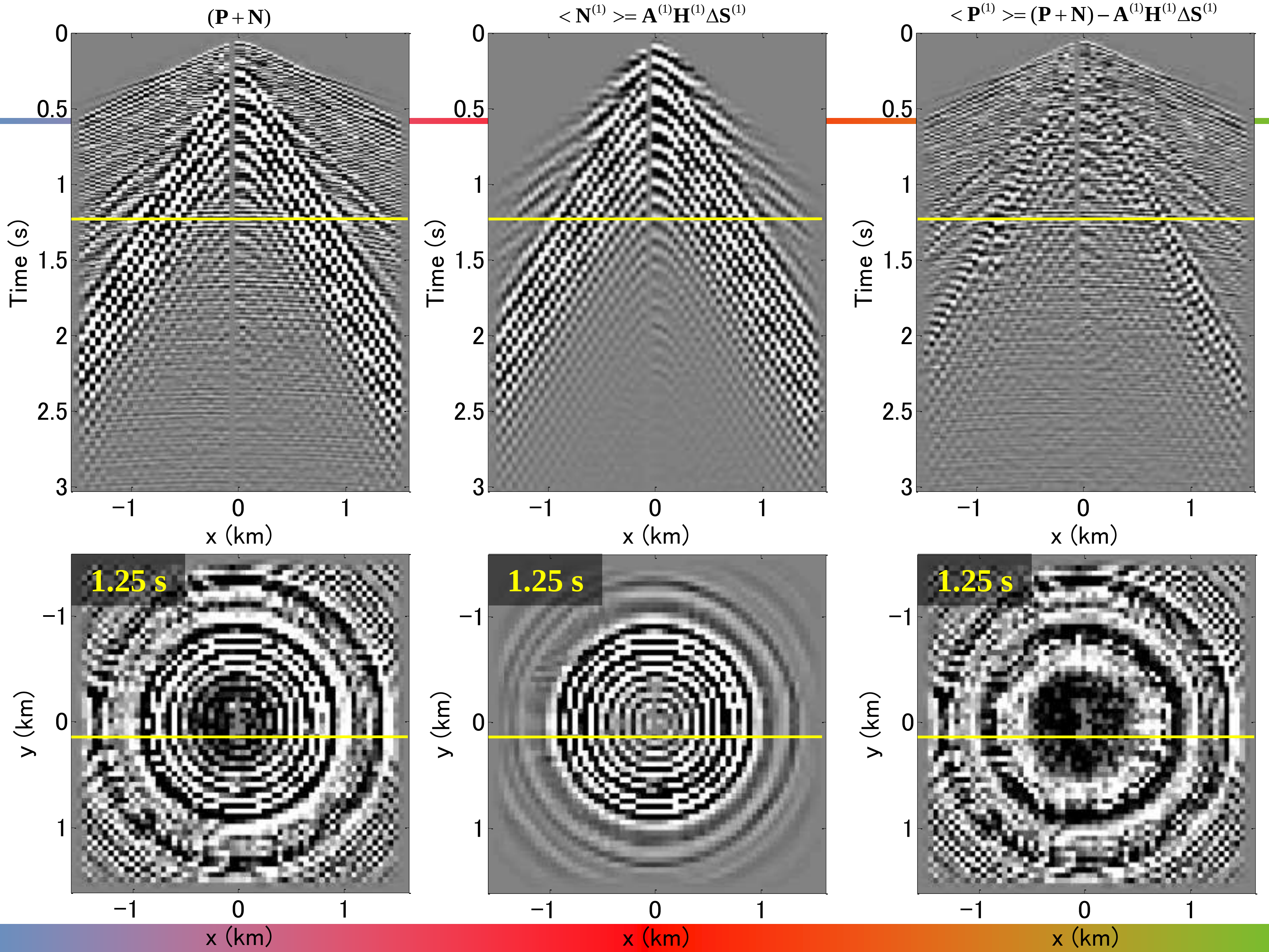
(P + N)
< N^(1) >= A^(1)H^(1)ΔS^(1)
< P^(1) >= (P + N) − A^(1)H^(1)ΔS^(1)
Time (s)
x (km)
y (km)
1.25 s

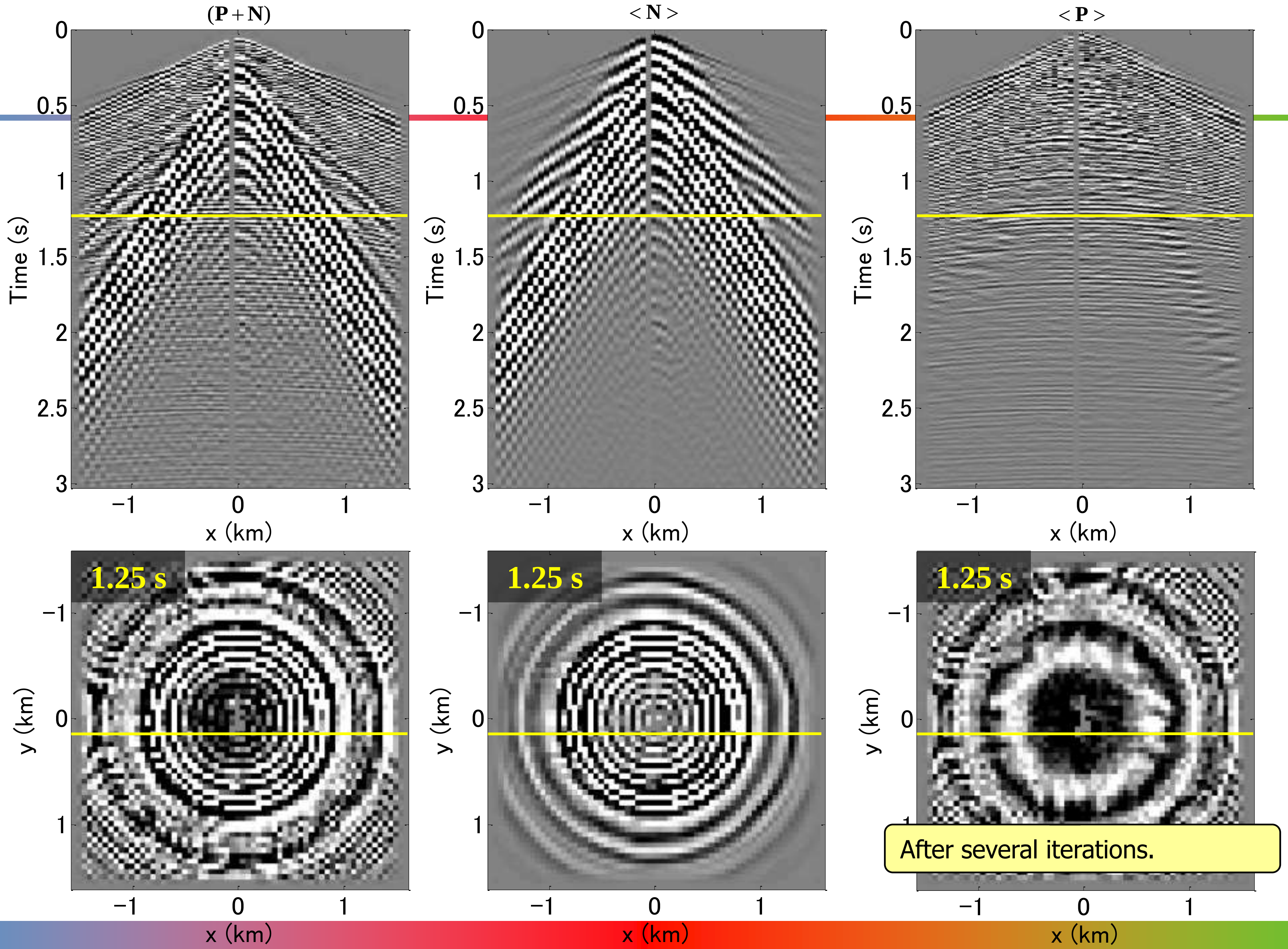
(P + N)
< N >
< P >
Time (s)
x (km)
y (km)
1.25 s
After several iterations.

Methods of surface-wave separation

- Slowness/velocity-based filtering methods
  (e.g. Yilmaz, 2001)
- Data-driven, data-adaptive and model-based method
  (AROGA; Le Meur et al., 2008, 2010)
- Data-driven, data-adaptive and model-based method using an iterative closed loop
  (SWES+; Ishiyama et al., 2014, 2015)
- Near-surface model-based method
  (SWAMI; Strobbia *et al.*, 2010, 2011)
- FWI-based methods (e.g. Ernst, 2013)

Methods of surface-wave separation

- SWES+

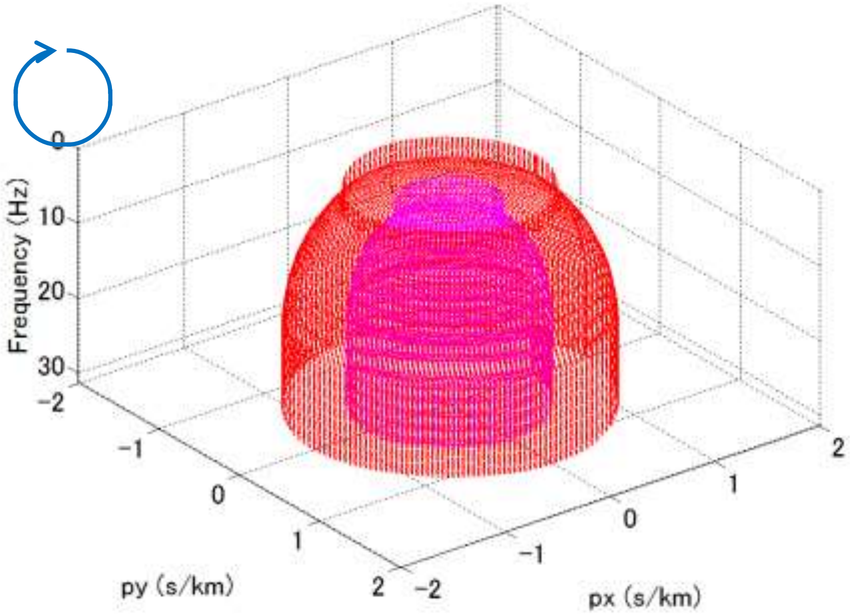

  - Simple (and robust) model
  - Parameterized by surface-wave properties: few parameters
  - Data-adaptive
  - Computationally affordable

- FWI

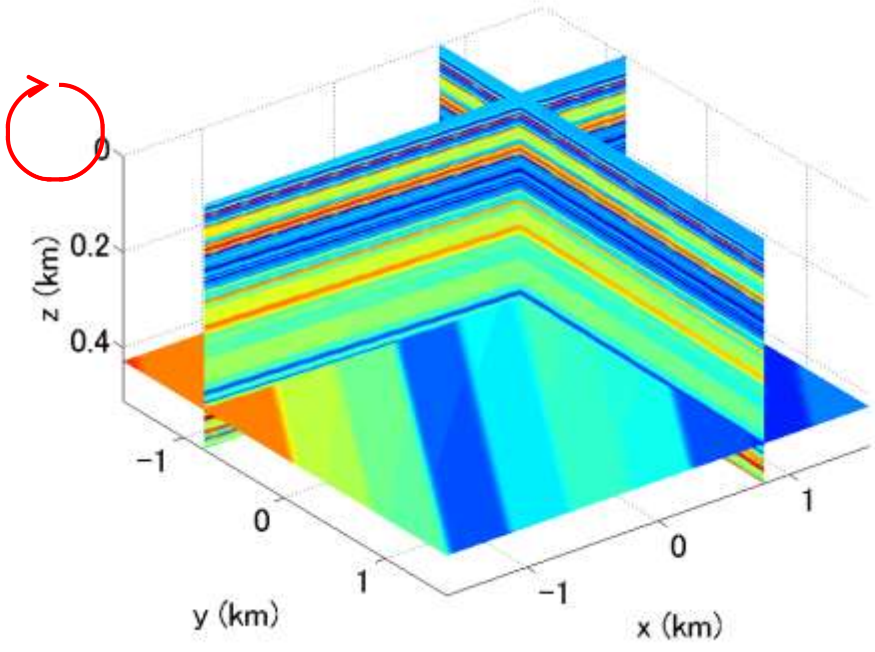

  - Complex (and sensitive) model
  - Parameterized by near-surface properties: many parameters
  - Computationally expensive

Outline

- Introduction
- Theory and method
- Real data examples
- Conclusions and remarks

Real data examples

- 3D land data acquired onshore Abu Dhabi
  (1) Less-aliased vertical geophone data
  (2) More-aliased vertical geophone data

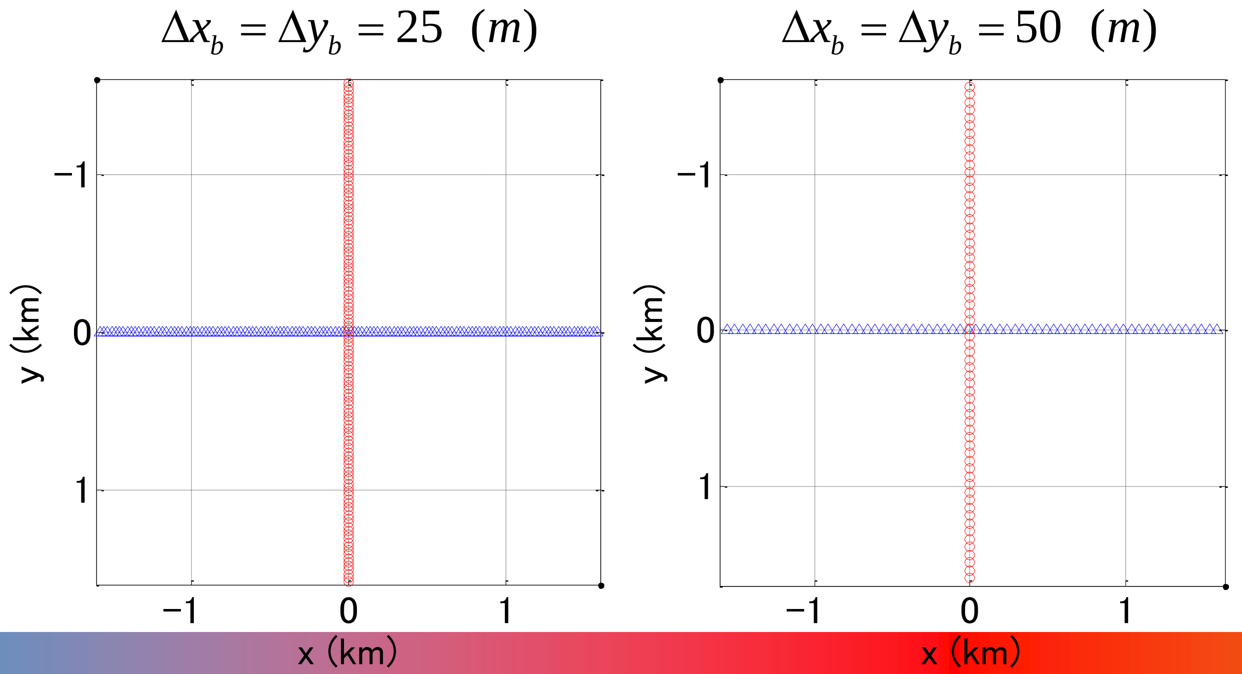

Receiver:
Arrayed geophones

Source:
Vibroseis with 6 Hz to 80 Hz linear sweep

Some aliased energy exists even around small wavenumbers.

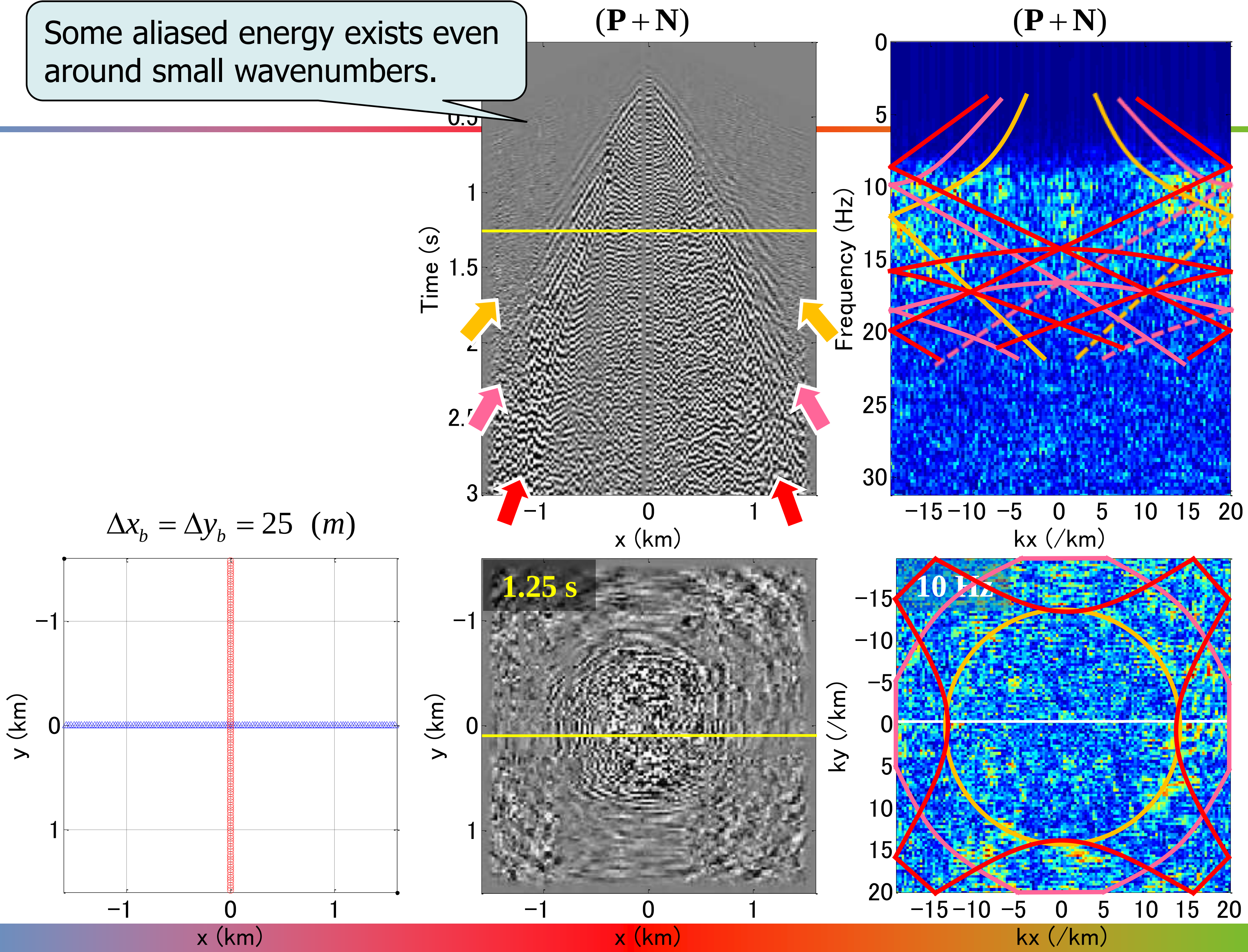

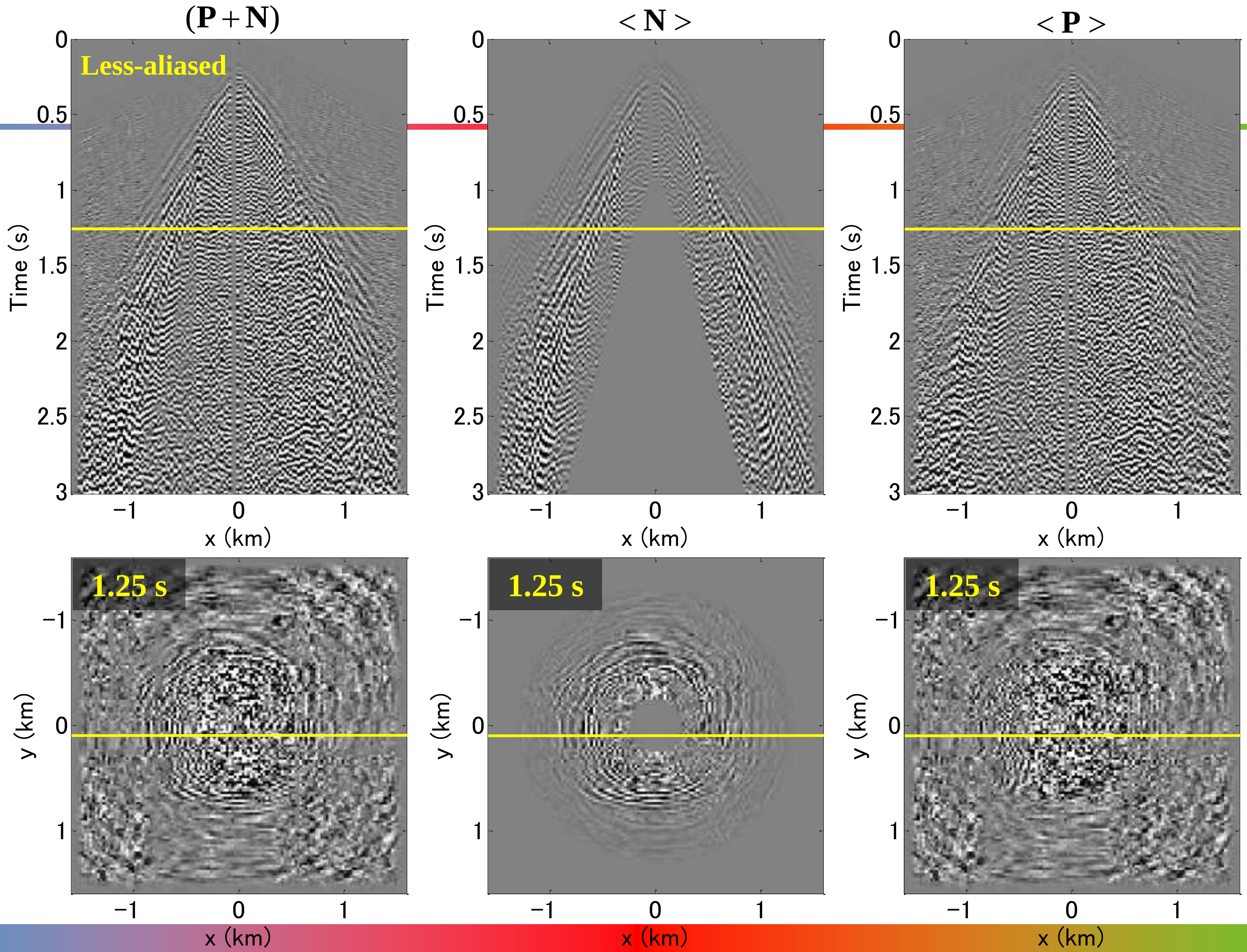
(P + N)
< N >
< P >
Less-aliased
Time (s)
x (km)
1.25 s
y (km)
x (km)

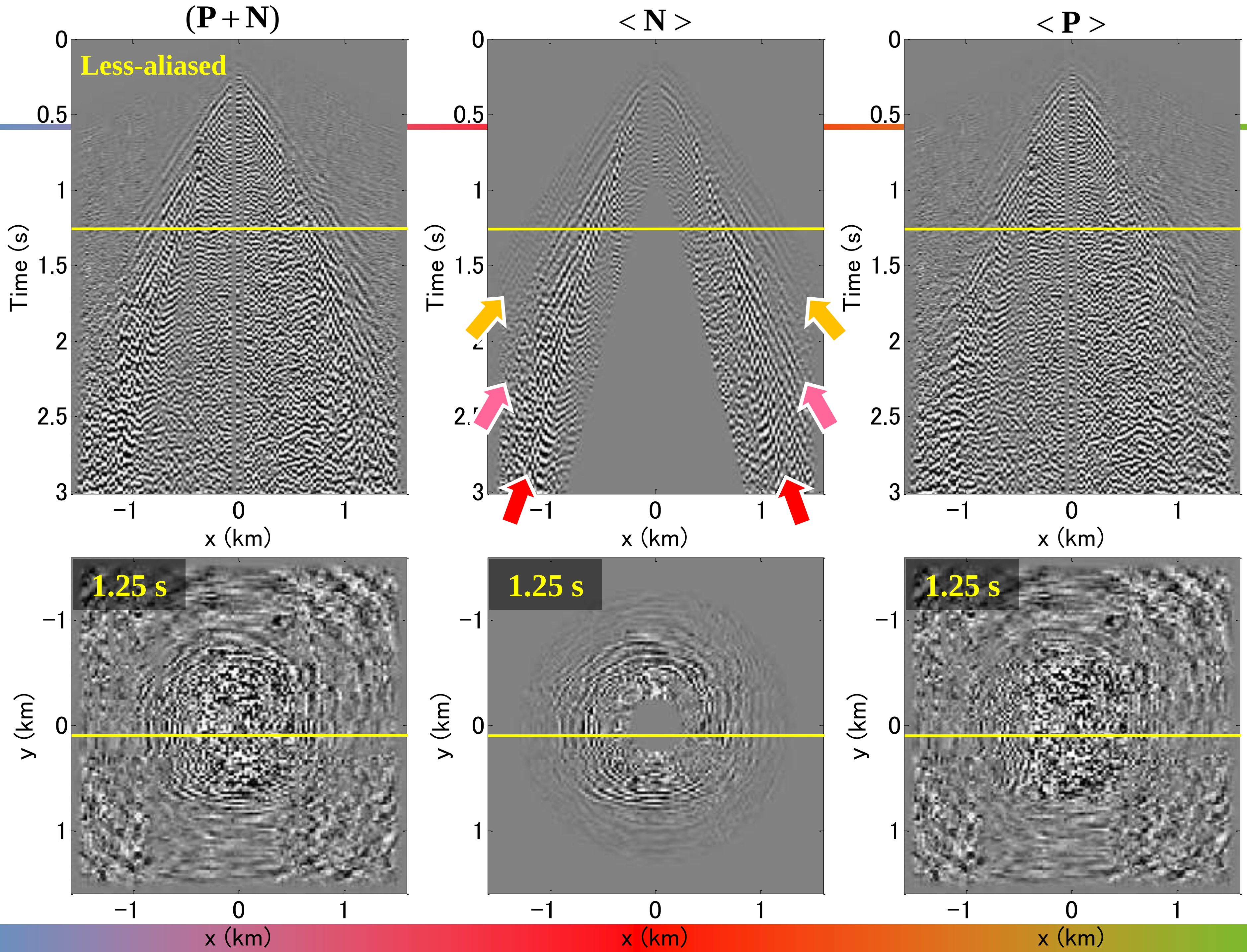
(P + N)
< N >
< P >
Less-aliased
Time (s)
x (km)
y (km)
1.25 s

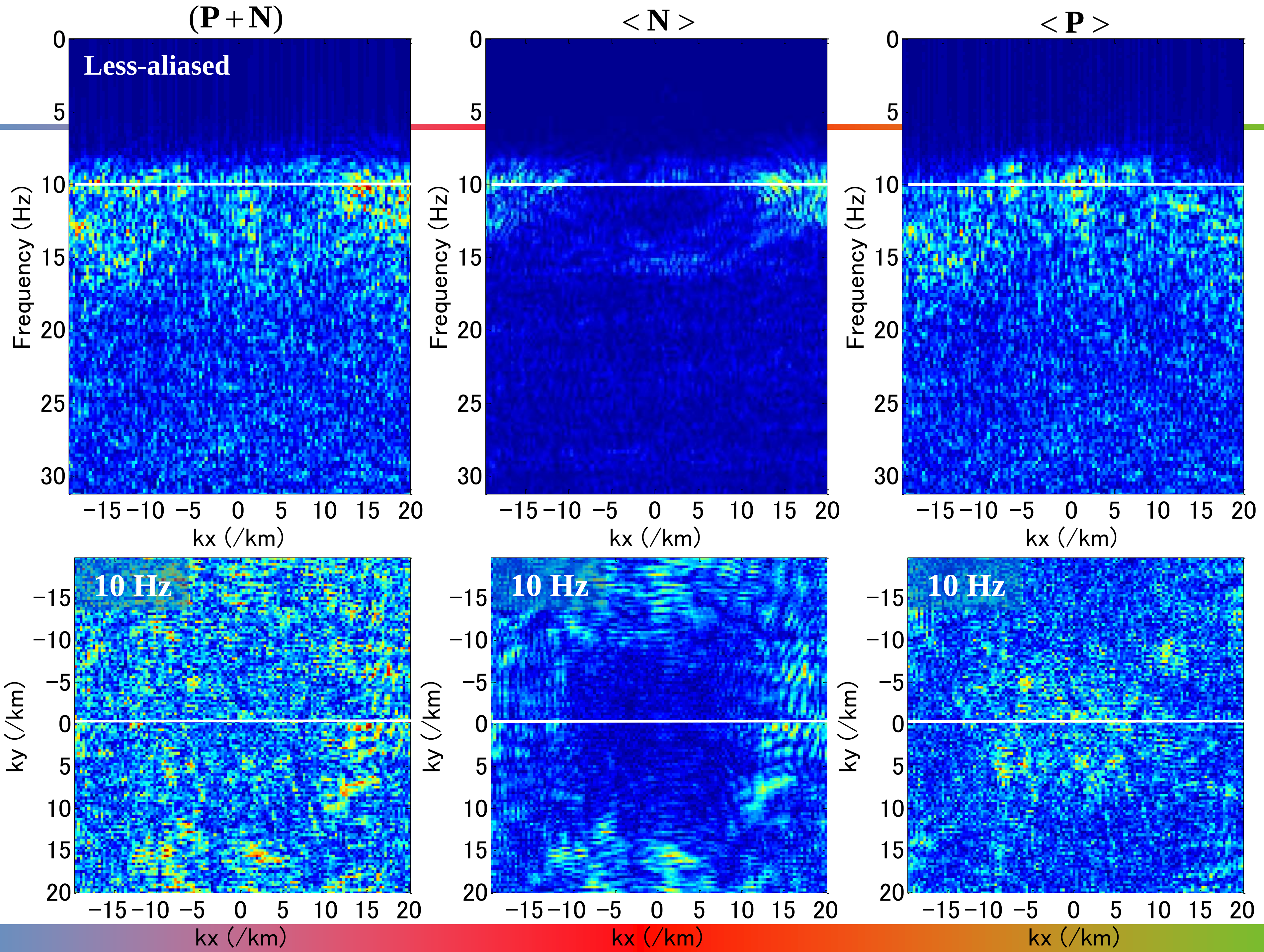
(P + N)
< N >
< P >
Less-aliased
10 Hz
10 Hz
10 Hz
Frequency (Hz)
kx (/km)
ky (/km)

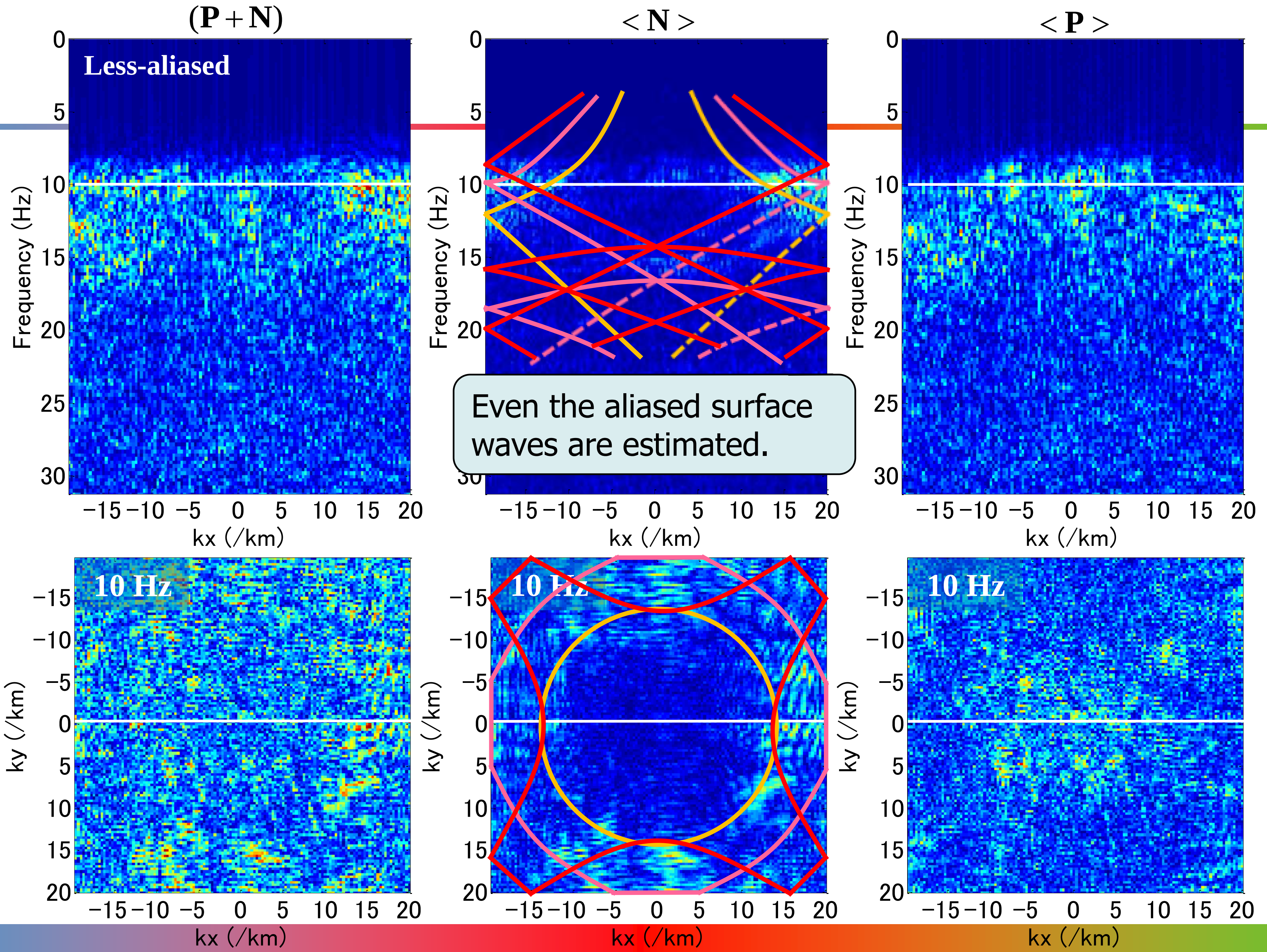
(P + N)
< N >
< P >
Less-aliased
Frequency (Hz)
kx (/km)
10 Hz
ky (/km)
Even the aliased surface waves are estimated.

Only aliased energy exists in the whole range of useful frequencies.

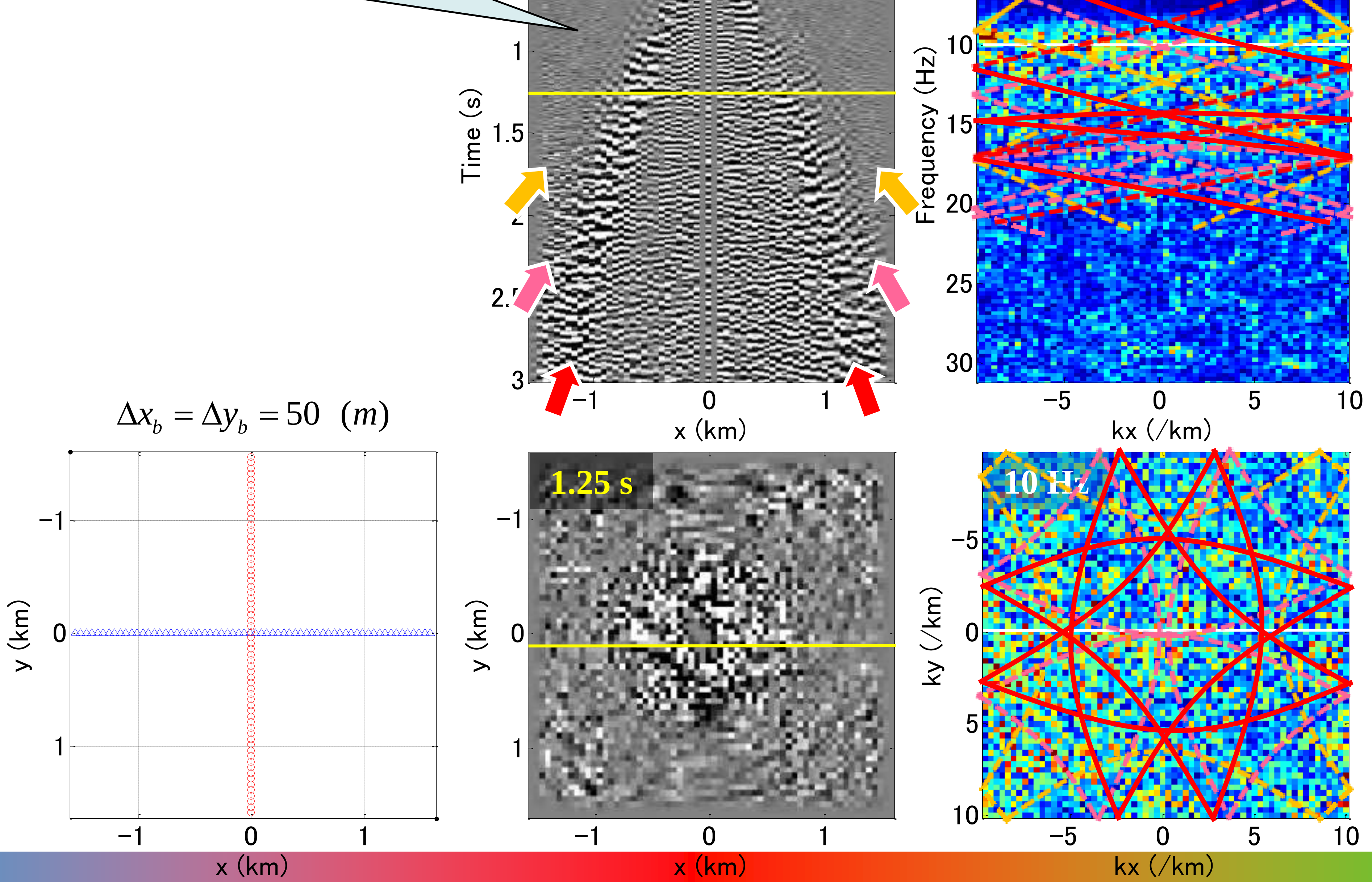

Delphi

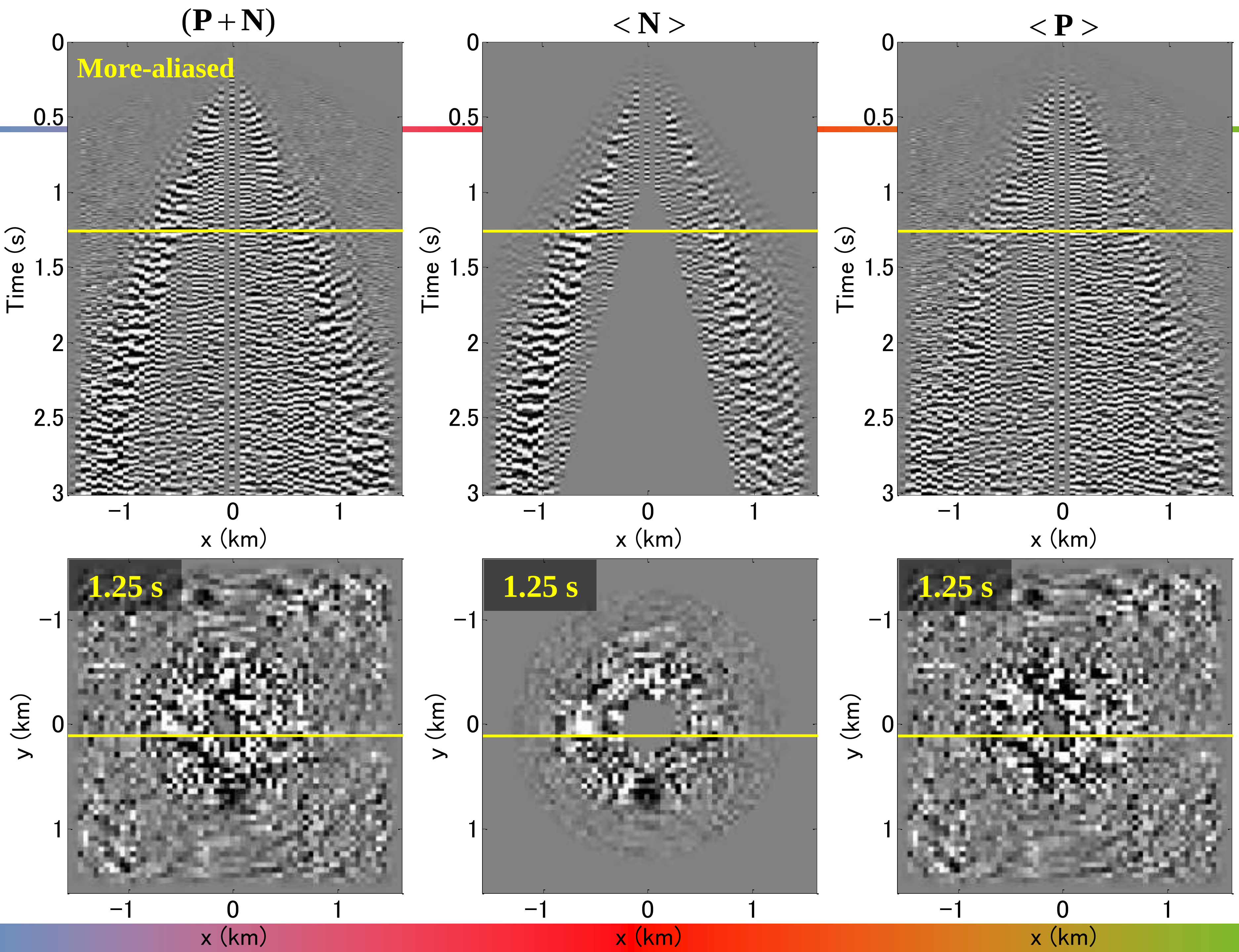
(P + N)
< N >
< P >
More-aliased
1.25 s
1.25 s
1.25 s
Time (s)
x (km)
y (km)
Delphi

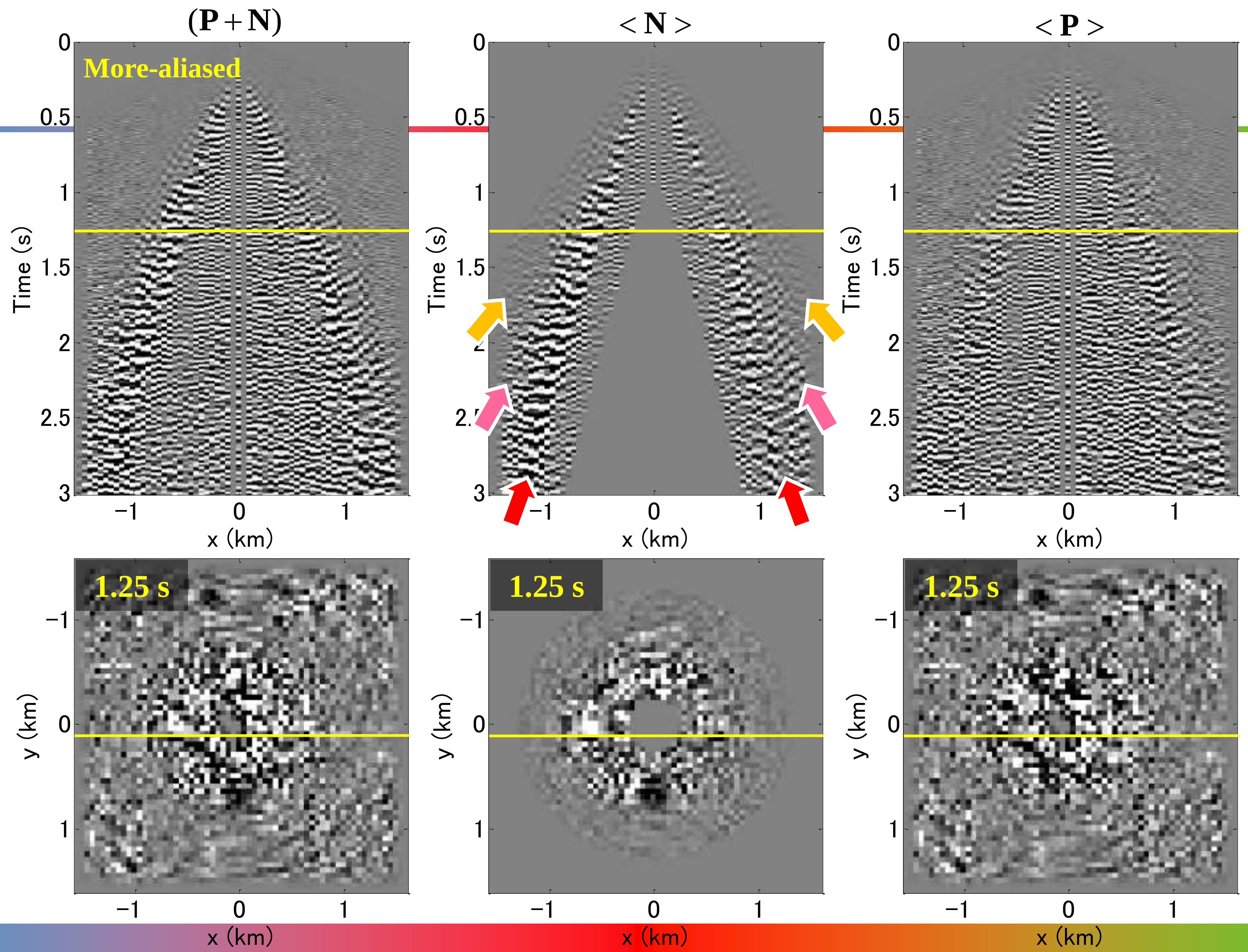

(P + N)
< N >
< P >
More-aliased
Time (s)
x (km)
y (km)
1.25 s

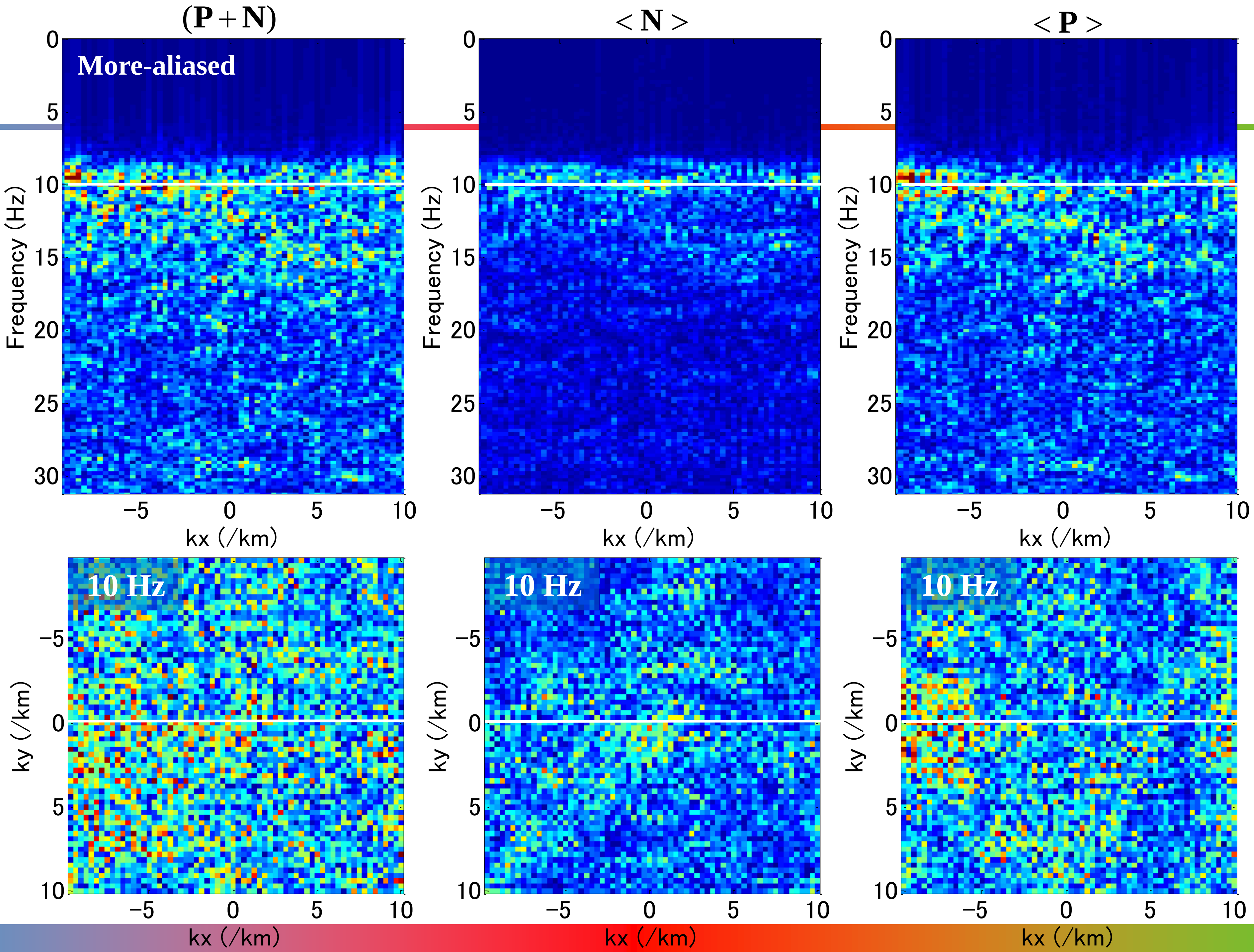
(P + N)
< N >
< P >
More-aliased
Frequency (Hz)
kx (/km)
ky (/km)
10 Hz
10 Hz
10 Hz

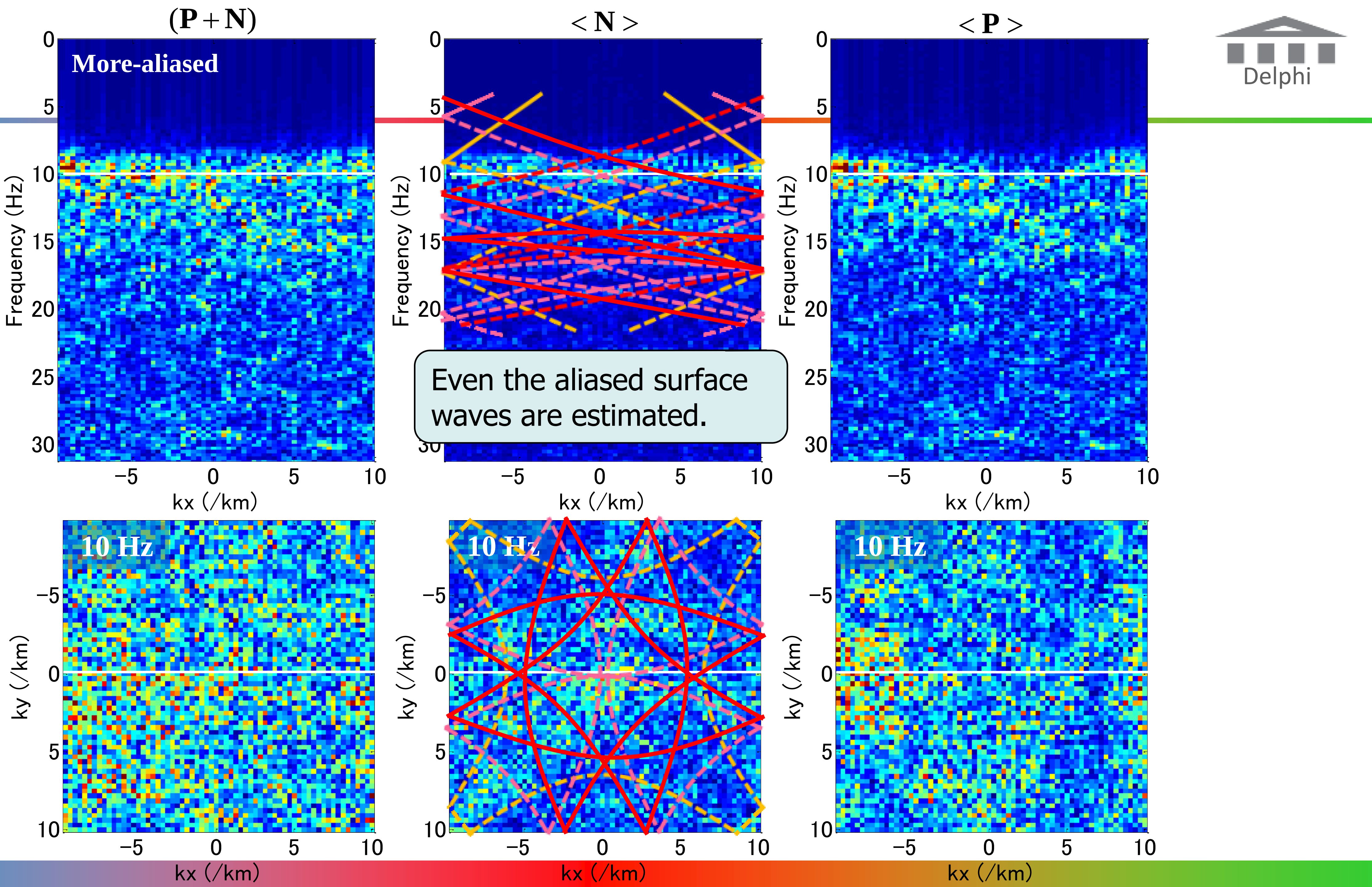

Even the aliased surface waves are estimated.

Real data examples

- 3D OBC data acquired offshore Abu Dhabi
  (1) Un-aliased hydrophone data
  (2) Aliased hydrophone data
  (2)' The above data with a conventional filtering method

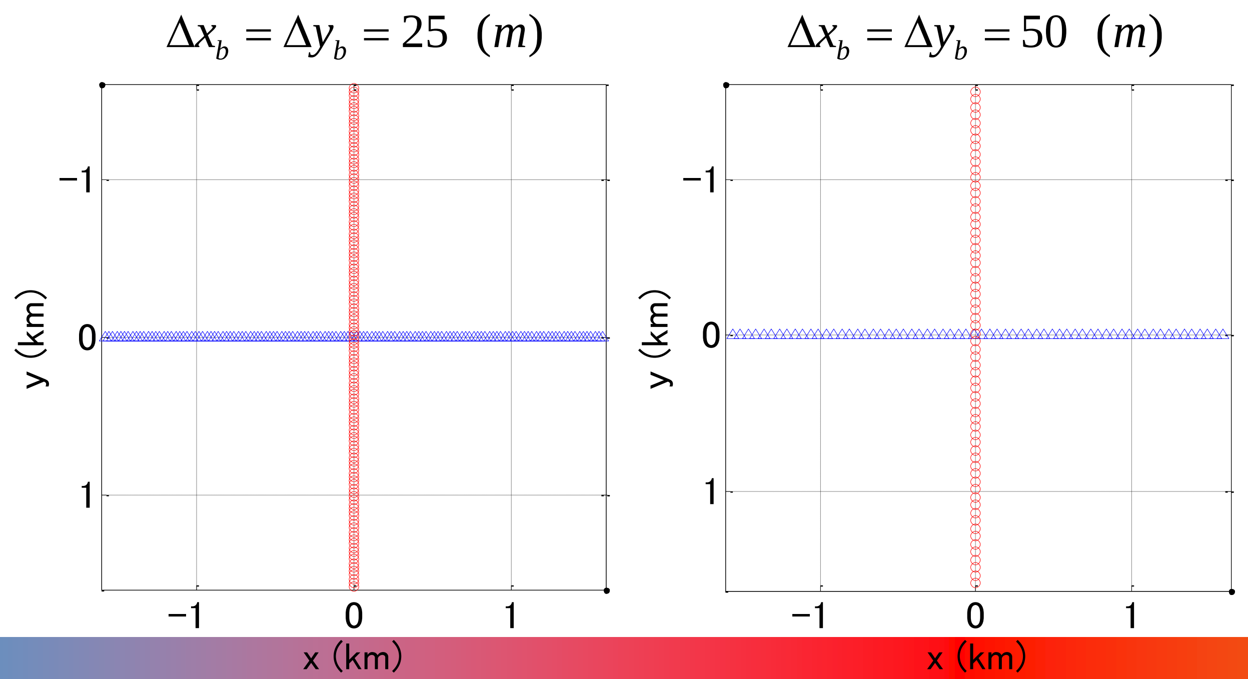

Receiver:
Single point hydrophone

Source:
Arrayed air-guns

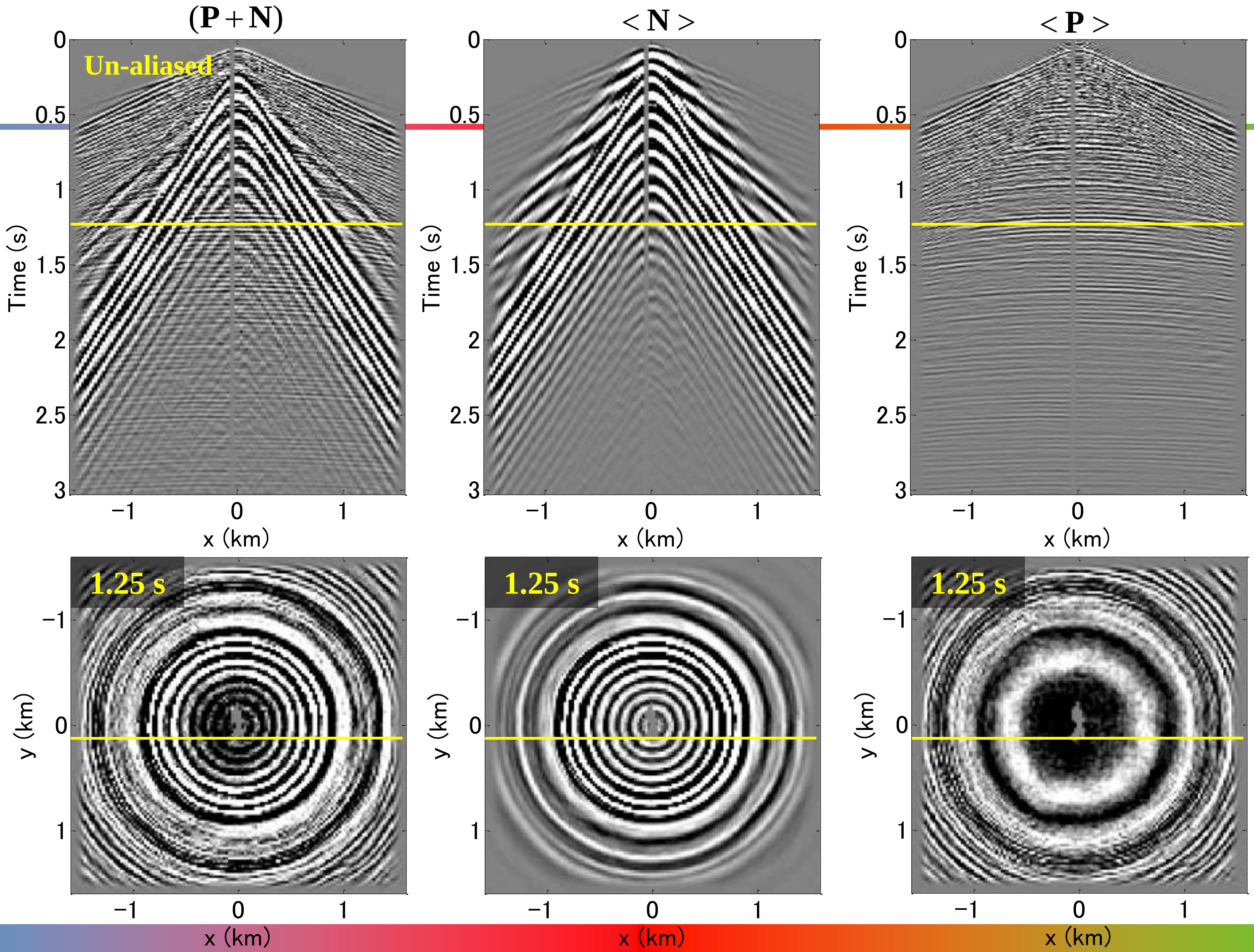

(P + N)
< N >
< P >
Un-aliased
Time (s)
x (km)
1.25 s
y (km)

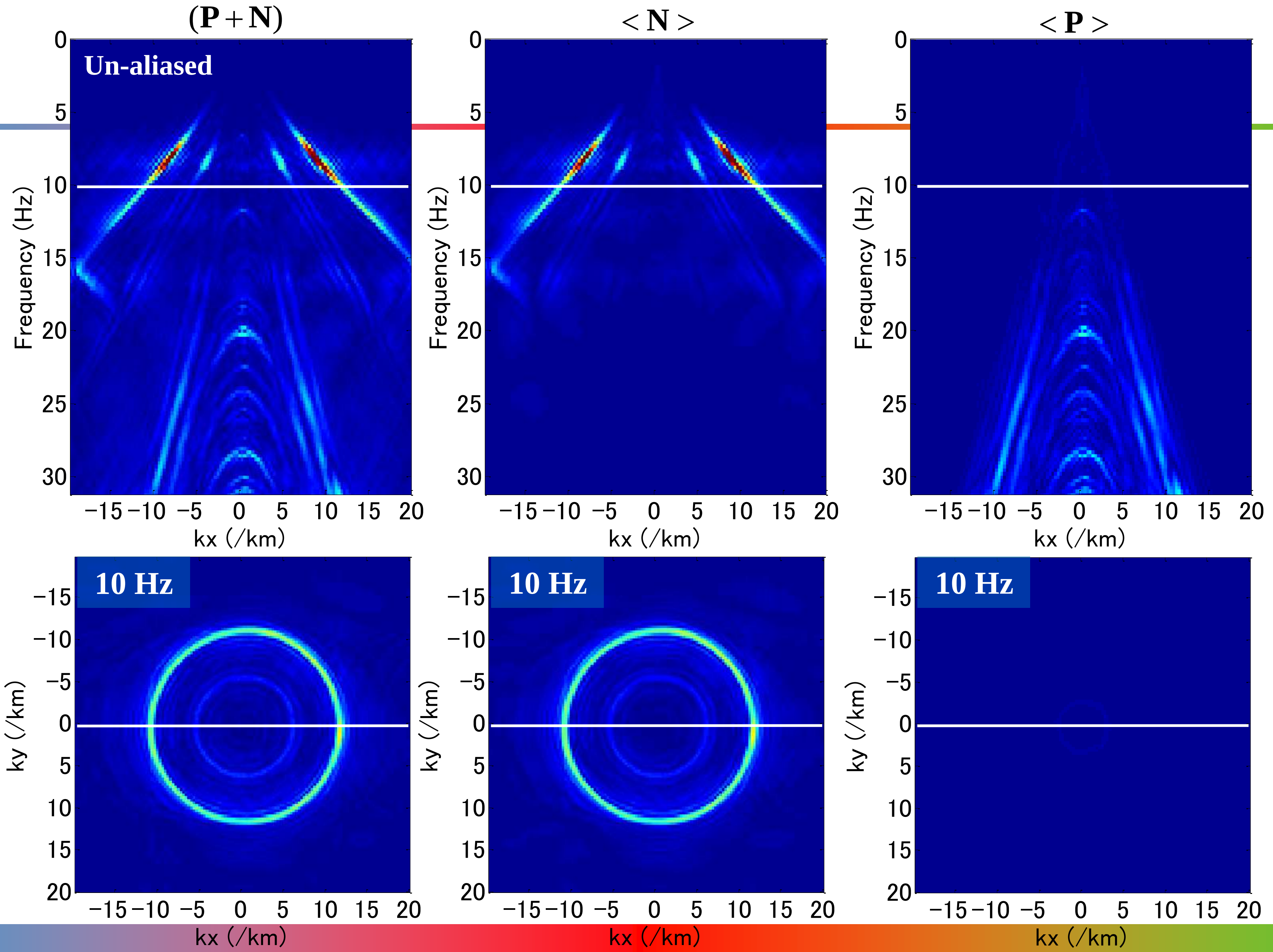
(P + N)
< N >
< P >
Un-aliased
Frequency (Hz)
kx (/km)
10 Hz
ky (/km)

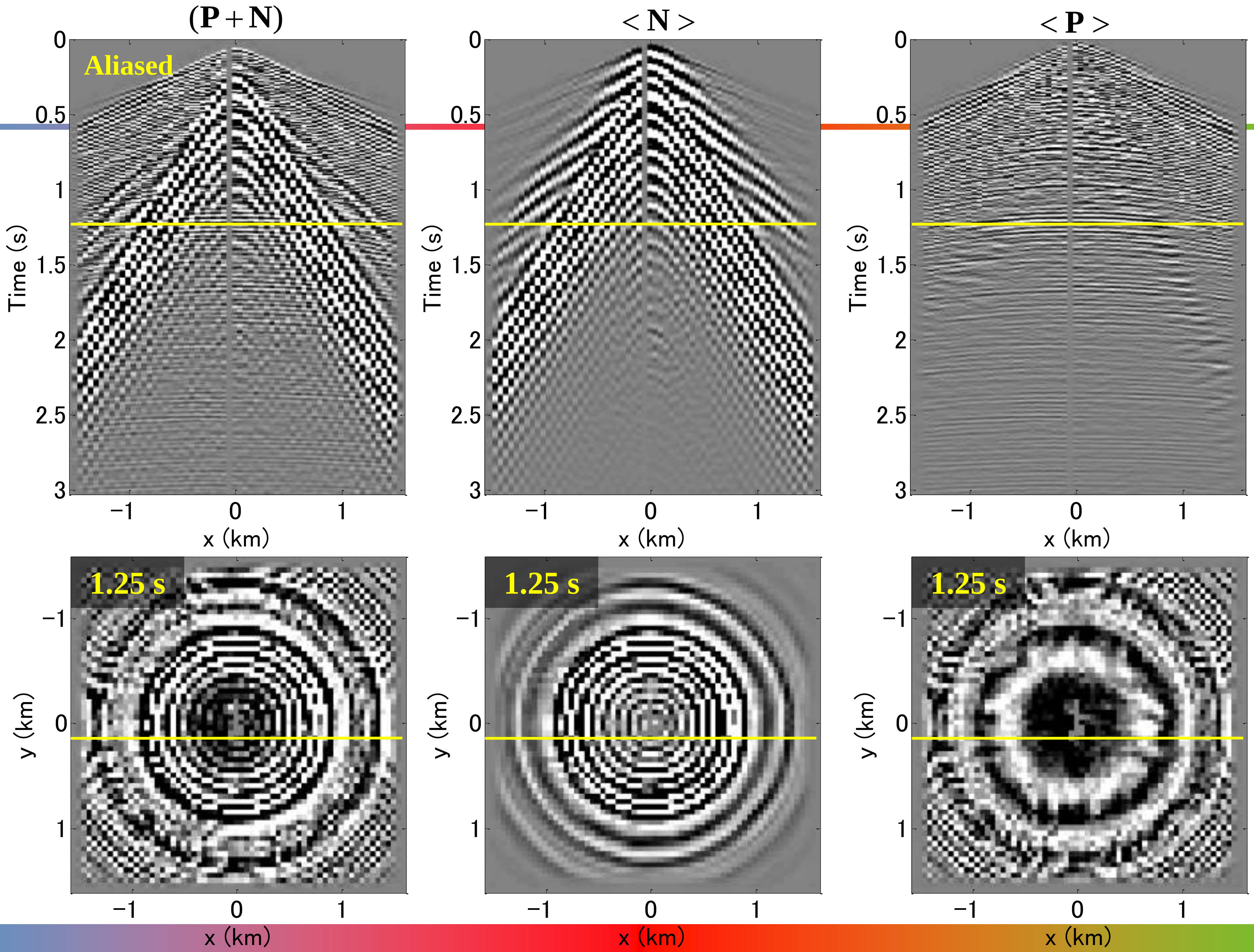
(P + N)
< N >
< P >
Aliased
Time (s)
x (km)
y (km)
1.25 s

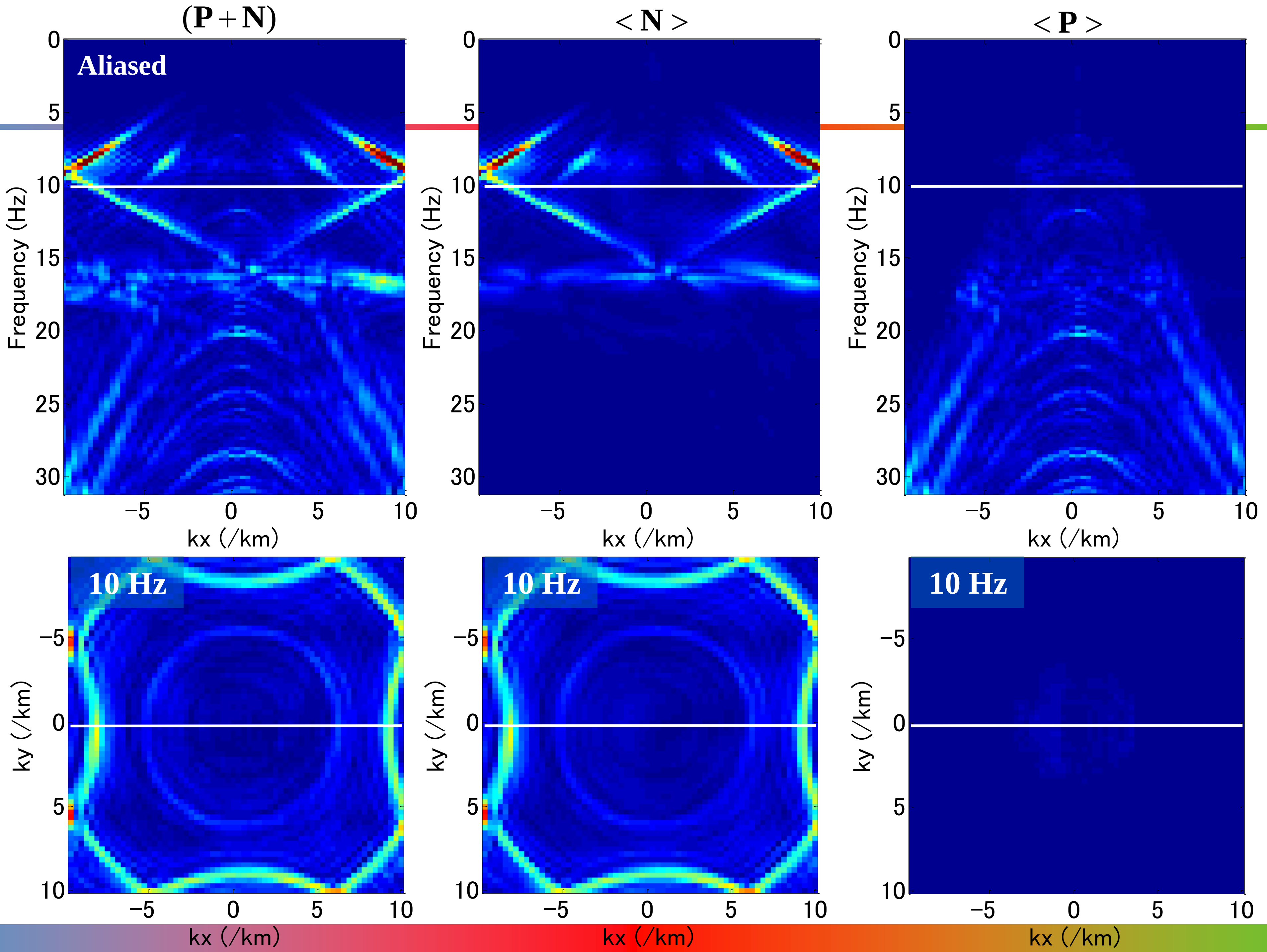
(P + N)
< N >
< P >
Aliased
10 Hz
10 Hz
10 Hz
Frequency (Hz)
kx (/km)
ky (/km)

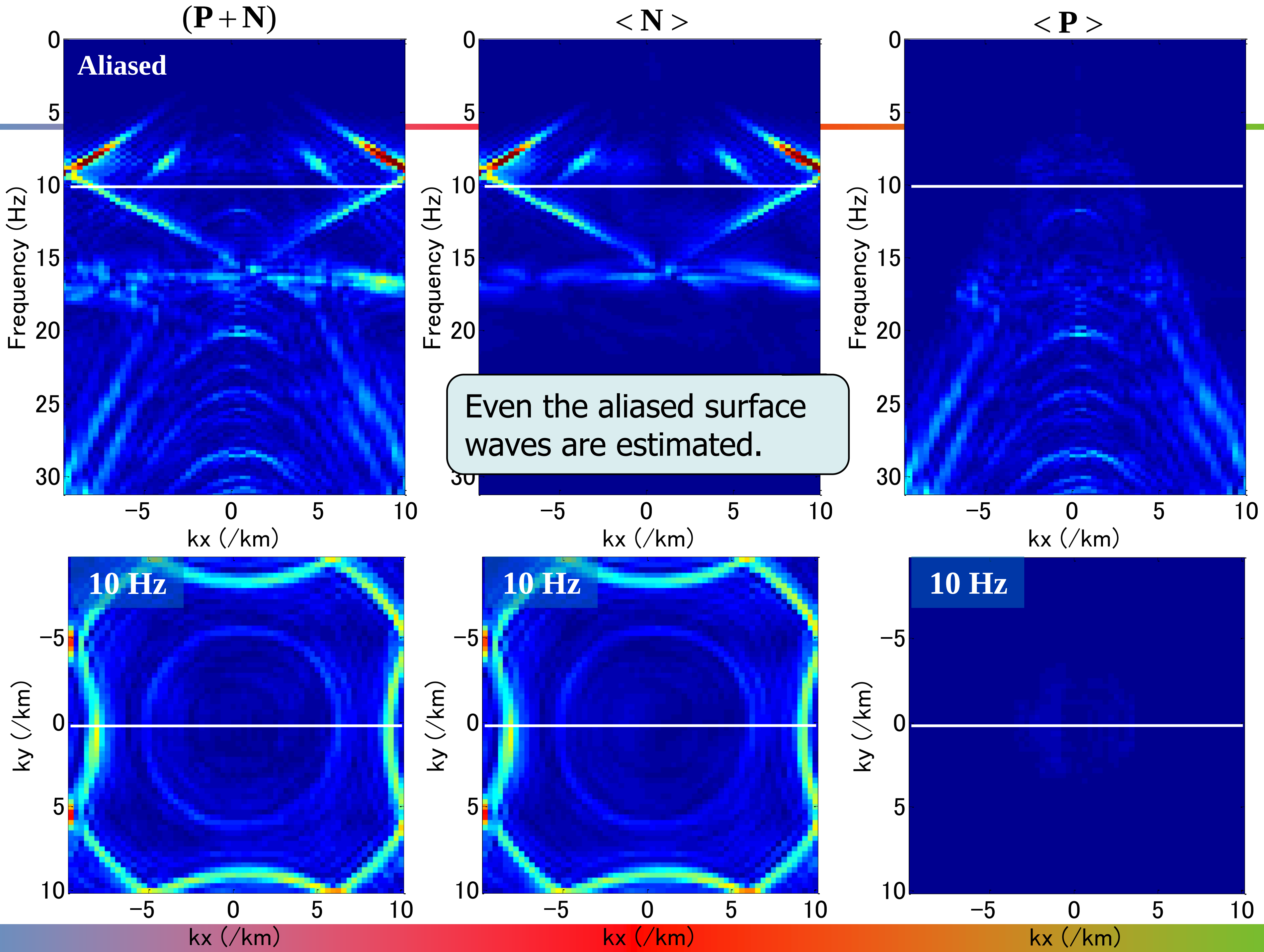

Even the aliased surface waves are estimated.

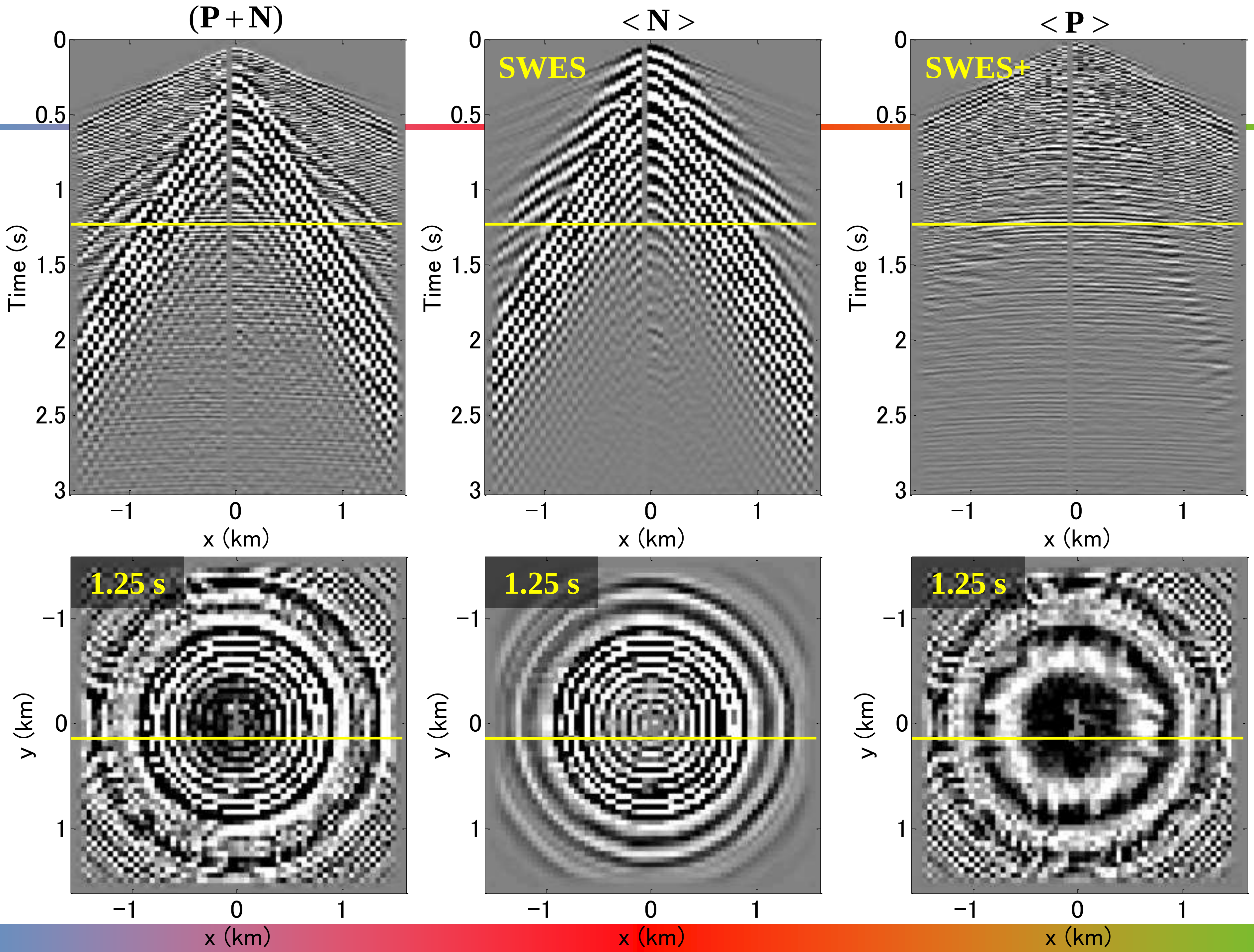
(P + N)
< N >
< P >
SWES
SWES+
Time (s)
x (km)
1.25 s
y (km)

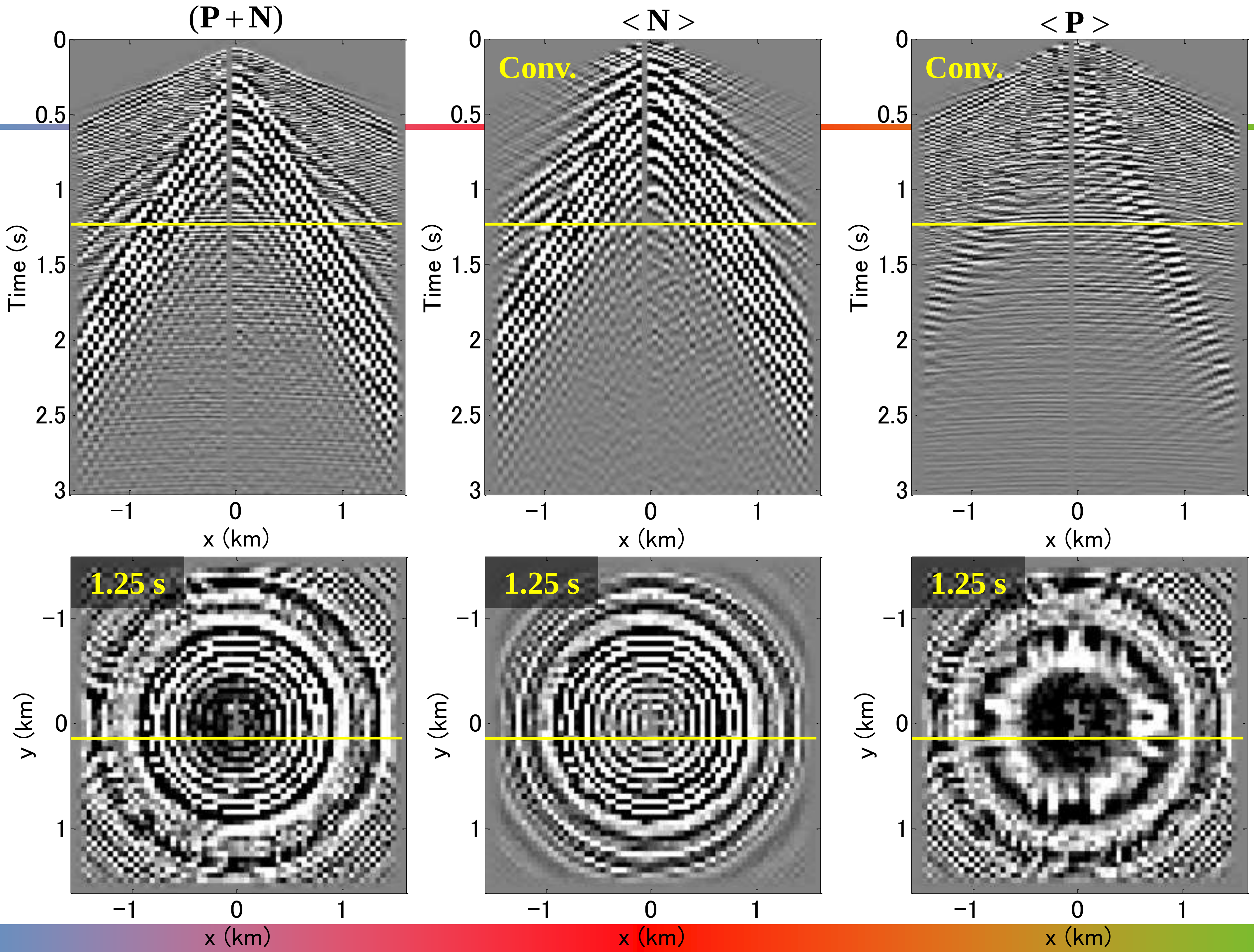
(P + N)
< N >
< P >
Conv.
Conv.
Time (s)
x (km)
1.25 s
1.25 s
1.25 s
y (km)
x (km)

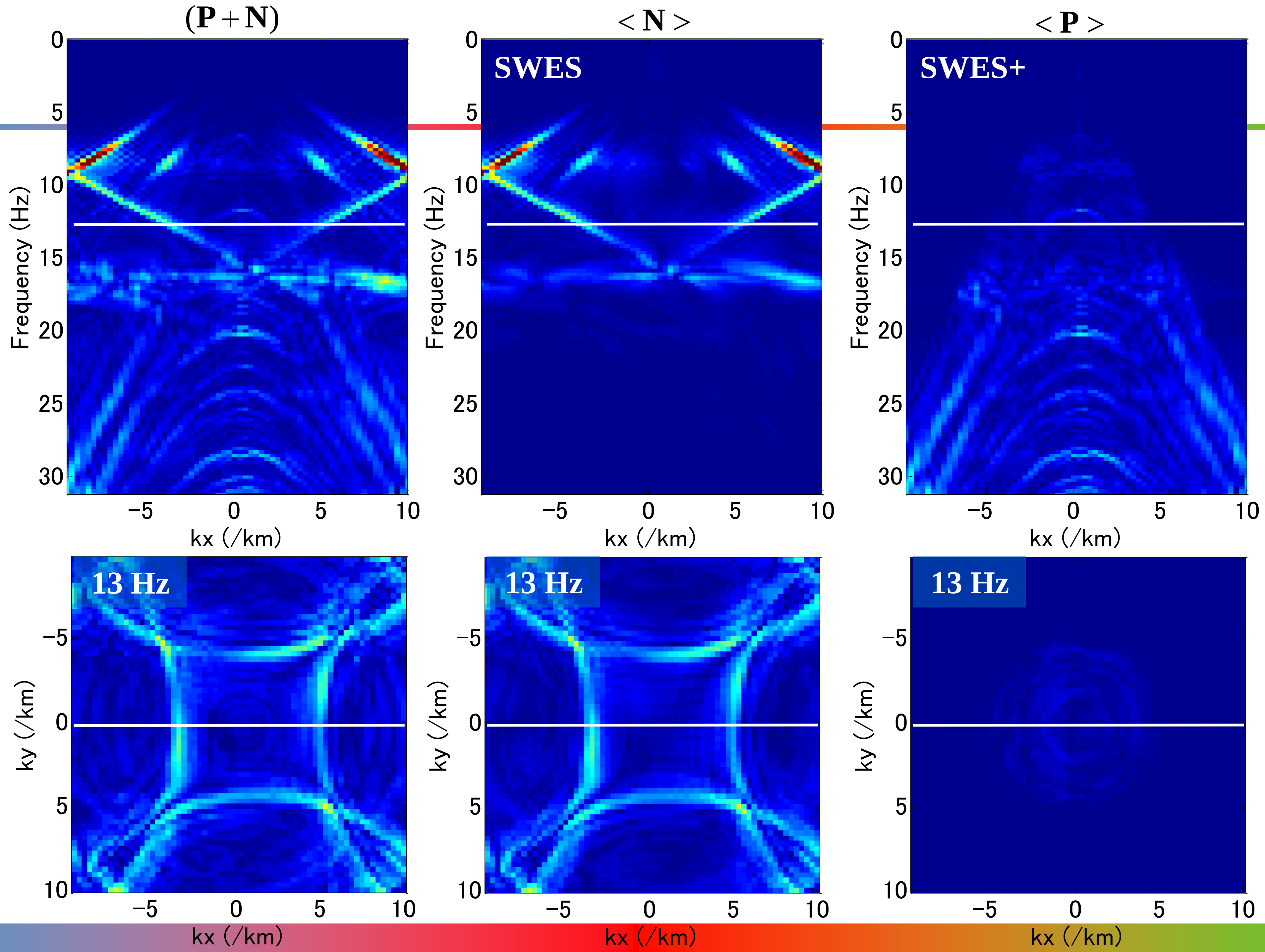
(P + N)
< N >
< P >
SWES
SWES+
Frequency (Hz)
kx (/km)
13 Hz
13 Hz
13 Hz
ky (/km)
kx (/km)
kx (/km)
kx (/km)

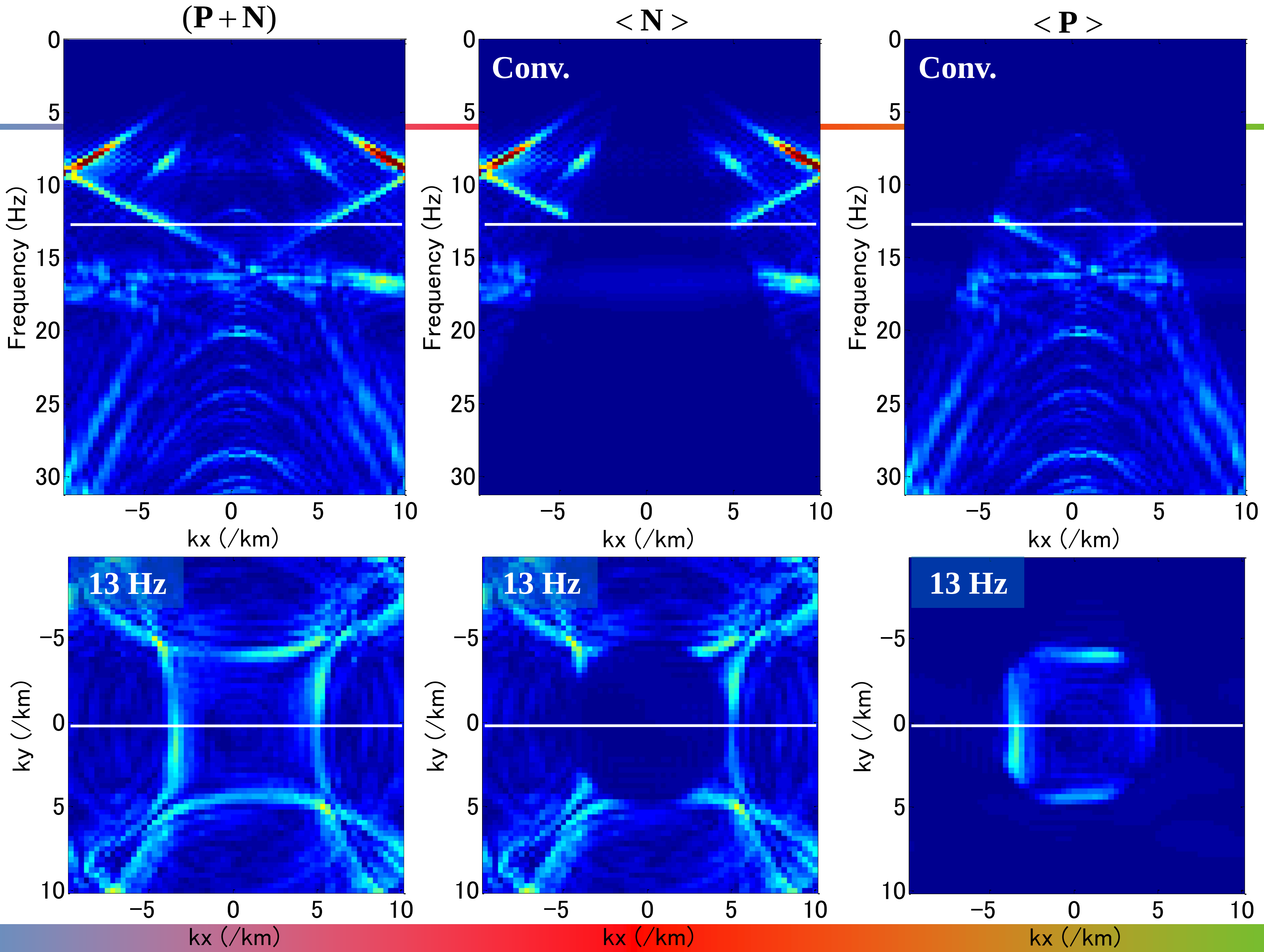
(P + N)
< N >
< P >
Conv.
Conv.
Frequency (Hz)
kx (/km)
13 Hz
13 Hz
13 Hz
ky (/km)
kx (/km)

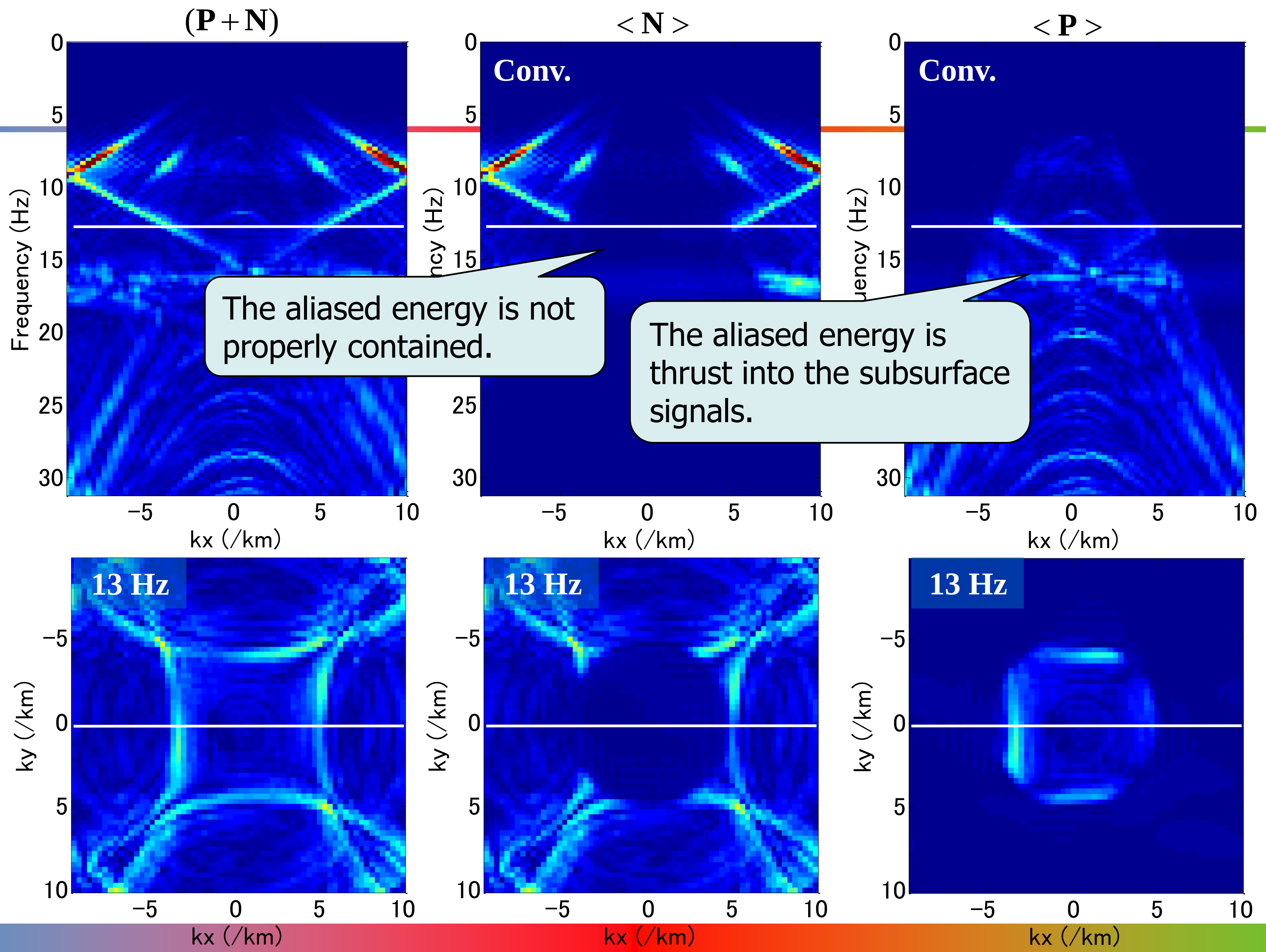
(P+N)
< N >
< P >
Conv.
Conv.
Frequency (Hz)
kx (/km)
ky (/km)
13 Hz
13 Hz
13 Hz
The aliased energy is not properly contained.
The aliased energy is thrust into the subsurface signals.

Real data examples

- 3D OBC data acquired offshore Abu Dhabi
  (1) Irregularly sampled hydrophone data
  (2) Blended hydrophone data

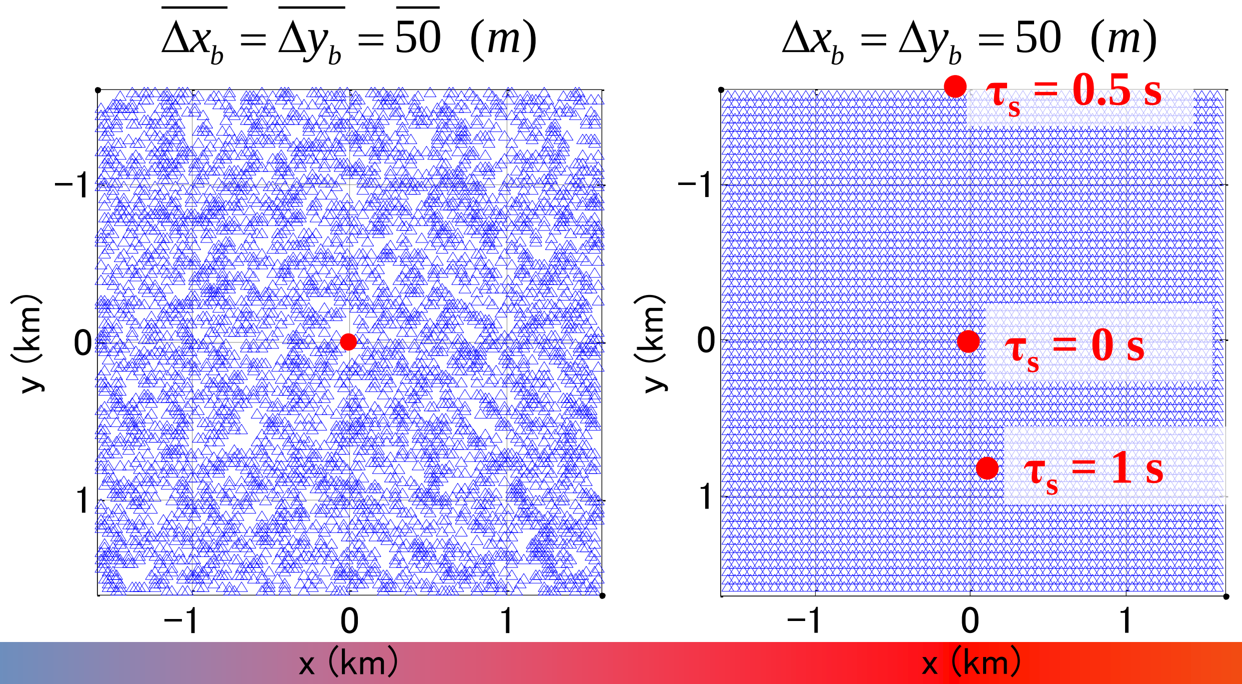

Receiver:
Single point hydrophone

Source:
Arrayed air-guns
as a single point source (1)
as a blended source (2)

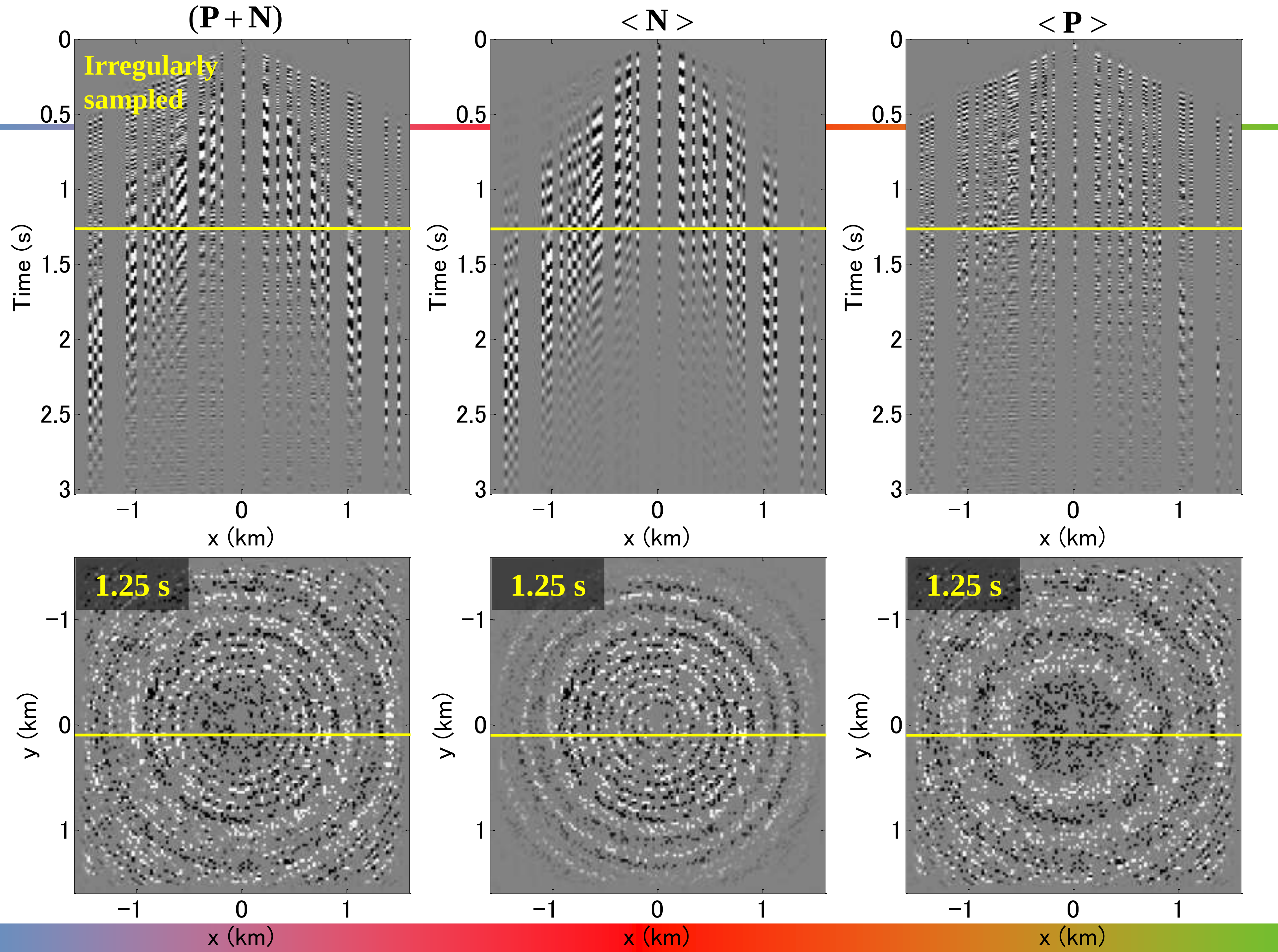

(P + N)
< N >
< P >
Irregularly sampled
Time (s)
x (km)
1.25 s
y (km)
Delphi

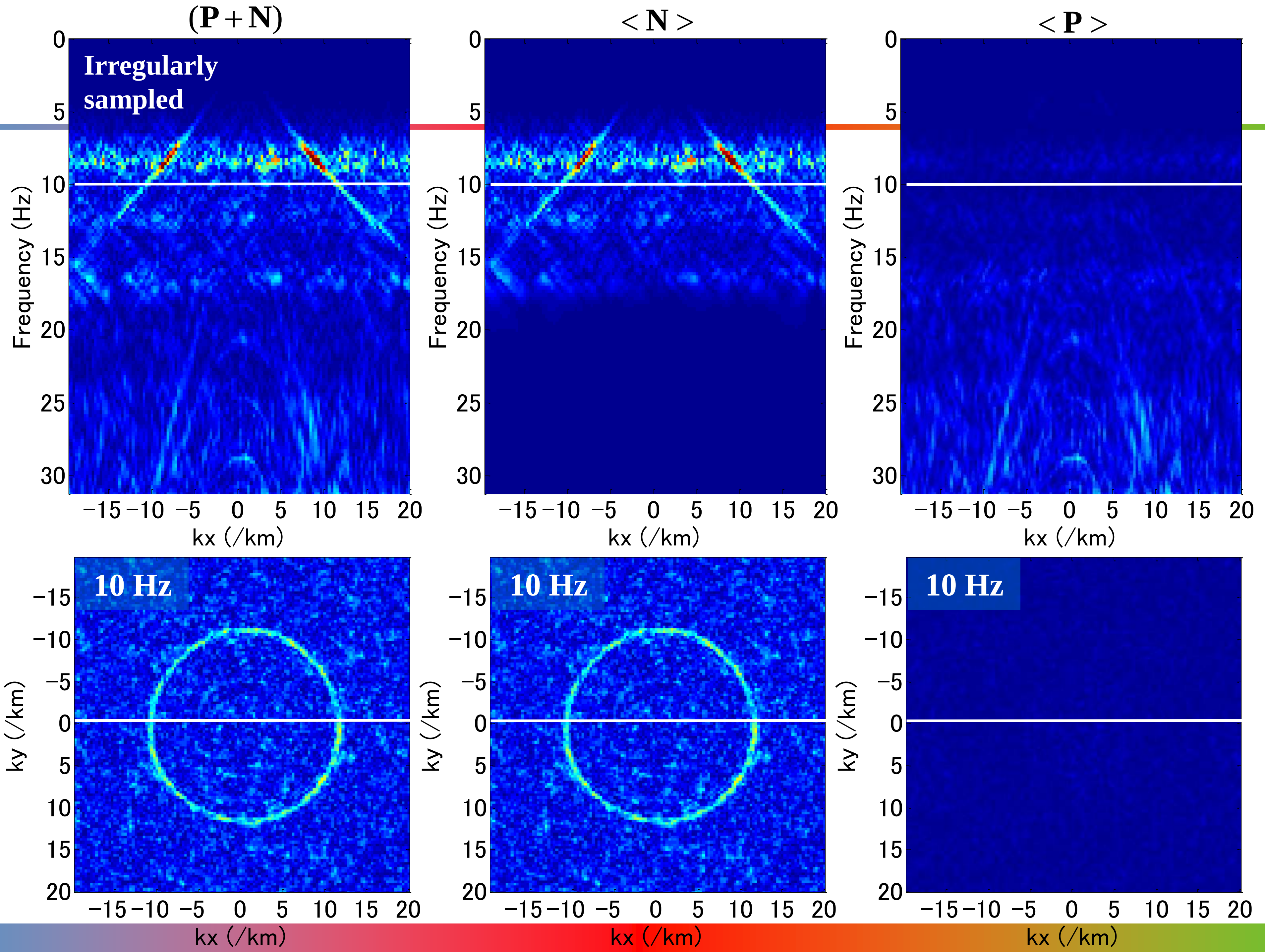

Delphi

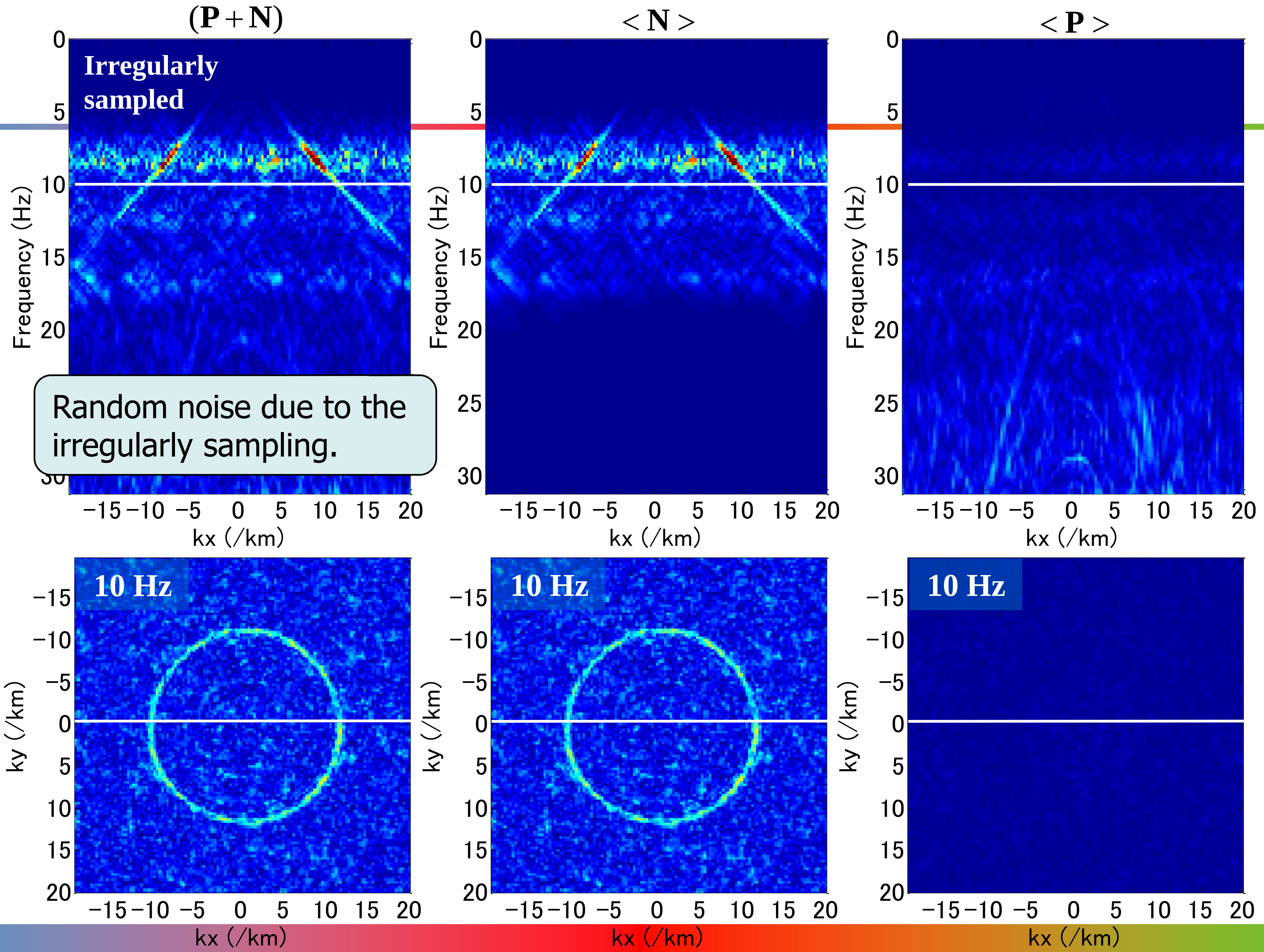

(P + N)
< N >
< P >
Irregularly sampled
Random noise due to the irregularly sampling.
Frequency (Hz)
kx (/km)
ky (/km)
10 Hz

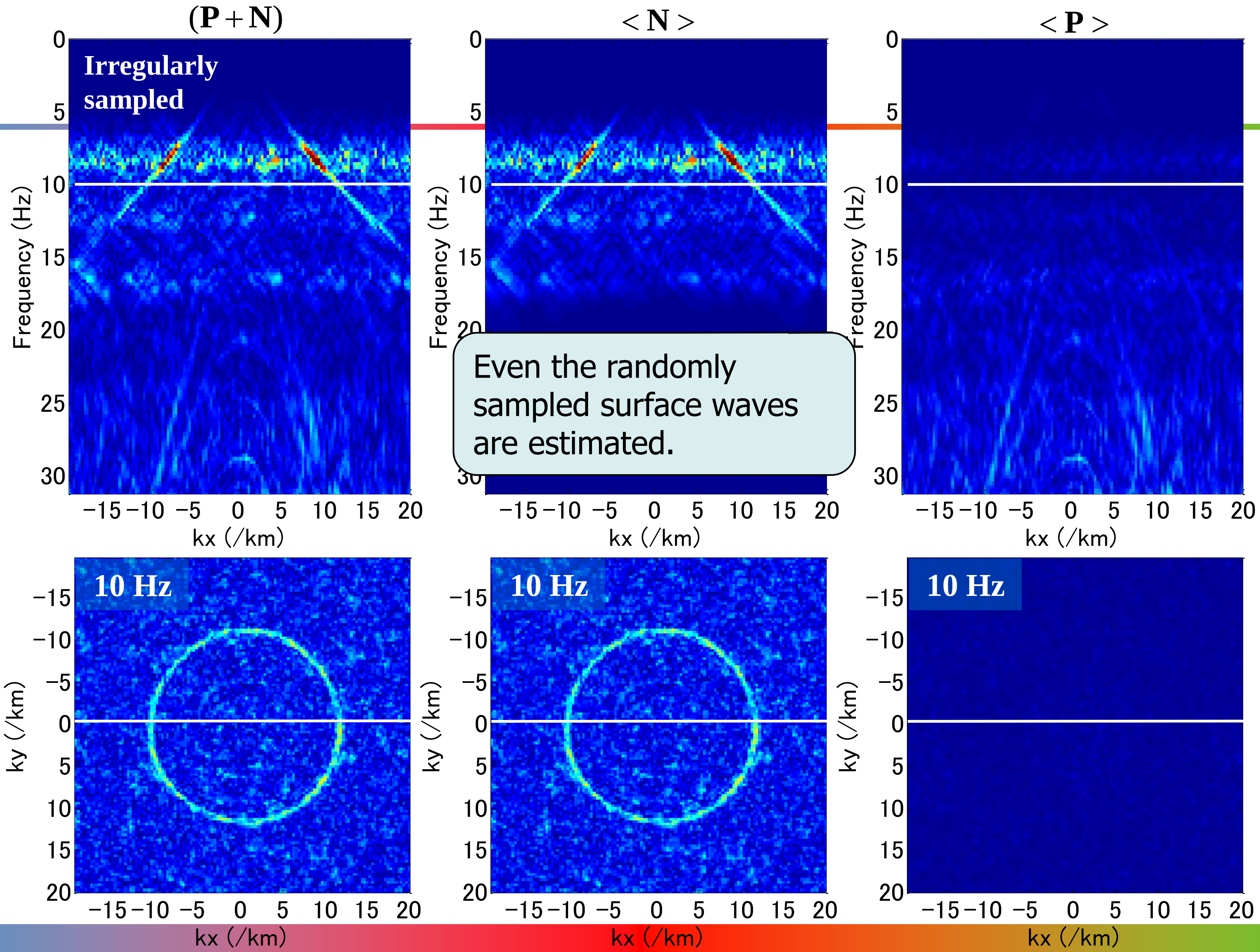

Even the randomly sampled surface waves are estimated.

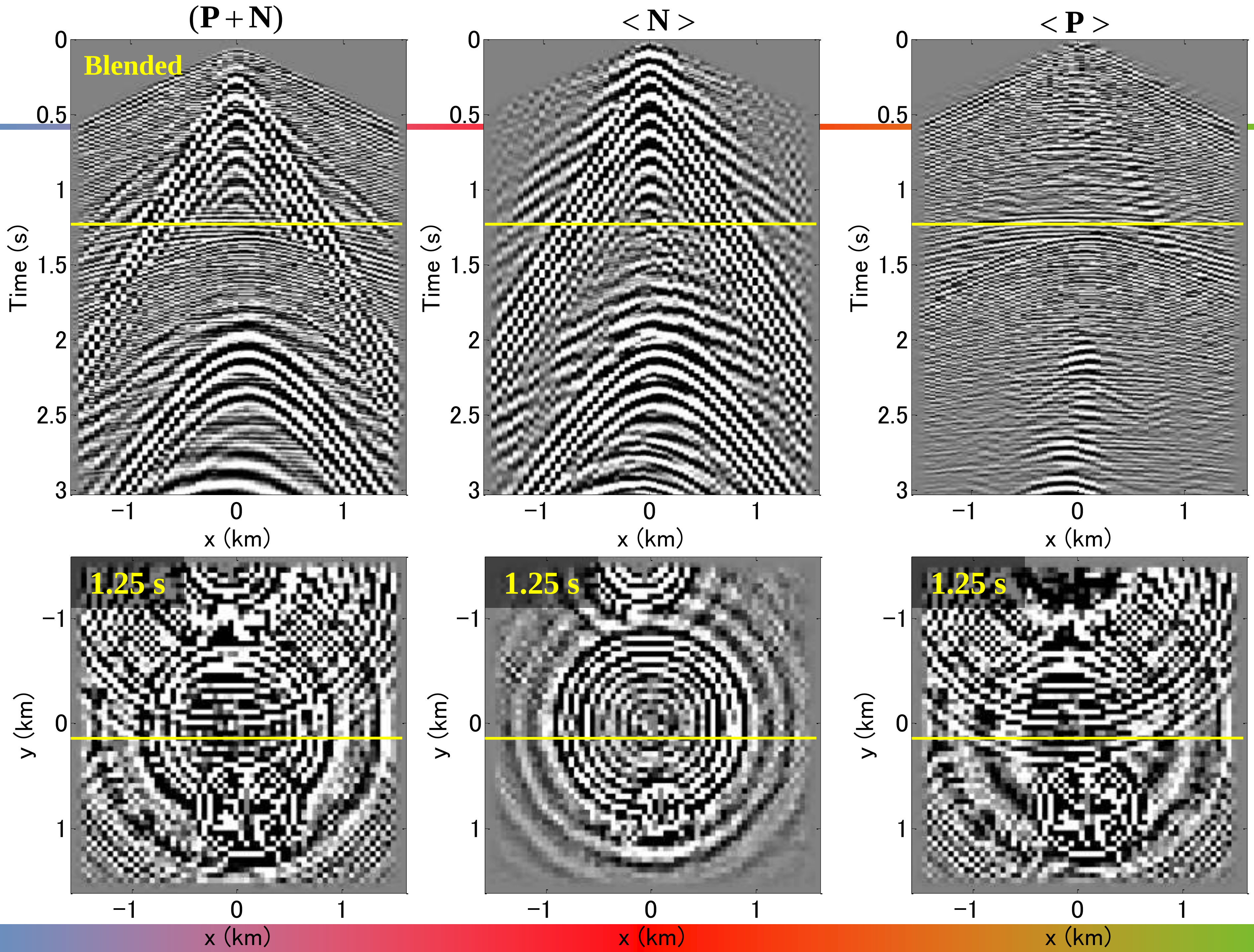

(P + N)
< N >
< P >
Blended
Time (s)
x (km)
y (km)
1.25 s
0
0.5
1
1.5
2
2.5
3
−1
0
1

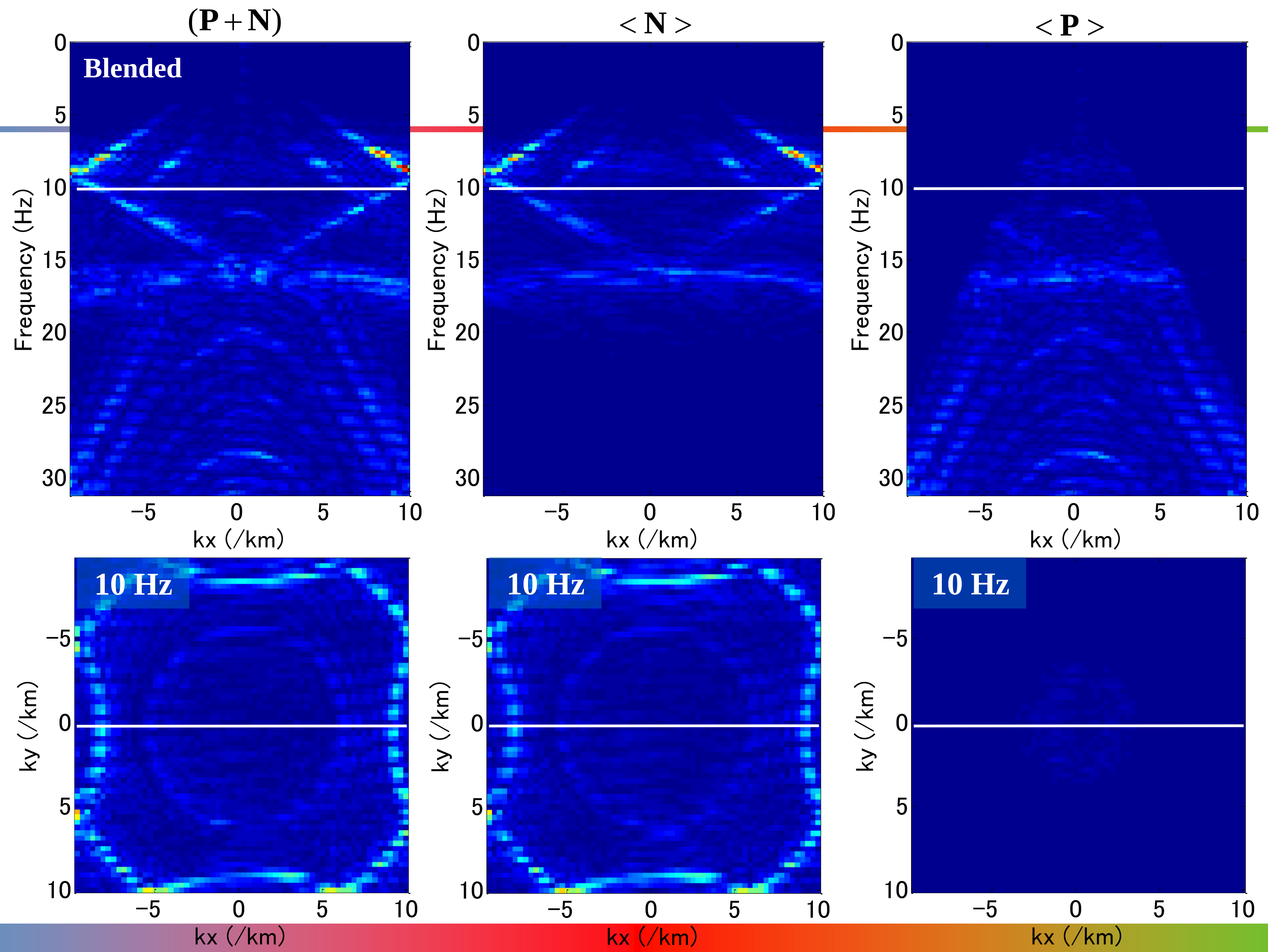
(P + N)
< N >
< P >
Blended
Frequency (Hz)
kx (/km)
10 Hz
ky (/km)
Delphi

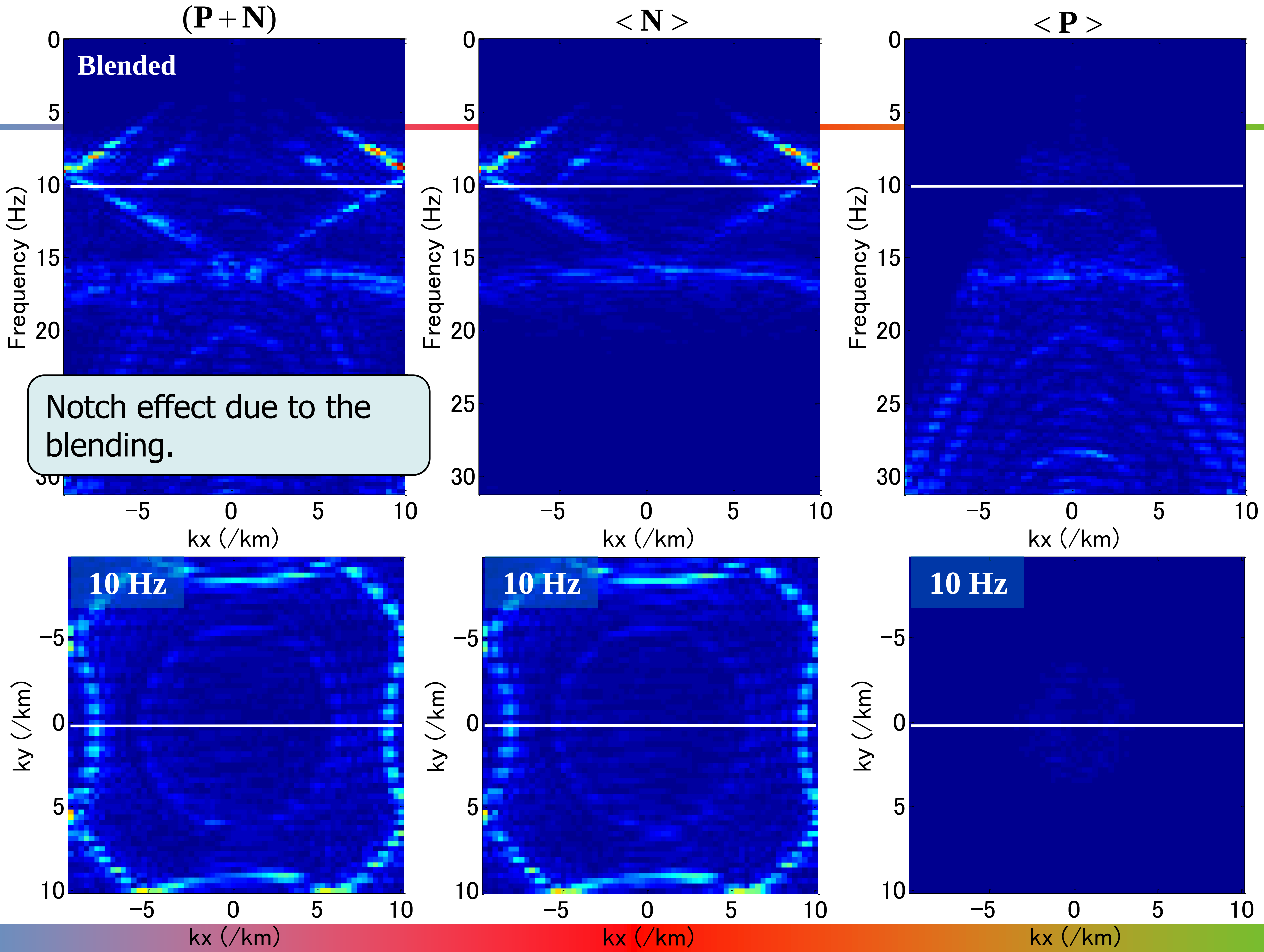

Notch effect due to the blending.

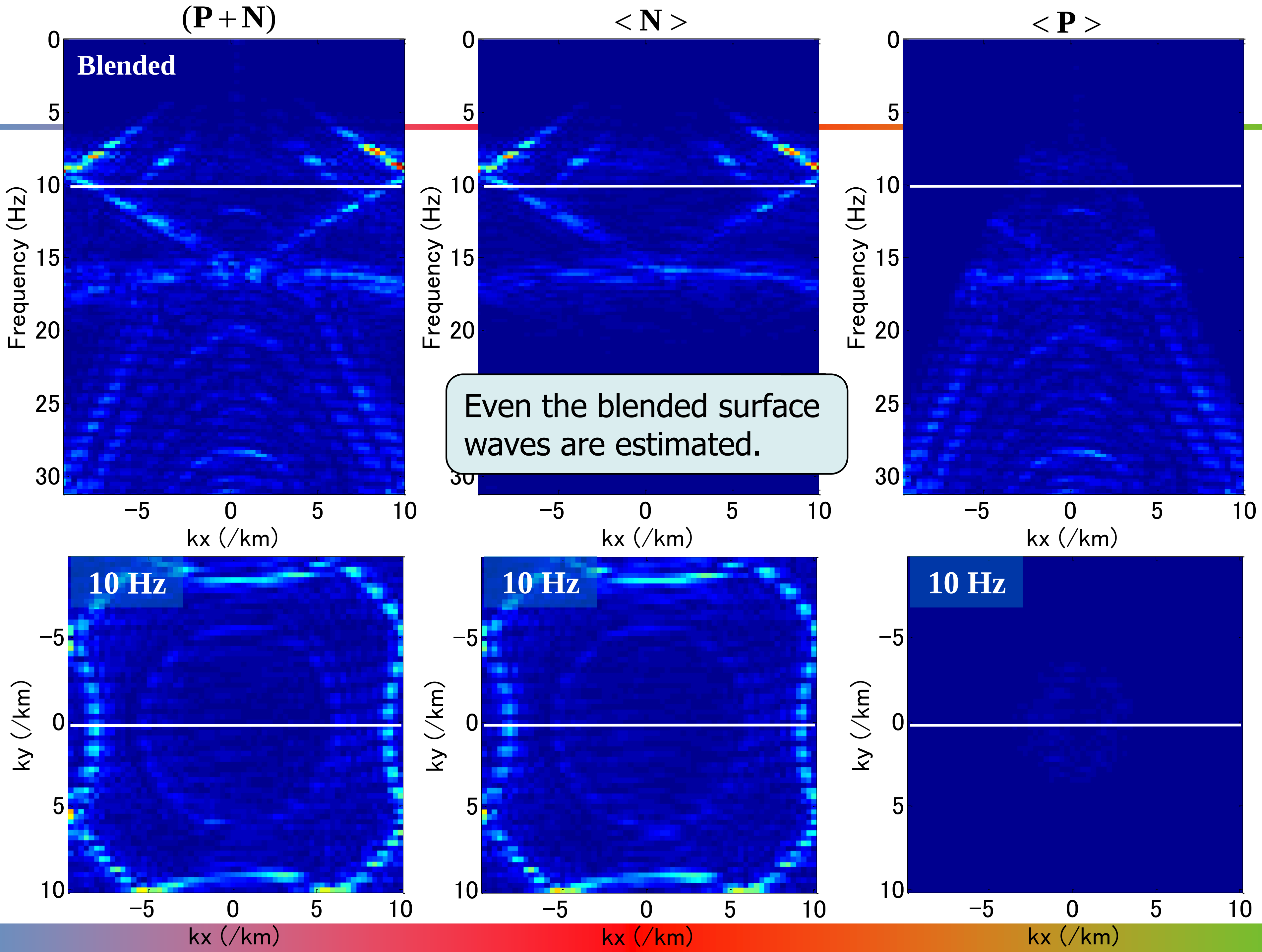

Even the blended surface waves are estimated.

Outline

- Introduction
- Theory and method
- Real data examples
- Conclusions and remarks

Conclusions and remarks

Delphi

- The proposed method addresses the surface-wave properties, i.e., dispersion and multi-modes.

- The method is data-driven and data-adaptive,
  automatically taking into account physical phenomena such as spatial variation, attenuation, anisotropy, etc.

- The method can be applied in any geometry domain, i.e., in any gathers.
  It can be applied to under-sampled, asymmetrically sampled, irregularly sampled and blended seismic data.

Conclusions and remarks

- This suggests the possibility of relaxing the spatial sampling interval, encourages random sampling / blending, and offers flexibility with respect to acquisition geometry.

Acknowledgements

- ADNOC R&D OSC / PI
- INPEX / JODCO
- DELPHI / TUD

Thank you.

GEO 2016

12th Middle East Geosciences Conference and Exhibition

Conference: 7 – 10 March 2016

Exhibition: 8 – 10 March 2016

BAHRAIN INTERNATIONAL EXHIBITION AND CONVENTION CENTRE

3-D Surface-wave estimation and separation using an iterative closed-loop approach

Tomohide Ishiyama, Inpex Corporation and
Gerrit Blacquiere, Delft University of Technology

AAPG

EAGE
EUROPEAN ASSOCIATION OF GEOSCIENTISTS & ENGINEERS

SEG
Society of Exploration Geophysicists
The international society of applied geophysics

ادارة المعارض العربية
Arabian Exhibition Management

INPEX Group

JODCO

TU Delft
Delft University of Technology